JOURNAL OF THE AMERICAN

ROCKET

SOCIETY

A journal devoted to rocket technology and the jet propulsion sciences

VOLUME 22 MAY-JUNE 1952 NUMBER 3

Fluctuations in a Spray Formed by Two Impinging Jets . . . . . *M. F. Heidmann and J. C. Humphrey* 127

Injector Spray and Hydraulic Factors in Rocket Motor Analysis . . *K. R. Stehling* 132

The Transfer Functions of Rocket Nozzles . . . . . *H. S. Tsien* 139

A Similarity Law for Stressing Rapidly Heated Thin-Walled Cylinders . . . . . *H. S. Tsien and C. M. Cheng* 144

Heat Flow in Composite Slabs . . . . . *E. Mayer* 150

A Comparison of Adiabatic and Isothermal Expansion Processes in Rocket Nozzles . . . . . *H. S. Seifert and D. Altman* 159

Letters to the Editor 162

Jet Propulsion News 163

American Rocket Society News 168

Technical Literature Digest 172

THIRD ASTRONAUTICAL CONGRESS, STUTTGART, GERMANY, SEPT. 1-6, 1952

that breaks the shackles of air-borne flight

Reaction Motors' 6000 pound thrust series of rocket engines has propelled man faster and higher than ever before. This single series of RMI rocket engines powers:

Bell X-1 (Air Force)
Bell X-1 Improved (Air Force)
Republic XF-91 (Air Force)
Douglas D558-2 (Navy)

RMI ***FOREMOST IN ROCKET POWER***

REACTION MOTORS, INC., ROCKAWAY, NEW JERSEY

EDITORIAL BOARD

D. ALTMAN
California Institute of Technology

L. CROCCO
Princeton University

P. DUWEZ
California Institute of Technology

R. D. GECKLER
Aerojet Engineering Corporation

C. A. GONGWER
Aerojet Engineering Corporation

C. A. MEYER
Westinghouse Electric Corporation

P. F. WINTERNITZ
Reaction Motors, Inc.

K. WOHL
University of Delaware

M. J. ZUCROW
Purdue University

JOURNAL OF THE AMERICAN
ROCKET
SOCIETY

PUBLICATION OFFICE:
20th and Northampton Sts., Easton, Pa.

EXECUTIVE OFFICES:
Engineering Societies Building
29 West 39th Street, New York 18, N. Y.

EDITOR-IN-CHIEF
MARTIN SUMMERFIELD
Princeton University

ASSOCIATE EDITORS
C. F. WARNER—*Jet Propulsion News*
Purdue University

H. K. WILGUS—*ARS News*
New York, N. Y.

H. S. SEIFERT—*Literature Digest*
California Institute of Technology

MANAGING EDITOR
H. K. WILGUS
New York, N. Y.

ADVISORS ON PUBLICATION POLICY

L. G. DUNN
Director, Jet Propulsion Laboratory
California Institute of Technology

T. C. FETHERSTON
General Publicity Department
Union Carbide and Carbon Corporation

R. E. GIBSON
Director, Applied Physics Laboratory
Johns Hopkins University

H. F. GUGGENHEIM
President, The Daniel and Florence
Guggenheim Foundation

LOVELL LAWRENCE, JR.
Engineering Consultant

D. L. PUTT
Major General, U.S. Air Force
Vice Commander, Air Research
and Development Command

T. VON KÁRMÁN
Chairman, Scientific Advisory Board
U.S. Air Force

W. E. ZISCH
General Manager
Aerojet Engineering Corporation

Scope of the Journal

The Journal of the American Rocket Society is devoted to the advancement of the field of jet propulsion through the publication of original papers disclosing new knowledge and new developments. The term "jet propulsion" as used herein is understood to embrace all engines that develop thrust by rearward discharge of a jet through a nozzle or duct, and thus includes systems utilizing atmospheric air and underwater systems, as well as rocket engines. The Journal is open to contributions, either fundamental or applied, dealing with specialized aspects of jet and rocket propulsion, such as fuels and propellants, combustion, heat transfer, high temperature materials, mechanical design analyses, flight mechanics of jet-propelled vehicles, astronautics, and so forth. The Journal endeavors, also, to keep its subscribers informed of the affairs of the Society and of outstanding events in the rocket and jet propulsion field.

Submission of Manuscripts

Manuscripts should be submitted in duplicate to the Editor-in-Chief, Martin Summerfield, Department of Aeronautical Engineering, Princeton University, Princeton, N. J. See instructions on the inside back cover.

Security Clearance

Manuscripts must be accompanied by written assurance as to security clearance in the event the subject matter of the manuscript is considered to lie in a classified area. Alternatively, written assurance that clearance is unnecessary should be submitted. Full responsibility for obtaining authoritative clearance rests with the author.

Advertisements

Information on advertising rates is obtainable from the Secretary of the Society.

Limitation of Responsibility

Statements and opinions expressed in the Journal are to be understood as the individual expressions of the authors and do not necessarily reflect the views of the Editors or the Society.

Copyright

Copyright, 1952, by the American Rocket Society, Inc. Permission for reprinting material in the Journal will be granted only upon application to the Secretary of the Society.

Subscription Rates

One year (six bimonthly issues)	$7.50
Foreign countries, including Canada	add .50
Single copies	1.25
Back numbers	1.50

Subscriptions and orders for single copies should be addressed to the Secretary of the Society.

Change of Address

Notices of change of address should be sent to the Secretary of the Society at least 30 days prior to the date of publication.

Explanation of Numbering of Issues

The September 1951 issue was the first of a new series of expanded scope and contents. This series is numbered on an annual volume basis, beginning each year with the January issue as Number 1. Correspondingly, the September issue was Number 5, and since 1951 was the 21st year of publication the new series started with Volume 21 Number 5. This replaced Number 86 of the previous series.

Published Bimonthly by the American Rocket Society, Inc.

Journal of the American Rocket Society, published bimonthly by the American Rocket Society at 20th and Northampton Streets, Easton, Pa., U.S.A. The Editorial Office is located at the Engineering Societies Building, 29 West 39th Street, New York 18, N.Y. Price $1.25 per copy, $7.50 per year. Entered as second-class matter at the Post Office at Easton, Pa., under the Act of March 3, 1879.

LIQUID OXYGEN

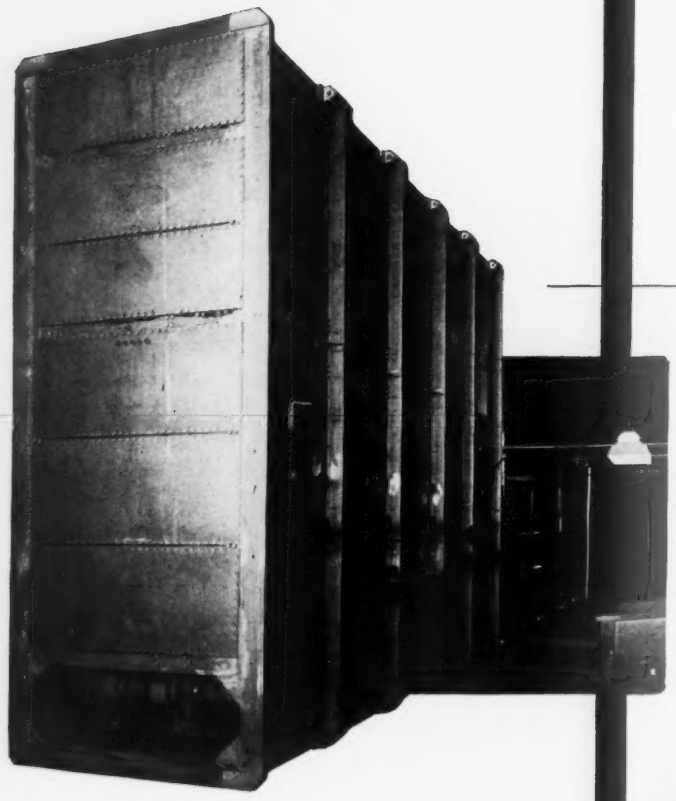

High performance, low cost, and relative ease of storage and handling make liquid oxygen not only the best oxidizer available but guarantee it a prominent place among high performance oxidizers in the future.

Liquid oxygen has certain advantages when comparing oxidizers:

1. **A potential supply unlimited**
2. **Production possible at source**
3. **Inexpensive**
4. **Non-toxic, non-corrosive, smoke-free combustion products**
5. **Easily ignited and smooth burning**
6. **Few limitations on component materials of construction**
7. **Not affected appreciably by ambient temperatures**

Arthur D. Little recently designed and constructed an air-transportable plant for the separation of oxygen from air. This plant was designed to produce 10 tons of liquid oxygen per day.

Experience in the technology of producing, handling and storing liquefied gases aided the Mechanical Division of Arthur D. Little in the design of this plant where minimum weight, small size and purity of product were the prime objectives. The Mechanical Division has further used its experience with liquid gases to design and produce the ADL Helium Refrigerator which is for the storage of liquid gases to reduce evaporation loss to zero.

Although liquid oxygen is produced in wartime chiefly for use as a propellant it may also be used for welding operations and breathing aids when converted to gas by the ADL Liquid-Oxygen Pump.

ADL
Mechanical Division

ARTHUR D. LITTLE, Inc.
Mechanical Division
30 MEMORIAL DRIVE • CAMBRIDGE, MASS.

Send for catalog R-2, describing these and other products and services of the Mechanical Division.

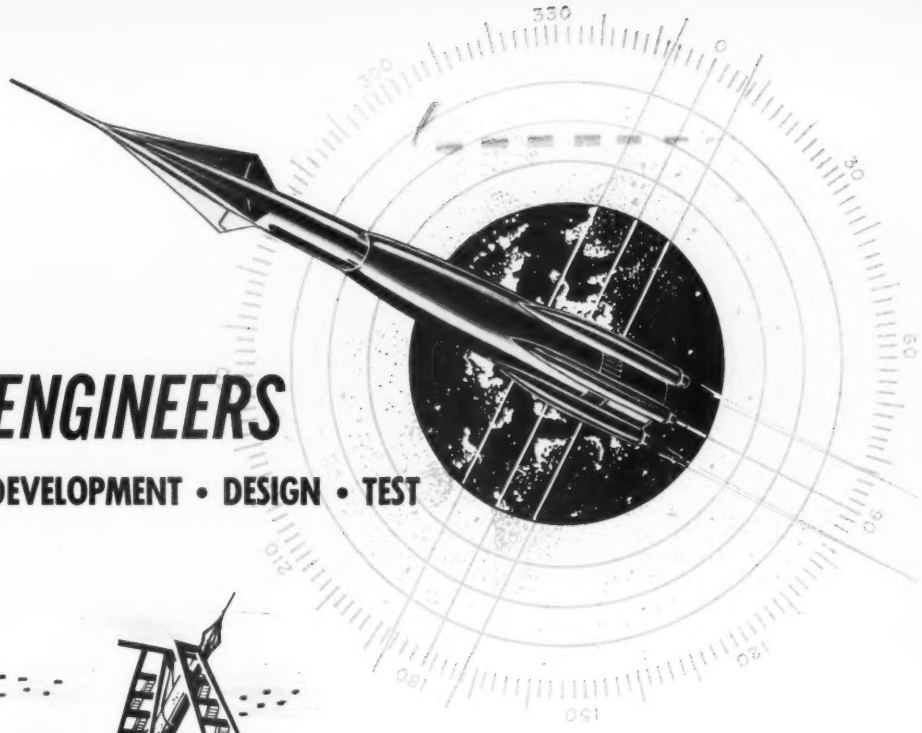

ROCKET ENGINEERS

RESEARCH • DEVELOPMENT • DESIGN • TEST

A long range program of research and development in guided missiles has created unlimited opportunities in all phases of rocket engineering.

Engineers with advanced degrees are needed for positions in Combustion Research and Physical Chemistry.

Engineers with or without advanced degrees are needed as:

RESEARCH ENGINEERS . . . for studies in heat transfer and Thermodynamics

DESIGN ENGINEERS . . . for design phases of liquid rocket power plants, thrust chambers, gas turbine pumps

FIELD ENGINEERS . . . for coordination of activities at field test sites

TEST ENGINEERS . . . for development and production testing of liquid rocket power plants and their components

COMPLETE ROCKET TESTING FACILITIES

Openings also for Design Draftsmen and Technicians
Send complete resume to: Manager, Engineering Personnel

BELL *Aircraft* CORPORATION
P. O. BOX 1, BUFFALO 5, NEW YORK

Many Engineers have not yet heard the good news:

...LOCKHEED IN CALIFORNIA HAS RAISED ENGINEERS' SALARIES

Lockheed Aircraft Corporation has raised engineers' salaries recently, in recognition of the importance and excellence of their work on both military and commercial aircraft.

The substantial increases make Lockheed engineers among the highest paid in the aircraft industry.

Engineers who join the Lockheed staff receive the benefits of these pay boosts.

In addition to increased salaries, Lockheed also offers engineers:

1. A "bonus" every day in better living—just because you live in Southern California, in an area where the climate is beyond compare.

2. A future that offers both security and advancement, helping create planes for defense, planes for the world's airlines in Lockheed's long-range development program.

3. Better *personal* working conditions among men who have built a reputation for leadership in aviation.

To forward-looking Engineers in non-aeronautical fields:

Become an Aircraft Engineer at Lockheed's Expense

The step up to Aircraft Engineering isn't as steep as you might expect. Aircraft experience isn't necessary. Lockheed takes your knowledge of engineering principles, your experience in other engineering fields, your aptitude, and adapts them to aircraft work. You learn to work with closer tolerances, you become more weight conscious. What's more, Lockheed trains you *at full pay*. You learn by doing—in Lockheed's on-the-job-training program. When necessary, you attend Lockheed classes. It depends on your background and the job you are assigned. But always, you learn at full pay.

To Engineers with Families:

Housing conditions are excellent in the Los Angeles area. More than 40,000 rental units are available in the Los Angeles area. Huge tracts for home ownership are under construction now. Thousands of homes have been built since the last war. Lockheed counselors help you get settled.

Lockheed also offers these extra benefits:

Generous Travel allowances • Outstanding Retirement Plan • Vacations with pay • Low cost group life, health, accident insurance • Sick Leave with pay • Credit Union, for savings and low-cost financing • Employees' Recreation Clubs • Regular performance reviews, to give you every opportunity for promotion • On-the-job training or special courses of instruction when needed.

Send today for illustrated brochure describing life and work at Lockheed in Southern California. Use this handy coupon.

ENGINEER TRAINING PROGRAM

Mr. M. V. Mattson, Employment Mgr. Dept. RT-4

Lockheed AIRCRAFT CORPORATION

Burbank, California

Dear Sir: Please send me your brochure describing life and work at Lockheed.

My Name

My Field of Engineering

My Street Address

My City and State

KOLLSMAN
for products of precision and dependability

Aircraft Instruments and Controls • • • Miniature AC Motors for Indicating and Remote Control Applications • • • Optical Parts and Optical Devices Radio Communications and Navigation Equipment

Today, Kollsman works without pause toward the fulfillment of America's defense needs. And to our nation's research scientists, the skill, ingenuity and creative drive of Kollsman Research Laboratories are available for the solution of instrumentation and control problems.

KOLLSMAN INSTRUMENT CORPORATION

ELMHURST, NEW YORK — GLENDALE, CALIFORNIA

SUBSIDIARY OF *Standard* COIL PRODUCTS CO. INC.

First AND *Foremost* IN *Ramjet* DESIGN & ENGINE

production

MARQUARDT AIRCRAFT CO VAN NUYS CALIF

MAY-JUNE 1952
VOLUME 22 NUMBER 3

JOURNAL OF THE AMERICAN ROCKET SOCIETY

Editor-in-Chief
MARTIN SUMMERFIELD

Fluctuations in a Spray Formed by Two Impinging Jets

MARCUS F. HEIDMANN[1] and JACK C. HUMPHREY[1]

National Advisory Committee for Aeronautics, Lewis Flight Propulsion Laboratory, Cleveland, Ohio

An investigation of the spray formed by two impinging jets of water indicated that upon impingement a ruffled sheet of liquid was formed which disintegrated intermittently to form groups of drops which appear as waves propagating from the point of impingement. The effect of various injector parameters on the frequency of wave formation and on the spray pattern was investigated because of its possible relation to combustion instability.

Introduction

COMBUSTION instability has been encountered during various phases of development of liquid-propellant rocket engines. This combustion instability is characterized by sustained oscillations in combustion chamber pressure over a wide frequency range. This problem has been the subject of a number of investigations (1, 2, 3).[2] The common concept of the analytical treatment of combustion oscillations is that the oscillations occur within a feedback loop. In general, it is assumed that oscillations in combustion chamber pressure result from a coupling between chamber pressure and energy addition to the chamber. In other words, a change in chamber pressure causes a change in energy addition which in turn causes an additional change in chamber pressure. The criteria for instability in such a system are that energy addition is in phase with the pressure change, and that the energy addition results in a pressure change of sufficient magnitude to overcome damping factors in the system. Such criteria necessitate a change in energy addition proportionately larger than the change in pressure, or that the gain factor in the feedback loop is greater than unity.

Low-frequency oscillations (in the range from approximately 20 to 200 cycles) appear to be a resonance in a feedback loop where propellant feed system and rocket combustion chamber are dynamically coupled. High-frequency oscillations (>200 cps) appear to be a feedback cycle within the combustion chamber itself, and hence is closely associated with propellant atomization, vaporization, burning rate, and related factors. Because of the role of the injector in influencing the burning, a study of the hydraulic characteristics of the injector as a possible source of high-frequency instability has been undertaken at the NACA Lewis Laboratory. The results of the initial investigation where spray fluctuations were observed in two impinging jets of water (4) are presented herein.

Impinging Jet Spray Characteristics

Spray Fluctuations

In the apparatus for study of the spray characteristics of two impinging jets, water was forced by regulated gas pressure through two precision-bore glass tubes with a L/D of approximately 75 and arranged so that angle of impingement and stream length could be conveniently varied. Several sets of glass tubes were used to vary stream diameter. In this manner the spray of the impinging jets as a function of jet velocity, jet diameter, impingement angle, and distance of the two jets to the point of impingement was observed. Microflash photographs of two impinging jets of water (Fig. 1) show that upon impingement a ruffled sheet of liquid is formed perpendicular to the plane of the two jets. The liquid sheet disintegrates intermittently, forming groups of drops which appear as waves propagating from the point of impingement. This wave propagation is better shown in Fig. 2 which shows a series of high-speed motion pictures of the same jets.

This phenomenon of wave propagation appears to be conducive to instability and may be an additional gain factor in a feedback loop. The photographs indicate that the flow rate in the spray may vary from a minimum of zero between waves to a maximum of a possible 200 per cent of average. If the fluctuations could be induced by small variation in chamber pressure or propellant flow, they would exhibit themselves as a very large gain factor in the feedback loop, which

Presented at the Annual Convention of the AMERICAN ROCKET SOCIETY, Atlantic City, N. J., November 30, 1951.

[1] Aeronautical Research Scientist.

[2] Numbers in parentheses refer to the References on page 167.

may be sufficient to cause sustained oscillations at high frequencies.

In view of the probable relation of spray fluctuations to combustion instability, a further investigation of the characteristics of the fluctuation was made. The fluctuations in a spray formed by two impinging jets of water were studied to determine the nature of the fluctuations and to evaluate the effect of injector parameters on the fluctuations. The frequency of wave formation in the spray was determined by allowing the wave to interrupt a beam of light focused on a photoelectric cell, and the resulting signal was analyzed by using either a frequency meter or recording oscilloscope. The measurements were made at a point where complete disintegration of the spray occurred, which was generally one inch from the point of impingement.

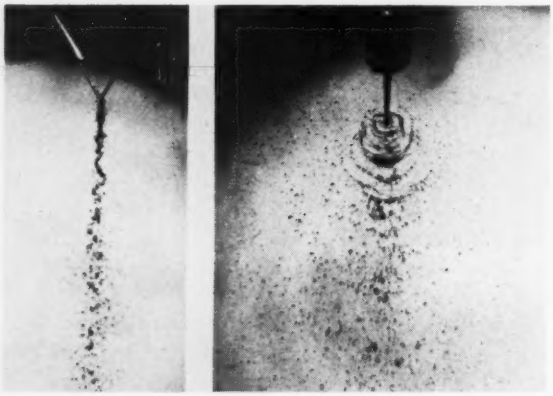

FIG. 1 MICROFLASH PHOTOGRAPHS OF FORMATION OF SPRAY BY TWO IMPINGING JETS OF WATER

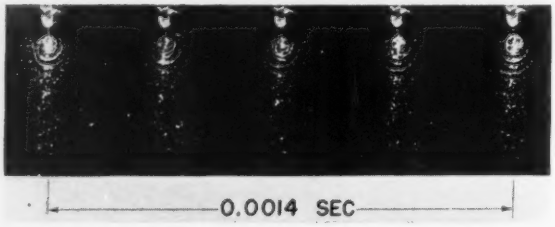

FIG. 2 SUCCESSIVE FRAMES FROM HIGH-SPEED MOTION PICTURES OF FORMATION OF SPRAY FROM TWO IMPINGING JETS OF WATER

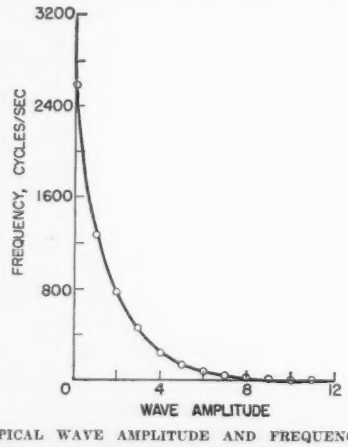

FIG. 3 TYPICAL WAVE AMPLITUDE AND FREQUENCY CHARACTERISTICS FOR FLUCTUATIONS RESULTING FROM IMPINGEMENT OF TWO JETS OF WATER

It will be noted in Figs. 1 and 2 that the groups of drops propagating from the point of impingement are of various sizes with irregular spacing between groups. A quantitative evaluation was made of wave intensity, the quantity of liquid per unit volume, and the frequency from an oscilloscope trace obtained for a typical spray. The evaluation was made assuming proportionality between oscilloscope deflection and quantity of liquid per unit volume intercepting the light beam directed at the photoelectric cell. The results of this evaluation are shown in Fig. 3, which shows frequency and intensity on an accumulative basis. For example, the frequency at an intensity of 3 is 450 cps, where 450 is the frequency based on the number of waves of intensity 3, plus all those larger than 3. The intensity scale used is linear, but the magnitude is arbitrary. Fig. 3 indicates that there is an abundance of low-intensity waves. Approximately one half the waves have an intensity of $^1/_{12}$ the maximum intensity. Although on first impression the fluctuations in the spray appear to be random in nature, on the basis of frequency and intensity the fluctuations do have defined characteristics, as illustrated in Fig. 3. Under constant operating conditions, these characteristics are reproducible and the frequency of wave formation over a finite time interval is constant. Although Fig. 3 presents the frequency distribution in the spray, in

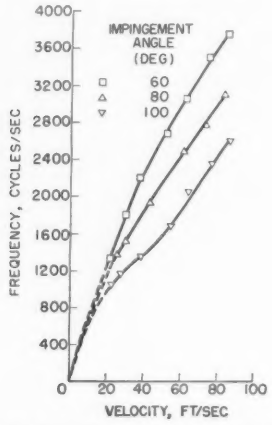

FIG. 4 EFFECT OF JET VELOCITY AND WAVE FREQUENCY FOR SEVERAL IMPINGEMENT ANGLES. EFFECT IS SHOWN FOR IMPINGING JETS 0.025 IN. IN DIAM

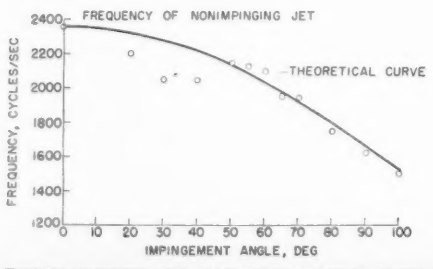

FIG. 5 EFFECT OF IMPINGEMENT ANGLE ON WAVE FREQUENCY FOR 0.040-IN. DIAM JETS AT VELOCITY OF 40 FPS

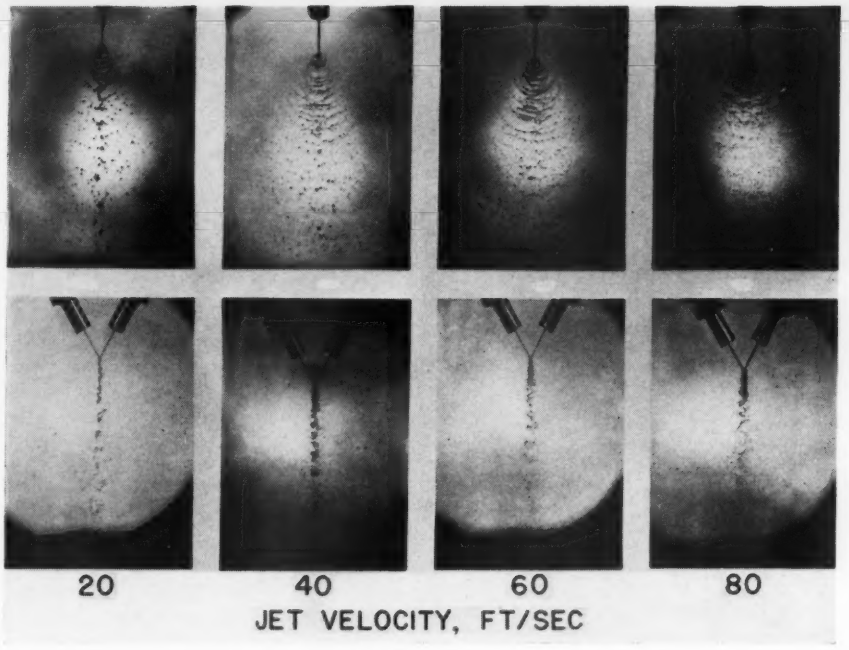

FIG. 6 EFFECT OF JET VELOCITY ON SPRAY PATTERN. CONDITIONS: JET DIAM, 0.023 IN.; IMPINGEMENT ANGLE, 60 DEG

subsequent references to spray frequency the frequency based on all waves formed will be used, which, in the case of Fig. 3, is 2580 cps.

Effect of Injection Parameters on Wave Frequency

Jet Velocity and Impingement Angle

The effect of jet velocity on wave frequency over a jet velocity range of 20 to 80 fps for impingement angles of 60, 80, and 100 deg was determined for 0.025-in.-diam jets. The relation between frequency and velocity at the various impingement angles is shown in Fig. 4. Fig. 4 shows that frequency increases with velocity, with the relation approaching direct proportionality. The frequency gradient is approximately 30-cps velocity. Although no data were taken below a velocity of 20 fps, the nature of the curves indicates extrapolation to the origin.

The trend of increasing frequency with decreasing impingement angle, indicated in Fig. 4, is more clearly shown in Fig. 5. In this case, the effect of impingement angle on frequency was determined, using 0.040-in.-diam jets. The frequency was determined over the maximum impingement-angle range of the apparatus, including the frequency measured in the nonimpinging jet, at a point where complete disintegration of the jet exists. The curve shown in Fig. 5 is a theoretical curve of frequency based on the change in resultant spray velocity with impingement angle (assuming conservation of momentum). Good agreement with the theoretical curve was obtained at impingement angles of 50 deg and above. The frequencies obtained at low impingement angles are reproducible; however, some of the deviation from the theoretical curve may be attributed to the indistinct nature of the waves at low impingement angles.

The variations in the spray pattern resulting from changes in jet velocity are shown in Fig. 6. The patterns for velocities of 20, 40, 60, and 80 fps at an impingement angle of 60 deg are shown for 0.025-in.-diam jets. These photographs illustrate that the wave pattern is not substantially altered by jet velocity. Smaller drops, however, are formed at the higher velocities.

The wave patterns for impingement angles of 30, 60, and 90 deg at a jet velocity of 60 fps for 0.025-in.-diam jets are shown in Fig. 7. These photographs indicate greater definition of wave pattern as well as a shorter distance for complete disintegration of the liquid sheet as impingement angle increases.

Jet Diameter

Frequency measurements were made over a velocity range of from 20 to 80 fps and at an impingement angle of 80 deg for jet diameters of 0.025, 0.040, and 0.057 in. These results are shown in Fig. 8. An increase in frequency with decreasing diameter at constant velocity is indicated; however, the effect of diameter is comparatively small. A diameter range of from 0.025 to 0.057 in. at constant velocity represents a flow range of approximately 5 and resulted in a frequency variation of from 200 to 300 cps. Inasmuch as velocity based on flow calibration was used in the comparison, the small variations in frequency are insufficient to predict the effect of diameter beyond that the effect is small in comparison to the effect of impingement angle and velocity.

The effect of diameter on the spray pattern is illustrated in the photographs shown in Fig. 9. The spray

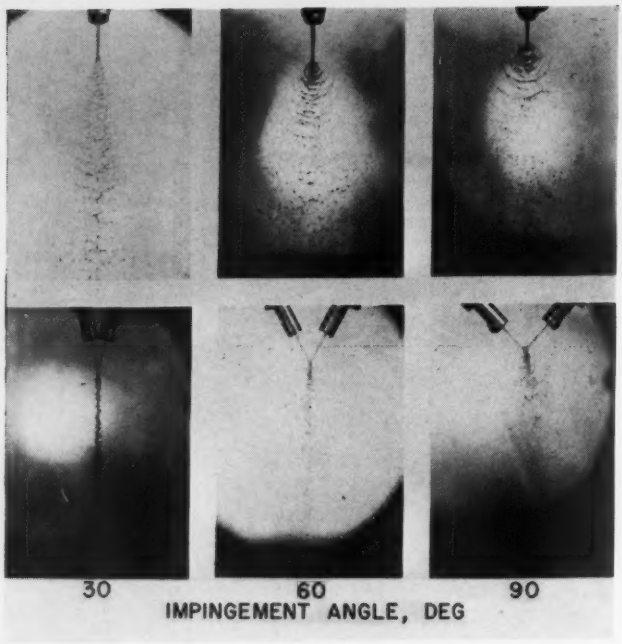

FIG. 7 EFFECT OF IMPINGEMENT ANGLE ON SPRAY PATTERS. CONDITIONS: JET DIAM, 0.025 IN.; JET VELOCITY, 60 FPS

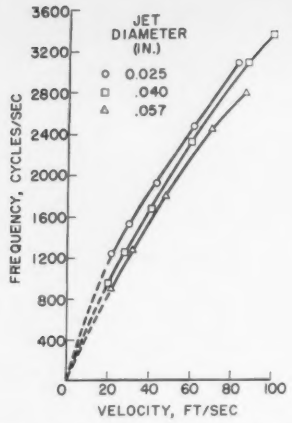

FIG. 8 EFFECT OF JET DIAMETER ON RELATION BETWEEN FREQUENCY AND JET VELOCITY AT IMPINGEMENT ANGLE OF 80 DEG

patterns for the 0.025, 0.040, and 0.057-in.-diam jets at a velocity of 50 fps and an impingement angle of 70 deg are shown. Beyond that, the size of the resulting spray changes with diameter, and only small differences are detectable. Fig. 9 gives the appearance of successive enlargements of the same picture.

Jet Length

The length of the jets before impingement was varied under several conditions to determine the effect of this parameter on wave frequency. The effect of changing jet length over a range of 6 to 80 diam had a negligible effect on spray frequency. The effect of jet length, however, is more pronounced in spray pattern. Fig. 10 portrays the effect on the 0.025-in.-diam jets at a velocity of 40 fps and angle of 60 deg. Stream lengths of 10, 20, 40, and 60 diam are shown. It will be noted that dispersion of the spray increases as stream length increases. At a stream length of 60 diam, the jet has become very unstable and almost complete separation occurs. Beyond this length it is possible for a fraction of liquid from one jet to pass through the path of the other jet without interference or impingement. The spray patterns perpendicular to those in Fig. 10 are not presented because the spray pattern in this plane was substantially unaffected.

Discussion

The results of this initial investigation of fluctuations in a spray formed by two impinging jets indicate that the major effect on the fluctuations was obtained by a change in the velocity of the sheet formed by the two jets. If, in Fig. 4, the jet velocity and sheet velocity are assumed to be directly proportional for a constant impingement angle, the frequency is shown to vary proportionately with sheet velocity. Also in Fig. 5, as impingement angle is changed, the sheet velocity should vary as the cosine of one half the impingement angle (based on conservation of momentum).

This relation applied to the experimental effect of impingement angle is shown in Fig. 5. The correlation appears good for impingement angles between 50 and 100 deg, and the frequency of a nonimpinging jet corresponds to the frequency for a 0-deg impingement angle. Lack of correlation at small impingement angles, however, indicates that the frequency is not a unique function of the sheet velocity. One other factor apparently affecting the ruffling of the sheet and the subsequent frequency is the irregular nature of the jets before impingement. This effect is indicated by the photographs in Fig. 10. In this case, increasing the jet length amplifies the irregularities in the jets, and a greater dispersion of the spray is obtained. Other factors may also influence the frequency; however, a complete theory on the formation of these fluctuations in the spray can be obtained only by a continuation of the investigation of the parameters affecting the spray formation.

In determining the effect of injector parameters on the spray formation, it was found that changes in the injector parameters had no effect on the basic mechanism of spray formation. Under all conditions, the spray was formed from a ruffled sheet of liquid that disintegrated intermittently, and the changes obtained in the measured frequency of wave formation with injector parameters were comparatively uniform.

The frequency of wave formation is important to the problem of combustion instability, for it indicates that the propellant flow rate in the spray can vary with sufficient rapidity to promote high-frequency pressure fluctuations, screaming, in combustion. The relation of the fluctuations in the spray to combustion instability, however, appears to be dependent on the problem of inducing fluctuations of a definite frequency

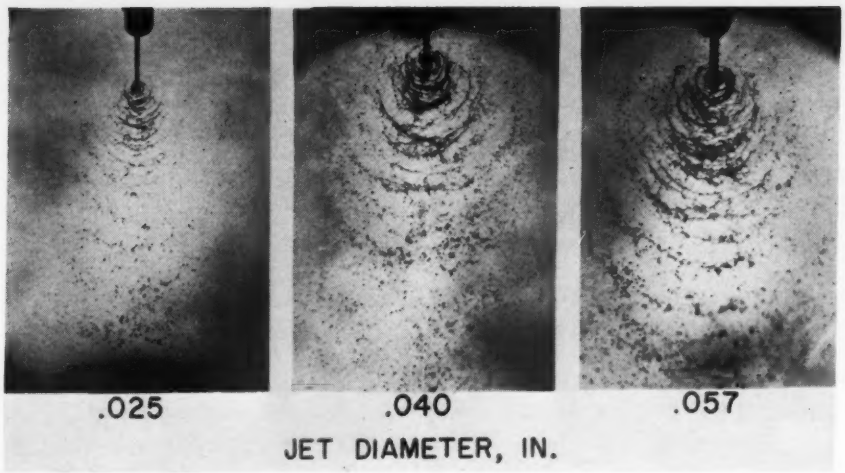

FIG. 9 EFFECT OF JET DIAMETER ON SPRAY PATTERN. CONDITIONS: JET VELOCITY, 50 FPS; IMPINGEMENT ANGLE, 70 DEG

n the spray. Limited experiments with sound waves have shown that fluctuations in a spray formed by two impinging jets of water cannot be readily induced. Sound waves produced by an oscillator and speaker and concentrated on the spray gave inconclusive results. At lower frequencies the spray could be disrupted, but this appeared to result from the air turbulence caused by the high concentration of sound energy. Waves were not induced but, rather, the spray or sheet was virtually torn apart independent of the wave formation. At induced frequencies approaching the natural frequency in the spray, the sound waves had no apparent effect on spray formation. Experiments with liquid pressure pulsators and with mechanical vibrators have also indicated that fluctuations in the spray are not readily induced.

Preliminary experiments on the effect of viscosity and surface tension on spray formation have shown that, although spray formation changes considerably with higher viscosity, the effect of surface tension is small. The effect of viscosity is presently being explored to provide data on a theory of spray formation and the resulting fluctuations. Such a theory will be useful in determining whether fluctuations can be induced and their relation to combustion instability.

Summary of Results

From the investigation of the fluctuations in the formation of a spray from two impinging water jets, the following results were obtained:

1 Upon impingement of two jets, a ruffled sheet of liquid was formed, perpendicular to the plane of the two jets. The liquid sheet disintegrates intermittently, forming groups of drops which appear as waves propagating from the point of impingement.

2 The intermittent disintegration of the liquid sheet resulted in irregular spacing between waves and in variable wave intensity. There was an abundance of small waves with the number of waves above a given intensity decreasing as the intensity increased.

3 The frequency of wave formation was constant over a finite time interval under constant operating conditions. The frequency varied between 1000 and 4000 cps for the range of test conditions used in this investigation.

4 The spray parameter having the major effect on spray frequency was found to be the velocity of the sheet formed on impingement. The relation between

(*Continued on page 167*)

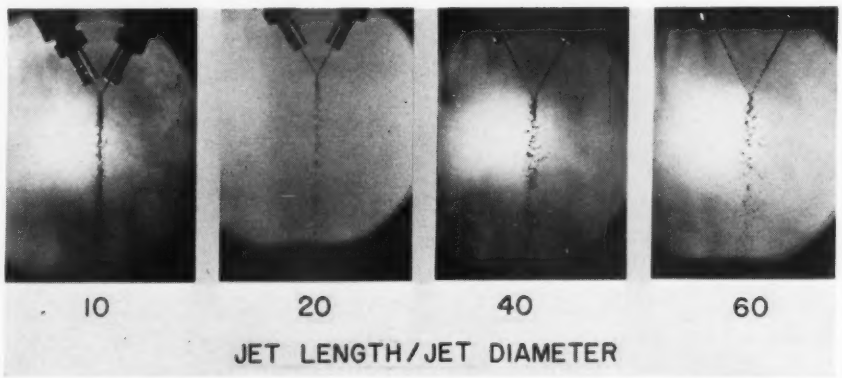

FIG. 10 EFFECT OF RATIO OF JET LENGTH TO JET DIAMETER ON SPRAY PATTERN. CONDITIONS: JET DIAM, 0.025 IN.; JET VELOCITY, 40 FPS; IMPINGEMENT ANGLE, 60 DEG

Injector Spray and Hydraulic Factors in Rocket Motor Analysis

KURT R. STEHLING[1]

Bell Aircraft Corporation, Buffalo 5, New York

HYDRAULICS RESEARCH LABORATORY

A comparison of various types of thrust chamber injection systems is outlined. The applicability and relative merits of several common injector heads are emphasized. The use of dyed-water flow analysis and high-speed photography in injector head spray research is described. It is shown that dye flow permits distinction of the "propellants" in the spray and enables the designer to take corrective steps if poor distribution is indicated. Methods of analyzing droplet size and atomization rates are reviewed and compared. The cause and effect of hydraulic "flip" in orifice jets are discussed, as are the effects of cavitation and feedback in the hydraulic system.

Introduction

LIQUID-FUEL rocket motor systems are characterized by flows of large quantities of liquids at high pressures and velocities. This characteristic inevitably results in anomalous hydraulic behavior and severe design criteria for the various components of the motor complex. The propellants must begin to flow from a reservoir (tank) through a maze of piping and valves, possibly through a cooling jacket, ultimately through an injector head, into the environment of the chamber. During its travels, the liquid must fight an uphill battle (energywise), against pipe, fitting, valve and jacket friction, the injector head orifice holes, and, finally, the high chamber pressure. It can derive its initial energy from pressurized tanks, or it may start out at a low energy level and get a boost along the way by a pump.

It is difficult to treat any one element distinctly and separately from the rest of the hydraulic circuit; however, some distinction is possible if interaction is neglected.

One of the more important components of the rocket motor system, the injector head, will be discussed briefly, assuming that it is independent of the remainder of the hydraulic circuit.

Injector Head Design

Basically, the injector head has the functions of introducing the propellants into the thrust chamber in the most efficient and auspicious manner (i.e., it should expedite the transfer of the propellant from the liquid to the gaseous phase as quickly as possible). The injection can either be random or indiscriminate, leaving the functions of atomization and mixing to the vagaries of the chamber; or, the injection system can prepare the propellants for combustion by performing these functions, utilizing some of the kinetic energy of the moving liquids.

A brief classification of injection systems, using the criteria of mixing and atomization, is as follows:

Random (Fig. 1): A typical example of this injection system is the "random showerhead" injector. It usually consists of a matrix of holes drilled in the flat face of the injector. Oxidizer and fuel are injected into the chamber through adjacent orifices. The rate and ultimate atomization of the liquid streams depend upon the chamber environment, such as the chamber gas density, temperature, and injection velocity. The mixing depends upon the collision between the droplets and the subsequent mingling.

Generally, random injectors have shown low efficiency with nonhypergolic propellants, probably due to their poor mixing and distribution characteristics. The mixing may be improved by increasing the number of orifices; however, the manifolding design and construction problems increase disproportionately. Since the combustion with this injector tends to be smooth with common propellants, further research is warranted to improve the combustion efficiency of this head, while retaining its stable combustion characteristics.

Presented at the Annual Convention of the American Rocket Society, Atlantic City, N. J., November 30, 1951.

[1] Rocket Research Engineer. Member ARS.

Splash (Fig. 2): The principle of this type of injection is primarily one of the impingement of the propellant stream or streams upon the walls of the chamber or some protuberance of the injector head, such as an annular ring or "splash plate." This plate serves to break up the stream for rapid atomization. The inelastic collision of the stream also abruptly changes its velocity and direction, and results in burning close to the injector head. This mechanical stream breakup permits low injection pressures.

The German "Enzian" injector head is a classical example. This configuration has been tried with varying success in this country. It may yield high specific impulses with relatively smooth combustion at differential injection pressures up to 50 psi. However, the combustion pattern tends to be uneven with severe localized heat rejection, in extreme cases almost 5 Btu/sq in./sec. Also, the position and tolerance of the splash ring are critical and deviations from design can result in wide variations in performance. This condition has been remedied to some extent by knurling or serrating the splash ring face in order to break up and distribute the spray more efficiently.

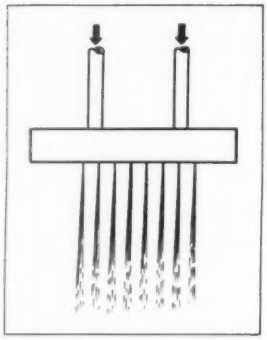

FIG. 1 RANDOM SHOWERHEAD INJECTION

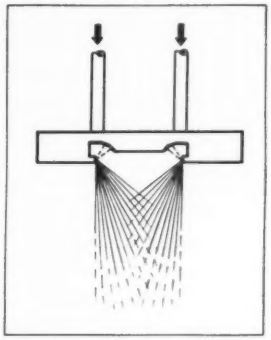

FIG. 2 SPLASH INJECTION

Liquid-Liquid (sometimes known as "forced action injection"): This injection method comprises the largest segment of current injector practice. Its chief virtue lies in its ability to break up and mix the propellant streams, using some of the kinetic energy of the liquids. In general, a well-designed head gives good mixing and distribution at any engine size from 100-lb thrust to existing upper limits (1).[2]

Some typical examples of injector heads based on this principle are:

a. The Impinging Showerhead

(Fig. 3): This is a favorite configuration, generally consisting of concentric rows of holes for fuel and oxidizer. It has proved advantageous to bring the propellant impingement points as close to the injector face as possible. This permits maximum utilization of the thrust chamber volume and results in smoother combustion, apparently due to the absence of unreactive vapor pockets near the injector face. With presently common nonhypergolic propellants, the well designed impinging showerhead can consistently yield specific impulses with values 90 per cent of theoretical; the value of the heat rejection may be reduced by designing for a spray envelope (usually fuel rich) whose mixture ratio differs from the rated value. Some evidence exists which indicates the injector is sensitive to sonic and transverse oscillations which influence the fluid stream impingement resulting in rough or unstable combustion.

This configuration is a close approach to a "standard" injector in the rocket motor industry.

b. The Hypoid Showerhead

(Fig. 4): Besides the normal impingement angle, the fluid streams are subjected to another degree of direction or "twist" by the alignment of the orifice holes so as to have not only impingement mixing, but also further forced mixing of the propellants, due to the hypoid action. The fishtails of mixed liquid impinge to form a sheet. Injector heads of this type can give a specific impulse at least as good as that obtained with "normal" impinging injectors, but with lower propellant injection pressures. These injectors can perform equally well with hypergolic or nonhypergolic propellants (which is not true for many other types of injectors). However, they are subject to face burning and occasionally give rise to high-frequency oscillations; furthermore, the hypoid configuration is not easily machined with common shop methods.

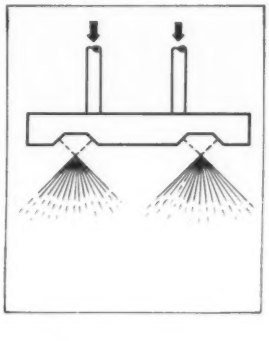

FIG. 3 IMPINGING (LIQUID-LIQUID) INJECTION

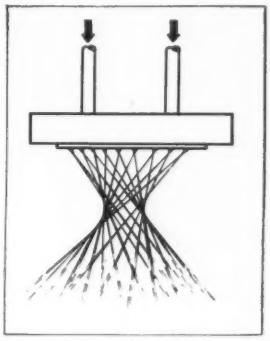

FIG. 4 HYPOID INJECTION

c. Concentric Ring

(Fig. 5): This is a variation of the impinging showerhead, depending for mixing and atomization upon the impingement of liquid sheets emitted by annular slots in the injector head. This configuration gives excellent extraneous-head mixing, since the effect of the impinging sheets is that produced by an infinite number of single, adjoining liquid streams (2). This contrasts with the mixing produced by double jet impingment, which may be erratic due to jet misalignment and oscillation. However, the considerable difficulty of manufacture of the concentric ring injector prevents its wide application. Also, excessive heat transfer rates have been experienced with this type of injector.

[2] Numbers in parentheses refer to References on page 138.

d. Variations of Liquid-Liquid

There are obviously many permutations of the above configurations. The designer can let his imagination revel at will, and produce types such as the like-on-like (fuel impinges on fuel, etc.) injector, or injector heads with inserts of swirler or common oil-burner nozzles (Fig. 6). These latter spray nozzles which are

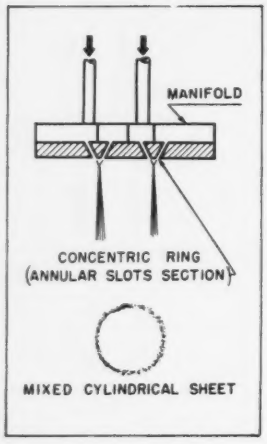

FIG. 5 CONCENTRIC RING

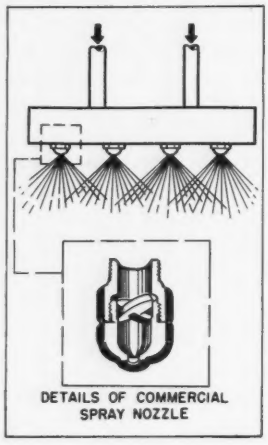

FIG. 6 SPRAY NOZZLE

commercially available, have been favorites of designers since the early days of rocket motor manufacture. It seemed simple enough to insert these nozzles into an injector-head face according to some empirical geometrical pattern. The wide angle of spray and good atomization were counted on to give good performance. However, this type of injector head is not widely applied. This may be due to several reasons, the principal one being that the specific impulse is somewhat less than for the other types.

An element of the commercial spray nozzle, the swirler or vane insert, which imparts angular momentum to the spray, is occasionally inserted into the plenum of normal head orifices in order to retain the atomizing features of the spray nozzle without sacrificing the flexibility and ease of manifolding of the conventional injector. Some success has been attained with differential injection pressures of 200–300 psi, obviously too high for practical applications.

Forced action, or "stream impinging" injectors will probably remain the primary injectors for some time to come, for motors up to five tons thrust. The configuration is flexible enough to permit ready adaptation to various sizes and types of thrust chambers. However, this type of injector must be accurately drilled, both for impingement angle and directness of impact, and for smoothness of the holes. Many otherwise well-impinging showerheads are discarded because of scored and burred holes, which affect the stream geometry.

Premix (Fig. 7): Premixing the propellants before introduction into the chamber would seem to be a most logical and obvious answer to the ills accompanying other injection methods.

In a typical premix injector nozzle, the propellants are individually injected into a plenum chamber and are partially mixed. They then flow through a swirl chamber, in which mixing is completed and an angular momentum is imparted to the liquid in order to produce a conical spray. If a conical spray is not desired, premixing is simplified, and is often accomplished by having two concentric annular nozzles, with the liquids mixing just before entry into the chamber. The V-2 injectors were, in a sense, premix types, with the alcohol and oxygen mingling in a small "ante-chamber."

Since premixing is a liquid-liquid interaction of combustibles, the flame front can progress upstream to a point where the mixture is inadequate to maintain burning. This usually happens, and if the burning reaches a confined domain, an explosion occurs. There are two ways to prevent this: either by increasing the injection pressure until the fluid velocity is greater than the flame velocity (whatever that may be), or by increasing the ignition lag, so that the liquid can leave the nozzle before burning occurs. Neither alternative is desirable or easily accomplished.

Despite these drawbacks, the theoretical advantages of a premix injector are attractive enough to warrant further research, expecially for very large thrust chambers, using nonhypergolic fuels where "standard" injectors would be too heavy, cumbersome, and expensive.

To summarize, it may be said that no single injector type or system is ideal or applicable to all circumstances. However, inevitably, greater standardization will occur, when more data on the significance of the injector are available, and when many of the empiricisms have been reduced to scientific foundations.

Injector Research

It is difficult to assess the absolute importance of the injector head when considering the over-all rocket motor system.

An "ideal" injector should result in the following desirable thrust chamber characteristics: (*a*) A high specific impulse; (*b*) stable combustion over a wide range of chamber pressure; (*c*) smooth start-up; (*d*) a low rate of heat injection, within the working limits of existing coolant flows and materials; (*e*) an absence of streaky or localized combustion; (*f*) minimum throat erosion; (*g*) efficient operation through wide variations of ambient temperatures.

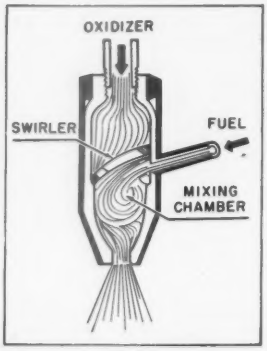

FIG. 7 PREMIX

This ideal head should also possess the following features: (*a*) Ease of manufacture and reproducibility; (*b*) a minimum of face erosion; (*c*) a low injection pressure; (*d*) adaptability to various propellant combinations: (*e*) a minimum of critical material; (*f*) insensitivity to vibrations of various types; (*g*) steady fluid jets.

Little quantitative data are available which directly relate the hydraulic injector constants with the above parameters. For this reason, experimental research is continuing and new methods of evaluation are constantly being tried.

In practice, each new injector head is first tested hydraulically, and, if satisfactory, is then checked in a carefully controlled firing test.

Hydraulic behavior, of course, is not necessarily a criterion of chamber behavior; however, hydraulic studies are at least a beginning and have shown that some correlation between test-stand performance is possible. The following are some of the injector head or orifice spray characteristics which seem to be important, and methods of their analysis.

Distribution of Propellants: A knowledge of the relative locations of oxidizer and fuel streams in the injector spray is often very useful. An oxidizer envelope may presage excessive chamber erosion or heat rejection. Discontinuities or streakiness may result in localized erosion or overheating of chamber or nozzle. A satisfactory qualitative analysis of this parameter has been evolved by the use of dye injection into the oxidizer or fuel water flow lines. Many dyes have been tried, but ultimately aniline "Wool Yellow"[3] and aniline "Niagara Sky Blue"[3] proved the best, for photographic and visual observation.[4] A further aid is a "strobolux" or other flashing stroboscopic light which slows down the spray velocity enough to permit detailed visual observation. A mechanical sampling method which has been a standby since the early days of spray studies, is the test-tube collector (Fig. 8). A large number of tubes are exposed to the spray and then checked for liquid level individually, to correlate with the geometrical location of the tube. This method is cumbersome and rather difficult to interpret for large flow rates.

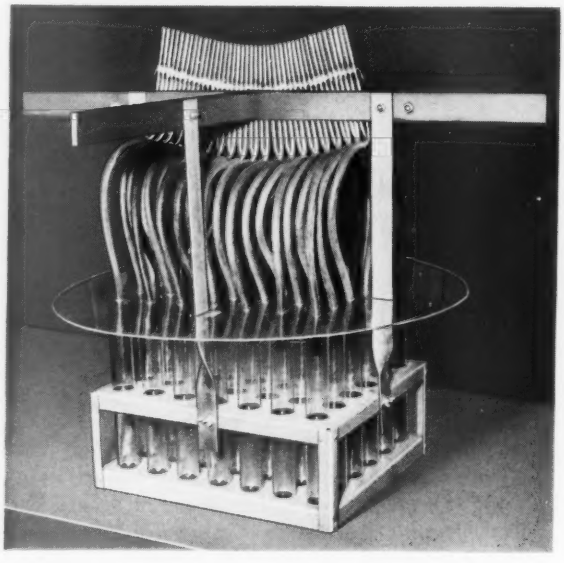

FIG. 8 TEST-TUBE SPRAY SAMPLER

[3] Made by National Aniline Div., Allied Chemical Corp., Buffalo, N. Y.

[4] Equivalent dyes, soluble in water, can be used.

Mixing of Propellants: Actual tests have shown that rapid and efficient mixing favorably influences combustion efficiency and stability. Good mixing depends upon a number of factors, such as the miscibility of the liquids, the velocity and area of impact (in impinging streams), the size and surface tension of the droplets (if the streams are atomized before collision) and convective recycling of the vaporized fluids in the hot thrust chamber. The last factor can only be surmised, considering existing data and equipment. The other factors and the actual mixing can be evaluated mechanically with sampling tubes, using water, carbon tetrachloride, or other mixtures, acid-base mixtures for pH measurements of the tube contents, or color analysis with a colorimeter. In the later case, a small sampling tube is traversed across the dyed water spray and a sample is taken by momentarily opening and closing a little cap valve at the mouth of the tube. The colored sample is then compared with a standard reference sample in a colorimeter. Thus a polar plot of mixture ratio across the spray pattern may be made. Attempts have been made to reduce surface tension and promote mixing by the addition of surface active agents. So far, results have been inconclusive.

Velocity: The stream velocity, as stated before, may have a bearing on the mixing rate; furthermore, it influences penetration into the chamber before burning, rate of ligament formation in the stream, atomization rate, and the direction of the resultant stream (after impingement). This latter factor is actually a result of the momenta of the two liquids. The velocity can be easily computed from standard hydraulic equations relating discharge coefficient, weight flow, orifice area, and injection pressure. Droplet velocity may also be measured by high-speed photography with calibrated grids or timing lights.

Atomization Rate and Droplet Size: If the propellant mixture is finely atomized, the total available surface area exposed to the combustion process increases thousands of times. Similarly, a rapid rate of atomization is desirable since it disperses the liquids into this desirable state with the least delay, and burning can proceed efficiently, making the most of the available chamber volume.

Since the surface area of a droplet decreases more slowly than its volume, with decreasing diameter, the available surface area-to-volume relationship of finely atomized droplet sprays is quite favorable. This factor expedites the rate of transformation from the liquid-to-gas-to-combustion state. On the other hand, the rate of vaporization is influenced at once by the high chamber pressure, and the convective and radiative heat transfer to the droplets. Experiments have indicated that a high chamber pressure tends to retard the rate of evaporation more than the high temperature accelerates it. Further research is required to substantiate this and to develop techniques of direct measurement of the liquid evaporation (3).

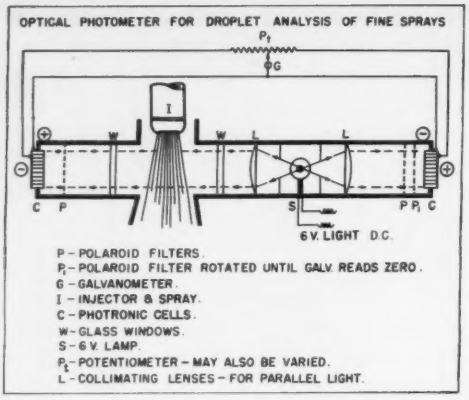

FIG. 9 SPRAY DROPLET PHOTOMETER DIAGRAM

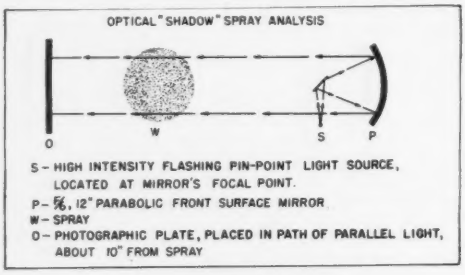
OPTICAL "SHADOW" SPRAY ANALYSIS
O
W
S
P
S - HIGH INTENSITY FLASHING PIN-POINT LIGHT SOURCE, LOCATED AT MIRROR'S FOCAL POINT.
P - 5/8, 12" PARABOLIC FRONT SURFACE MIRROR
W - SPRAY
O - PHOTOGRAPHIC PLATE, PLACED IN PATH OF PARALLEL LIGHT, ABOUT 10" FROM SPRAY

FIG. 10 OPTICAL SHADOW SYSTEM

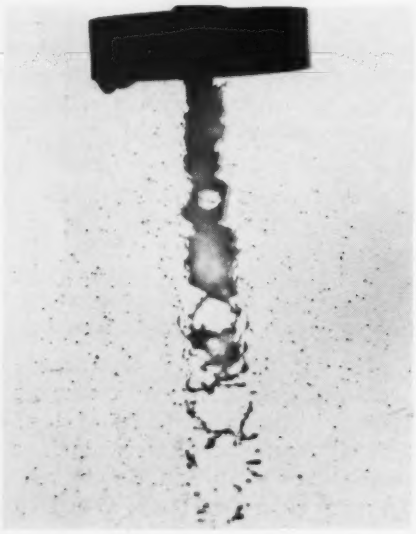

FIG. 11 SPRAY SHADOW PHOTOGRAPH

Much work has been done on the observation and measurement of spray droplet sizes and the factors affecting the rate of formation of drops from liquid streams, and the ultimate drop diameter. A favorite mechanical method of sampling the droplets has been by their impingement upon magnesium-oxide covered glass slides; the drops are assumed to leave an impact pattern analogous to their size (and distribution). The impact cavities, or the actual drops, with some types of slides, are then laboriously counted and measured with a calibrated microscope (4).

Another, indirect, method of measuring droplet sizes is an optical technique; a beam of light is passed through the spray and is received by a photo detector which measures the intensity of this transmitted beam, as compared to some reference beam. This is in effect a photometer (Fig. 9) which relates light transmission loss to droplet diameter and concentration (5).

The above methods are unsuitable for heavy, coarser rocket injector sprays; here photography is a useful method, especially high-speed photographs (5 microsec or less) which can "freeze" the spray pattern. If this is not too dense, the individual droplets can readily be counted and measured at random. A variation of normal photography is the "shadow" method (Fig. 10). Light from a pinhole source is paralleled by a concave mirror (or convex lens) and sent through the spray. A photographic plate may be placed at some distance beyond the spray and exposed by a high-speed flash light. The resultant image is full size and an exact silhouette of the droplet (Fig. 11).

No definite working relationships have been established for the prediction of spray droplet size and behavior in a thrust chamber (or even in the atmosphere). Considering the many existing propellants and variations in combustion conditions, such relationships may be impossible to establish rigorously. Factors, such as high injection and chamber pressure, low viscosity and surface tension, have been widely proved to favorably affect a rapid atomization and small droplet formation. A typical relationship established by Triebnigg (6) combines some of these factors (Fig. 12).

ULTIMATE DROPLET DIAMETER, d AND BREAKUP DISTANCE, N,

$$d = \left(\frac{g}{P_0 - P_1}\right)\left(\frac{S}{\varphi}\right)\left(\frac{\gamma_0^2}{\gamma_1}\right) \qquad N = \left(\frac{g}{P_0 - P_1}\right)\left(\frac{S}{\varphi}\right)\left(\frac{\gamma_0 d^2}{\gamma_1}\right)$$

WHERE P_0 = PROPELLANT INJECTION PRESSURE
P_1 = CHAMBER PRESSURE IN Kg/cm^2
γ_0 = SPEC. WEIGHT OF THE PROPELLANT GAS
γ_1 = SPEC. WEIGHT OF THE CHAMBER GAS
S = SURFACE TENSION OF PROPELLANT
φ = FRICTION COEFFICIENT BETWEEN PROPELLANT AND CHAMBER GAS

FIG. 12 EQUATION RELATING SPRAY FACTORS

The relation was determined for a diesel fuel injection system, but is typical of the conditions encountered in rocket practice.

It is difficult to measure the above quantities under actual working conditions; also the relative importance of atomization rate and droplet size in rocket combustion remains to be established.

Other Hydraulic Factors

Although the "normal" hydraulic behavior of the injector head is readily analyzed and plays a large part in rocket motor hydraulic research, other important fluid flow phenomena occur in the motor system and injector head which are not so easily evaluated. Some of these are:

Hydraulic "Flip" (Figs. 13 and 14): This condition of unstable orifice flow occurs in orifice holes with length/diameter ratios greater than those of knife-edged orifices, i.e., typical holes in an injector head.

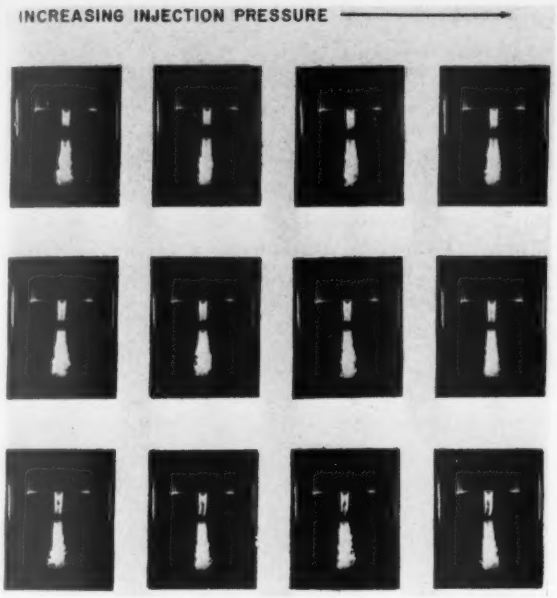

FIG. 13 PLEXIGLAS ORIFICE, HYDRAULIC "FLIP"

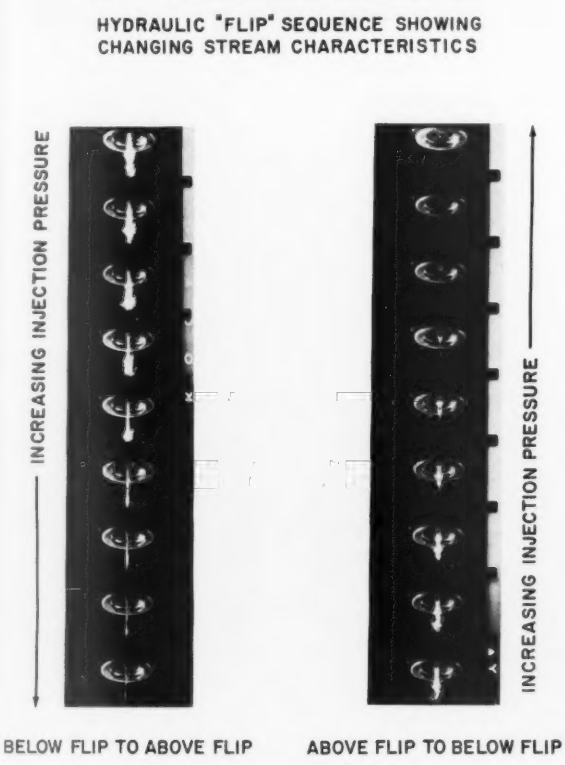

FIG. 14 HYDRAULIC "FLIP" SEQUENCE

At definite injection pressures, related to particular length/diameter (L/d) ratios, the water jet flowing through the orifice suddenly changes its characteristics as the injection pressure is increased slightly. Flow becomes quite turbulent and then smooth, with a rapid uncontrollable increase in pressure drop but no increase in the flow rate (Fig. 15).

This phenomenon has been adequately treated in a previous report (7); it suffices to say that the cause seems to be the breaking-away of the stream from the orifice walls except at the inlet edge, effectively establishing a knife-edged orifice. A reversible flip transition time of $^1/_{320}$ sec has been measured with water. If this transition time occurred with actual motors and if a reversible flip action took place continuously, a combustion frequency of approximately 320 cycles/second might be expected. Actually, frequencies near this value have been detected with injectors which had a hydraulic flip near the rated flow.

Impinging Jet Stability: It has been observed that impinging fluid jets tend to form a "Christmas tree" or "pagoda" pattern of fluid ligaments (Fig. 16). This formation seems to be caused by a combination of:

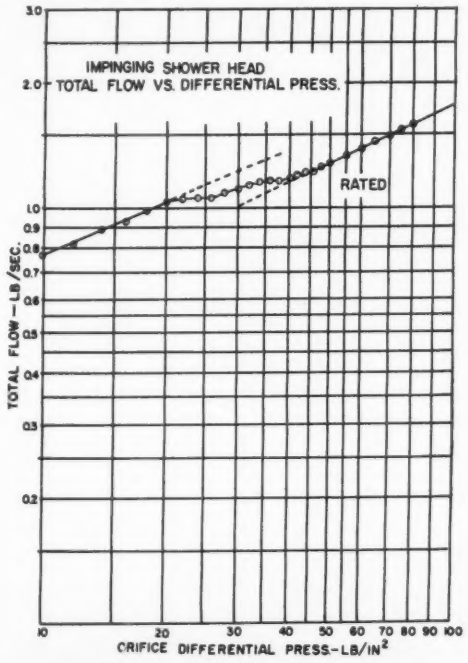

FIG. 15 HYDRAULIC WATER FLOW CHART

FIG. 16 SPRAY PAGODA STRUCTURE

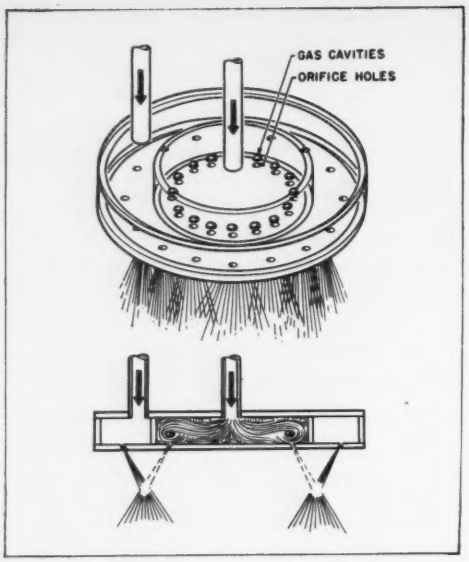

FIG. 17 GAS POCKETS IN INJECTOR MANIFOLDS

change in kinetic energy, surface tension, and air (or chamber gas) friction (8). This latter factor does not seem too important. Work done at Bell shows no change in frequency or number of these ligaments with low (vacuum) chamber pressure and 30-psig chamber pressures.

Some partial evidence exists relating 90 cycle pagoda frequencies (measured with a photoelectric counter) with combustion stability frequencies of 90–100 cycles.

Cavitation: Cavitation existing in pump-fed systems, and its effect is a common problem and need not be elaborated here. However, other instances of gas entrapment have been discovered in injector head manifolds. The gas pockets were detected by inserting a transparent back-plate in the manifold and observing the flow under stroboscopic illumination (Fig. 17).

It was assumed that these pockets could act as elastic cavities which would induce pulsations in the orifice jet and act as a source of burning instability. Attempts have been made to tap injector manifolds, and cooling jackets, in order to "bleed" off these trapped gas cavities and eliminate them as a possible source of burning instability. While some success has been obtained, it is apparent that further research is required in order to establish this form of cavitation as a definite source of instability. Also, further research may show other, hitherto unsuspected examples of gas pockets in the propellant feed system.

Acknowledgments

The author wishes to acknowledge the collaboration of Mr. F. Stratton in the photographic techniques, and the assistance of Mr. C. Kurland in the Hydraulics Laboratory, and invaluable contributions by various members of the Rocket Power Plant Division.

References

1 "Forced Action Mixing Nozzles for Rockets," by Eberhard J. Spohn, Report No. 68, Ordnance Guided Missile Center, Redstone Arsenal, Huntsville, Ala., June 1951.

2 "A Survey of Injector Designs for Use in Liquid Propellant Rocket Motors," by B. N. Abramson, ARS Reprint 1-49, 1949, p. 4.

3 "Theorie de Gemischaufbereitung in Stationären Feuerungen," by Eugen Sänger, *Brennstoff-Chemie*, vol. 32, no. 23–4, 1951, pp. 42–44.

4 "Experiments on the Distribution of Fuel in Fuel Sprays," by Dana W. Lee, *NACA, Report no.* 438, 1932, pp. 5–6.

5 "Application of the Photoelectric Photometer to the Study of Atomization," by J. M. Schmidt, Jet Propulsion Laboratory, California Institute of Technology, July 1946.

6 "Mechanism of Disintegration of Liquid Jets," by P. H. Schweitzer, The Pennsylvania State College, *Journal of Applied Physics*, vol. 8, August 1937, pp. 514–516.

7 "Flow Stability in Small Orifices," by R. P. Northup, General Electric Co., Project Hermes, ARS Reprint 49–51, 1951.

8 "Fluctuations in a Spray Formed by Two Impinging Jets," by Marcus F. Heidmann and Jack C. Humphrey, *NACA Technical Note* 2349, April 1951, Lewis Flight Propulsion Laboratory, Cleveland, Ohio.

Manuscripts Invited for Presentation at the Fall Meeting of the ARS

This meeting is to be held in Chicago, Illinois, September 9–10*, 1952, during the Centennial of Engineering (September 3–13), an event sponsored jointly by the principal engineering societies in the United States in commemoration of the founding of the first engineering society one hundred years ago.

Brief abstracts should be submitted as soon as possible to:

Dr. M. J. Zucrow
Program Chairman, ARS
c/o School of Mechanical Engineering
Purdue University
Lafayette, Indiana

Please refer to page 121, this issue of the JOURNAL, for acceptable scope of subject matter. Manuscripts are to be prepared in accordance with style instructions on inside back cover.

* *This date was erroneously given as Sept. 1–5 in the March–April issue of the Journal.*

The Transfer Functions of Rocket Nozzles

H. S. TSIEN[1]

Daniel and Florence Guggenheim Jet Propulsion Center,
California Institute of Technology, Pasadena, Calif.

The transfer function is defined as the fractional oscillating mass flow rate divided by the fractional sinusoidal pressure oscillation in the rocket combustion chamber. This is calculated as a function of the frequency of oscillation. For very small frequencies, the transfer function is approximately 1 with a small "lead component." For very large frequencies, the transfer function is considerably larger than 1, and is approximately 1 + $(\gamma M_1)^{-1}$ where γ is the ratio of specific heats of the gas, and M_1 is the Mach number at entrance to the nozzle.

RECENTLY, the problem of combustion instability of rocket motor has been studied by several authors (1, 2, and 3).[2] In these investigations, it is assumed that the percentage increase of the mass rate of flow through the nozzle is equal to the percentage increase of pressure in the rocket cylinder. It is, however, not certain whether this assumption is correct. Since this flow condition enters in a direct manner into the instability calculation, the relation between flow variations and the pressure variations should be determined more carefully. It is the purpose of this paper to do this. The result of the present study is expressed as the transfer function of the rocket nozzle, i.e., the ratio of the fractional increases in mass flow and the chamber pressure as function of the frequency of the oscillation. It indicates that the transfer function is rather a complex function of the nozzle geometry and the frequency of oscillation, and that the previous very simple assumption is only justified for very small frequencies of oscillation.

Flow Conditions

The flow in the nozzle will be considered as one-dimensional, i.e., at each nozzle section the conditions are taken to be uniform and the independent variables of the problem are then the time t and the distance x along the nozzle axis in the direction of flow (Fig. 1). Let p be the pressure, ρ the density, and u the velocity. The primed quantities are the oscillating quantities; thus ρ' is the density oscillation. Similarly, the unprimed quantities are the steady-state or undisturbed quantities. Therefore p'/p is the oscillating pressure at x expressed as fraction of the steady-state pressure at x. These fractional quantities are assumed to be small so that only first order terms need to be considered. Since the mass rate of flow per unit area is

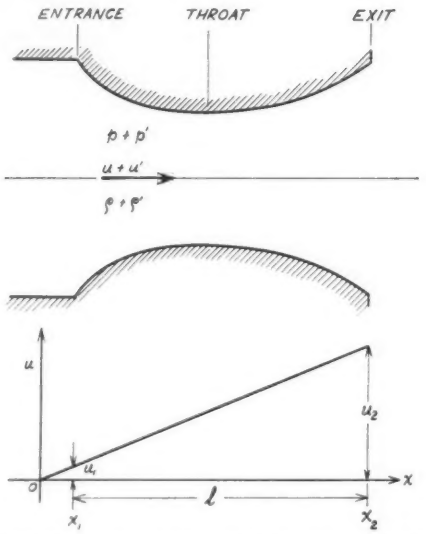

FIG. 1 ROCKET NOZZLE WITH LINEAR VELOCITY DISTRIBUTION

equal to the product of density and velocity, the fractional increment of the mass rate of flow is $\left(\frac{\rho'}{\rho} + \frac{u'}{u}\right)$. Hence the purpose of this paper can now be stated as simply to compute the ratio $\left(\frac{\rho'}{\rho} + \frac{u'}{u}\right) \Big/ \left(\frac{p'}{p}\right)$ at the entrance to the nozzle as a function of the oscillation frequency ω. This ratio will be called the transfer function of the rocket nozzle.

The conditions at the entrance to the nozzle are fixed by the plausible assumption that the temperature of the combustion gas is not changed by variations in pressure. Let the gas be considered as a perfect gas, and let the subscript 1 denote the entrance to the nozzle; then

$$\left(\frac{p'}{p}\right)_1 - \left(\frac{\rho'}{\rho}\right)_1 = 0 \quad \ldots\ldots\ldots\ldots\ldots\ldots [1]$$

Since the flow in the divergent part of the rocket nozzle is supersonic, the obvious additional condition for the complete determination of the flow is simply that the propagation of oscillations must be toward the downstream direction. For instance, if $U(x)$ is the velocity of the propagation of density oscillations at the section x, then for an observer who travels with the speed U, the density is stationary, i.e.,

$$\frac{\partial}{\partial t}\left(\frac{\rho'}{\rho}\right) + U\frac{\partial}{\partial x}\left(\frac{\rho'}{\rho}\right) = 0 \quad \ldots\ldots\ldots\ldots\ldots [2]$$

This is the equation for determining the velocity of

Received January 2, 1952.

[1] Robert H. Goddard Professor of Jet Propulsion.

[2] Numbers in parentheses refer to References on page 162.

propagation. The condition of downstream propagation means positive U. Thus, in the nozzle the signs of $\partial\left(\frac{\rho'}{\rho}\right)/\partial t$ and $\partial\left(\frac{\rho'}{\rho}\right)/\partial x$ must be opposite. Similarly, the signs of $\partial\left(\frac{u'}{u}\right)/\partial t$ and $\partial\left(\frac{u'}{u}\right)/\partial x$ must also be opposite in the nozzle.

Formulation of the Problem in Nozzle

In the nozzle, if A is the cross section of the nozzle at x, then the continuity equation is

$$A\frac{\partial\rho'}{\partial t} + \frac{\partial}{\partial x}[A(\rho+\rho')(u+u')] = 0 \quad \ldots\ldots [3]$$

The steady-state flow or the undisturbed flow satisfies, however, the simpler continuity equation

$$A\rho u = \text{const}$$

By eliminating A from Equation [3] by this equation, and by retaining only the first-order terms of the oscillating quantities, one obtains the linearized continuity equation as

$$\frac{\partial}{\partial t}\left(\frac{\rho'}{\rho}\right) + u\frac{\partial}{\partial x}\left(\frac{\rho'}{\rho}+\frac{u'}{u}\right) = 0 \quad \ldots\ldots [4]$$

Similarly, the dynamic equation is

$$\frac{\partial}{\partial t}\left(\frac{u'}{u}\right) + \left(\frac{p'}{\rho}+2\frac{u'}{u}\right)\frac{du}{dx} + u\frac{\partial}{\partial x}\left(\frac{u'}{u}\right) = \left(\frac{p'}{p}\right)\frac{du}{dx} - \frac{p}{\rho u}\frac{\partial}{\partial x}\left(\frac{p'}{p}\right) \quad \ldots\ldots [5]$$

For any fluid mass, the entropy is maintained. Therefore, if γ is the ratio of specific heats of the gas,

$$\left(\frac{\partial}{\partial t}+u\frac{\partial}{\partial x}\right)\left[\left(\frac{p'}{p}\right)-\gamma\left(\frac{\rho'}{\rho}\right)\right] = 0 \quad \ldots\ldots [6]$$

Equations [4], [5], and [6] are three equations for the three dependent variables (ρ'/ρ), (p'/p), and (u'/u).

It is convenient in the following calculations to introduce a specific nozzle shape such that the steady velocity in the nozzle increase simply linearly with x (Fig. 1). The simplest way to specify this is

$$u = \frac{u_1}{x_1}x \quad \ldots\ldots [7]$$

where the subscript 1 denotes again quantities at the entrance to the nozzle. x_1 is thus the x-coordinate at the entrance to the nozzle. Therefore, the origin of the x-axis is not generally at the entrance to the nozzle; it is there only if the steady velocity at entrance is equal to zero. With Equation [7], Equation [6] becomes

$$\left(\frac{\partial}{\partial t}+\frac{u_1}{x_1}\frac{\partial}{\partial \log x}\right)\left[\left(\frac{p'}{p}\right)-\gamma\left(\frac{\rho'}{\rho}\right)\right] = 0 \quad \ldots\ldots [8]$$

Therefore, if the entropy oscillations at the entrance to the nozzle is $\epsilon e^{i\omega t}$, i.e.,

$$\left(\frac{p'}{p}\right)_1 - \gamma\left(\frac{\rho'}{\rho}\right)_1 = \epsilon e^{i\omega t} \quad \ldots\ldots [9]$$

then, according to Equation [8] in general

$$\left(\frac{p'}{p}\right) - \gamma\left(\frac{\rho'}{\rho}\right) = \epsilon\exp\left[i\omega\left(t-\frac{x_1}{u_1}\log\frac{x}{x_1}\right)\right] \quad \ldots\ldots [10]$$

By eliminating (p'/p) between Equations [5] and [10], the resultant equation together with Equation [4] constitute a system of two equations for the two unknowns (ρ'/ρ) and (u'/u).

Now let x_2 be the x-coordinate at the exit of the nozzle, or if l is the length of the nozzle,

$$x_2 = x_1 + l \quad \ldots\ldots [11]$$

Define a nondimensional independent variable ξ as

$$\xi = x/x_2 \quad \ldots\ldots [12]$$

Then

$$\xi_1 = x_1/x_2 = x_1/(x_1+l) = 1/\left(1+\frac{l}{x_1}\right) \quad \ldots\ldots [13]$$

The oscillating quantities with frequency ω can now be written as

$$\left(\frac{\rho'}{\rho}\right) = f(\xi)e^{i\omega t} \quad \ldots\ldots [14]$$

$$\left(\frac{u'}{u}\right) = g(\xi)e^{i\omega t} \quad \ldots\ldots [15]$$

By introducing these expressions into the differential equations for ρ'/ρ and u'/u, equations for f and g are derived. The results can be, however, written more compactly if one uses the reduced frequency β, defined as

$$\beta = \frac{\omega x_1}{u_1} = \frac{\omega x_2}{u_2} = \frac{\omega l}{u_2}\frac{1}{1-\xi_1} \quad \ldots\ldots [16]$$

where u_2 is the exit velocity of the nozzle. β is then the ratio of the angular frequency ω and the velocity gradient u_1/x_1 along the nozzle axis. Then from Equations [4], [5], and [10] the equations for the f and g are obtained as

$$\xi\left[\frac{df}{d\xi}+\frac{dg}{d\xi}\right] + i\beta f = 0 \quad \ldots\ldots [17]$$

and

$$(2+i\beta)g + (1-i\beta)f - \xi\frac{df}{d\xi} = \gamma f - \frac{1}{M^2}\xi\frac{df}{d\xi} + \epsilon\left(\frac{\xi}{\xi^1}\right)^{i\beta}\left[1+\frac{i\beta}{\gamma M^2}\right] \quad \ldots\ldots [18]$$

where M is the local Mach number of the undisturbed flow at x or ξ. In fact, for the assumed linear velocity distribution in the nozzle,

$$M^2 = \frac{M_1^2\xi^2}{\xi_1^2 - \frac{\gamma-1}{2}M_1^2(\xi^2-\xi_1^2)} = \frac{M_1^2\left(\frac{x}{x_1}\right)^2}{1-\frac{\gamma-1}{2}M_1^2\left(\frac{x^2}{x_1^2}-1\right)} \quad \ldots\ldots [19]$$

M_1 is the Mach number at the entrance to the nozzle.

By eliminating $g(\xi)$ from Equations [17] and [18], a single second-order equation for $f(\xi)$ is obtained. The result can, however, be reduced to more convenient form by using a new independent variable z defined as

$$z = \frac{\frac{\gamma+1}{2}M_1^2(\xi/\xi_1)^2}{1+\frac{\gamma-1}{2}M_1^2} \quad \ldots\ldots [20]$$

It is easy to show that z is actually the square of the ratio of u to the so-called critical sound speed. Thus $z = 1$ at the throat of the nozzle. In terms of z, the differential equation for f is

$$z(1-z)\frac{d^2f}{dz^2} - \left\{2 + \frac{2i\beta}{(\gamma+1)}\right\} z\frac{df}{dz} - \frac{i\beta(2+i\beta)}{2(\gamma+1)} f =$$

$$-i\beta\,\epsilon\left(\frac{z}{z_1}\right)^{-i(\beta/2)}\left[\frac{1-i\beta\dfrac{\gamma-1}{2\gamma}}{2(\gamma+1)} + \frac{2+i\beta}{4\gamma}\frac{1}{z}\right] \quad \ldots\ldots [21]$$

The relation between $f(z)$ and $g(z)$ is

$$(2+i\beta)g(z) = [(\gamma-1)+i\beta]f(z) - (\gamma+1)(1-z)\frac{df}{dz} +$$

$$\epsilon\left(\frac{z}{z_1}\right)^{-i(\beta/2)}\left[1 - \frac{i\beta(\gamma-1)}{2\gamma} + \frac{i\beta(\gamma+1)}{2\gamma}\frac{1}{z}\right] \quad \ldots\ldots [22]$$

z_1 is, of course, the value of z corresponding to ξ_1 as given by Equation [13]; i.e.,

$$z_1 = \frac{\dfrac{\gamma+1}{2}M_1^2}{1 + \dfrac{\gamma-1}{2}M_1^2} \quad \ldots\ldots [23]$$

The initial condition needed to solve Equation [21] is specified by Equations [1] and [9]. That is, at $z = x_1$ or $z = z_1$,

$$f(z_1) = -\frac{\epsilon}{\gamma-1} \quad \ldots\ldots [24]$$

The complete solution requires the cognizance of the fact that the propagation of oscillations must be toward the downstream direction as discussed in the previous section.

When $f(z)$ is determined, one can compute $g(z)$ by Equation [22]. Then the density oscillations and the velocity oscillations are determined as functions proportional to the amplitude of entropy oscillation ϵ. Since the point of interest is the ratio of the oscillations, the arbitrary ϵ does not really enter into the final result. In fact, according to Equation [1], the ratio of the fractional increase in mass rate of flow and that of pressure, or the transfer function $G(\beta)$ is

$$G(\beta) = \left[\left(\frac{\rho'}{\rho}\right)_1 + \left(\frac{u'}{u}\right)_1\right] \Big/ \left(\frac{p'}{p}\right)_1 =$$

$$\left[\left(\frac{\rho'}{\rho}\right)_1 + \left(\frac{u'}{u}\right)_1\right]\left(\frac{\rho'}{\rho}\right)_1 = 1 + \frac{g(z_1)}{f(z_1)} \quad \ldots\ldots [25]$$

Therefore $G(\beta)$ is unity as assumed by previous investigators of combustion instability only if there is no velocity oscillation at the entrance, or $(u'/u)_1 = 0$. It is perhaps worthwhile to point out the fact that the present definition of transfer function $G(\beta)$ corresponds to the practice of servomechanism analysis, if the pressure oscillation $(p'/p)_1$ is taken as the "input" and the mass flow oscillation as the "output." Hence the transfer function $G(\beta)$ will be useful also in the synthesis of the systems for servocontrol or servostabilization of the rocket motor, as suggested by W. Bollay (4).

Solution for Small Frequency

The basic differential equation with linear velocity distribution in the nozzle as given by Equation [21] can be reduced to the hypergeometric differential equation by the substitution $f(z) = z \cdot w(z)$. $w(z)$ is then the hypergeometric function. However, the calculation is rather difficult. For a first discussion, only cases of either very small frequency or very large frequency will be considered here.

If the frequency β is very small, the functions $f(z)$ and $g(z)$ can be expanded in terms of this parameter

$$f(z;\ \beta) = f^{(0)}(z) + \beta f^{(1)}(z) + \ldots \quad \ldots\ldots [26]$$

$$g(z;\ \beta) = g^{(0)}(z) + \beta g^{(1)}(z) + \ldots \quad \ldots\ldots [27]$$

These expressions are appropriate if the interval of z concerned does not include $z = 0$. Fortunately, the physical problem generally specifies nonvanishing u at the entrance to the nozzle. Therefore, $\xi_1 \neq 0$ and thus $z_1 \neq 0$. The restriction on the validity of the expansions is thus generally complied. By substituting Equations [26] and [27] into the basic Equations [21] and [22], and then equating terms of same powers in β, one has

$$z(1-z)\frac{d^2f^{(0)}}{dz^2} - 2z\frac{df^{(0)}}{dz} = 0 \quad \ldots\ldots [28]$$

and

$$z(1-z)\frac{d^2f^{(1)}}{dz^2} - 2z\frac{df^{(1)}}{dz} = i\left\{\frac{2}{\gamma+1}z\frac{df^{(0)}}{dz} + \frac{1}{\gamma+1}f^{(0)} - \frac{\epsilon}{2}\left(\frac{1}{\gamma+1} + \frac{1}{\gamma z}\right)\right\} \quad \ldots\ldots [29]$$

Furthermore

$$2g^{(0)}(z) = (\gamma-1)f^{(0)}(z) - (\gamma+1)(1-z)\frac{df^{(0)}}{dz} + \epsilon \quad \ldots [30]$$

$$2g^{(1)}(z) = (\gamma-1)f^{(1)}(z) - (\gamma+1)(1-z)\frac{df^{(1)}}{dz} + i[f^{(0)}(z) - g^{(0)}(z)] - \frac{i\epsilon}{2}\left[\log\left(\frac{z}{z_1}\right) + \frac{\gamma-1}{\gamma} - \frac{\gamma+1}{\gamma z}\right] \quad \ldots\ldots [31]$$

The initial condition of Equation [24] now becomes

$$f^{(0)}(z_1) = -\frac{\epsilon}{\gamma-1} \quad \ldots\ldots [32]$$

$$f^{(1)}(z_1) = 0 \quad \ldots\ldots [33]$$

A straightforward calculation will give the following relation for the propagation velocity U for the density fluctuation defined by Equation [2],

$$\frac{U}{u} = -\frac{i\beta f(z)}{2z\dfrac{df}{dz}} = -\frac{1}{2z}\frac{i\beta[f^{(0)}(z) + \beta f^{(1)}(z) \ldots\ldots]}{\dfrac{df^{(0)}}{dz} + \beta\dfrac{df^{(1)}}{dz} + \ldots\ldots} \quad \ldots [34]$$

where u is, of course, the undisturbed flow velocity at the section concerned. Therefore, in order that the propagation speed be finite even for small β, $f^{(0)}(z)$ must be a constant. Hence the appropriate solution of Equation [28] together with the condition of Equation [32] is

$$f^{(0)}(z) = -\frac{\epsilon}{\gamma-1} \quad \ldots\ldots [35]$$

Then Equation [30] gives immediately

$$g^{(0)}(z) = 0 \quad \ldots\ldots [36]$$

Up to this order of approximation then, $G = 1$, as shown by Equation [25]. Therefore the assumption of the previous investigators of the combustion in-

stability of rocket motor is indeed correct if the frequency is vanishingly small.

With $f^{(0)}(z)$ given by Equation [35], the equation for $f^{(1)}(z)$, Equation [29], can be written as

$$\frac{d}{dz}\left[(1-z)^2\frac{df^{(1)}}{dz}\right] = -\frac{i\epsilon}{2}\left[\frac{1}{\gamma-1}+\frac{1}{\gamma z}\right]\frac{1-z}{z}$$

Therefore the solution is

$$\frac{df^{(1)}}{dz} = -\frac{i\epsilon}{2}\left[\frac{1}{\gamma(\gamma-1)}\frac{\log z}{(1-z)^2}+\frac{1}{(\gamma-1)}\frac{1}{(1-z)}-\frac{1}{\gamma}\frac{1}{z(1-z)}\right]+\frac{C}{(1-z)^2}$$

The quantity inside the square bracket is finite and positive for $z > 0$, while the last term is infinite at the throat of the nozzle where $z = 1$. Hence, according to Equation [34], the condition for *finite* positive propagation speed U requires $C = 0$. Therefore[3]

$$\frac{df^{(1)}}{dz} = \frac{i\epsilon}{2}\left[-\frac{1}{\gamma(\gamma-1)}\frac{\log z}{(1-z)^2}-\frac{1}{(\gamma-1)}\frac{1}{(1-z)}+\frac{1}{\gamma}\frac{1}{z(1-z)}\right] \quad [37]$$

This equation together with Equations [31] and [33] then gives

$$g^{(1)}(z_1) = \frac{i\epsilon}{4\gamma}\left\{\frac{\gamma+1}{\gamma-1}\frac{\log z_1}{1-z_1}+1\right\} \quad [38]$$

Therefore, up to the first order in β, the transfer function $G(\beta)$ is

$$G(\beta) \cong 1+\frac{\beta g^{(1)}(z_1)}{f(z_1)} = 1+i\beta\left\{\frac{\gamma+1}{4\gamma}\frac{\log\left(\frac{1}{z_1}\right)}{1-z_1}-\frac{\gamma-1}{4\gamma}\right\}, \qquad \beta \ll 1 \quad [39]$$

Therefore, when the frequency β is not exactly zero, the transfer function has a small "lead component," proportional to the frequency.

Solution for Large Frequencies

If the value of β is very large, one must find the asymptotic solution of Equation [21]. The dominating terms in Equation [21] are

$$z(1-z)\frac{d^2f}{dz^2}-\frac{2i\beta}{\gamma+1}z\frac{df}{dz}+\frac{\beta^2}{2(\gamma+1)}f = \beta^2\epsilon\left(\frac{z}{z_1}\right)^{-(i\beta/2)}\frac{1}{4\gamma}\left[\frac{1}{z}-\frac{\gamma-1}{\gamma+1}\right] \quad [40]$$

For the particular integral f^*, take

$$f^*(z) = Z(z)\left(\frac{z}{z_1}\right)^{-(i\beta/2)}$$

where $Z(z)$ is a function of z not involving β. Therefore, by retaining only the highest order term,

$$\frac{df^*}{dz} \cong -\frac{i\beta}{2}\frac{Z(z)}{z}\left(\frac{z}{z_1}\right)^{-(i\beta/2)}$$

$$\frac{d^2f^*}{dz^2} \cong -\frac{\beta^2}{4}\frac{Z(z)}{z^2}\left(\frac{z}{z_1}\right)^{-(i\beta/2)}$$

By substituting these derivatives into Equation [40], it is found that

$$Z(z) = -\frac{\epsilon}{\gamma}$$

thus

$$f^*(z) = -\frac{\epsilon}{\gamma}\left(\frac{z}{z_1}\right)^{-(i\beta/2)} \quad [41]$$

To find the complementary function, let

$$f(z) = e^{i\beta\lambda(z)}$$

then

$$\frac{df}{dz} = i\beta e^{i\beta\lambda(z)}\frac{d\lambda}{dz}$$

$$\frac{d^2f}{dz^2} \cong -\beta^2 e^{i\beta\lambda(z)}\left(\frac{d\lambda}{dz}\right)^2$$

By substituting these into the homogeneous equation corresponding to Equation [40], one has

$$\frac{d\lambda_{1,2}}{dz} = \frac{1}{(\gamma+1)(1-z)}\left[1\pm\sqrt{1+\frac{\gamma+1}{2}\frac{1-z}{z}}\right]$$

Thus

$$\lambda_1(z) = \frac{1}{\gamma+1}\int_{z_1}\frac{dz}{1-z}\left[1+\sqrt{1+\frac{\gamma+1}{2}\frac{1-z}{z}}\right], \quad \lambda_1(z_1)=0$$

and

$$\lambda_2(z) = \frac{1}{\gamma+1}\int_{z_1}\frac{dz}{1-z}\left[1-\sqrt{1+\frac{\gamma+1}{2}\frac{1-z}{z}}\right], \quad \lambda_2(z_1)=0 \quad [42]$$

The complete solution for large β is thus

$$f(z)e^{i\omega t} = -\frac{\epsilon}{\gamma}e^{i\beta\left[\frac{u_2}{x_2}t-\frac{1}{2}\log\left(\frac{z}{z_1}\right)\right]}+Be^{i\beta\left[\frac{u_2}{x_2}t+\lambda_1(z)\right]}+De^{i\beta\left[\frac{u_2}{x_2}t+\lambda_2(z)\right]} \quad [43]$$

The first term is the particular integral; it satisfies the condition of downstream propagation of disturbances. The same condition requires, however, that $\lambda(z)$ be negative and increasingly negative as z increases from z_1. $\lambda_1(z)$ does not satisfy this condition and hence has to be rejected. Therefore, $B = 0$. D is fixed by the initial condition of Equation [24], and is $-\epsilon/\gamma(\gamma-1)$. Therefore, finally

$$f(z) = -\frac{\epsilon}{\gamma}\left[\left(\frac{z}{z_1}\right)^{-(i\beta/2)}+\frac{1}{\gamma-1}e^{i\beta\lambda_2(z)}\right] \quad [44]$$

where $\lambda_2(z)$ is given Equation [42].

By taking the dominating terms of Equation [22] for large β, one has

$$g(z) = f(z)-(\gamma+1)(1-z)\frac{1}{i\beta}\frac{df}{dz}+\epsilon\left(\frac{z}{z_1}\right)^{-(i\beta/2)}\left[\frac{\gamma+1}{2\gamma}\frac{1}{z}-\frac{\gamma-1}{2\gamma}\right]$$

with $f(z)$ as given Equation [44], then $g(z)$ is determined as

$$g(z) = -\frac{\epsilon}{\gamma(\gamma-1)}\sqrt{1+\frac{\gamma+1}{2}\frac{1-z}{z}}\,e^{i\beta\lambda_2(z)}, \qquad \beta \gg 1 \quad [45]$$

[3] Professor L. Crocco has very kindly pointed out that the condition for positive finite propagation speed U is equivalent to the suppression of all singularities at the sonic point. This observation may simplify the analysis for general values of β.

Therefore, the transfer function $G(\beta)$ for large β is

$$G(\beta) = 1 + \frac{1}{\gamma}\sqrt{1 + \frac{\gamma + 1}{2}\frac{1 - z_1}{z_1}}, \quad \beta \gg 1$$

But z_1 is specified by Equation [23], therefore

$$G(\beta) = 1 + \frac{1}{\gamma M_1}, \qquad \beta \gg 1 \ldots\ldots\ldots\ldots [46]$$

Therefore, for large frequencies the transfer function is again real and positive, i.e., the mass flow oscillations and the pressure oscillations at the entrance to the nozzle are again in phase. However, the mass flow oscillations are considerably larger than the pressure oscillations; the ratio is given by Equation [46].

Concluding Remarks

In the previous section the calculation of the transfer function of the rocket nozzle is considered as a problem in nonsteady one-dimensional flow. For very small frequencies of oscillations, the transfer function is indeed approximately equal to unity, as assumed by previous investigators of combustion instability. However, the present calculation also shows that the transfer function is a complex number and has a lead component increasing with increase in frequency. For very large frequencies, the analyses give results indicating larger mass flow oscillations than supposed before. But the transfer function for infinite frequency β is again a positive real number. Therefore, the Nyquist diagram of the transfer function $G(\beta)$ is a curve, not a line. As an example, for $\gamma = 1.22$, and $M_1 = 0.2$, according to Equations [39] and [46]

$$\begin{aligned} G(\beta) &\cong 1 + 1.438i\beta, && \text{for } \beta \ll 1 \\ &\cong 5.1, && \text{for } \beta \gg 1 \end{aligned}$$

The accuracy of the present results is limited by the underlying assumptions. First of all, the nozzle shape is such as to give a linear velocity distribution in the nozzle. Then the gas is assumed to be perfect and nonreacting. In reality, viscosity, heat conduction, and residual chemical reactions in the exhaust gas will modify the result. At large frequencies or for very short nozzles, the wave length may be small in comparison with the nozzle length, then the one-dimensional flow assumption may introduce appreciable error. For these reasons, it is desirable to measure the transfer function of the rocket nozzle experimentally. Here, however, one must remember that the flow phenomenon in connection with the combustion stability is profoundly influenced by the entropy oscillations generated in the combustion processes. Direct stability measurements on rocket motor with artificially oscillated propellant flow will be necessary. The present analysis indicates, however, that the nozzle could be cut short with practically no divergent part as the transfer function is not influenced by the particular exit velocity so long as the exit velocity is supersonic. The propellant flow rate will then be smaller than a full-

(*Continued on page 162*)

ARS Preprints

PRICE PER COPY:

25 cents to members

50 cents to nonmembers

Code No.	*Title and Author*
35–51	"The United States Air Force Experimental Rocket Engine Test Station, Edwards, California," by R. A. Schmidt and D. L. Dynes
36–51	"Combustion Studies with a Rocket Motor Having a Full Length Observation Window," by K. Berman and S. E. Logan
37–51	"Some Experimental Dynamic Launching Techniques for Testing Aircraft Rockets," by A. W. Nelson
38–51	"Fluctuations in a Spray Formed by Two Impinging Jets," by M. F. Heidmann and J. C. Humphrey
39–51	"Attitude Stabilization for Supersonic Vehicles," by C. W. Besserer and A. J. Bell
40–51	"Isothermal Combustion Under Flow Conditions," by J. A. Bierlein and K. Scheller
41–51	"The Principle of the Concentric Nozzle," by W. F. Kaufman and B. N. Abramson
42–51	"Porous, Sweat and Film Cooling with Reactable Coolants," by Luigi Crocco
43–51	"Unusual Applications of the Momentum Principle," by T. F. Reinhardt
44–51	"Installation of Rocket Engines in Airplanes," by F. A. Coss
45–51	"Description of the NOTS Aeroballistics Laboratory," by E. I. Highberg
46–51	"High Flux Heat Transfer and Coke Deposition of JP-3," by J. B. Hatcher and D. R. Dartz
47–51	"Photographic Techniques Applied to Combustion Studies—Two Dimensional Transparent Thrust Chamber," by J. H. Altseimer and T. Thackrey
48–51	"Experimental Problems in High Pressure Combustion," by R. L. Wehrli
49–51	"Flow Stability in Small Orifices," by R. P. Northup
51–52	"Range Formulas for Rocket-Powered Aircraft with Comparison to Range of Airbreathing Aircraft," by Ralph W. Allen
52–52	"Large-Scale Production and Handling of Liquid Hydrogen," by H. L. Coplen
53–52	"The Role of Research in Rocket Development," by Paul F. Winternitz

American Rocket Society

29 W. 39th Street, New York 18, N. Y.

Please send me the preprints checked below:

☐ 35–51 ☐ 36–51 ☐ 37–51 ☐ 38–51 ☐ 39–51 ☐ 40–51 ☐ 41–51 ☐ 42–51 ☐ 43–51 ☐ 44–51 ☐ 45–51 ☐ 46–51 ☐ 47–51 ☐ 48–51 ☐ 49–51 ☐ 51–52 ☐ 52–52 ☐ 53–52

My (check) (M.O.) for $.....is attached.

Signed.....

Address.....

.....

A Similarity Law for Stressing Rapidly Heated Thin-Walled Cylinders[1]

H. S. TSIEN[2] and C. M. CHENG[3]

Daniel and Florence Guggenheim Jet Propulsion Center,
California Institute of Technology, Pasadena, Calif.

When a thin cylindrical shell of uniform thickness is very rapidly heated by hot high-pressure gas flowing inside the shell, the temperature of material decreases steeply from a high temperature at the inside surface to ambient temperatures at the outside surface. Young's modulus of material thus varies. The purpose of the present paper is to reduce the problem of stress analysis of such a cylinder to an equivalent problem in conventional cylindrical shell without temperature gradient in the wall. The equivalence concept is expressed as a series of relations between the quantities for the hot cylinder and the quantities for the cold cylinder. These relations give the similarity law whereby strains for the hot cylinder can be simply deduced from measured strains on the cold cylinder and thus greatly simplify the problem of experimental stress analysis.

THE cylinder of a solid propellant rocket is subjected to very rapid heating during its short duration of operation. The temperature distribution across the thin cylindrical wall, although approximately the same in every section, is not linear. This condition is most severe at the end of the combustion of the propellant grain. From the point of view of a materials engineer, this case is distinguished from others by the time rate of heating, which is so large as to not allow sufficient time for appreciable change in the structure of the material. The strength of the wall material under this operating condition is quite different from that under slow heating. This fact is clearly and conclusively shown by R. L. Noland in a recent paper (1).[4] From the point of view of a stress analyst, the rational design of a solid propellant rocket cylinder is thus complicated by the very large thermal stress and variable Young's modulus of the material across the wall as a result of the large temperature gradient. Furthermore, experimental stress determination under actual firing tests is rather difficult due to the short test time available and the high temperature.

It is believed that for these reasons the only case which has been analyzed by reliable rational method is the case of rocket cylinder under uniform internal pressure. The bending stresses due to canted nozzles, the stresses due to end enclosures, mounting lugs, etc., are only estimated by very rough methods. The purpose of this paper is to improve this situation by suggesting an approach which will reduce the general stress problem of hot cylinder to a problem of an equivalent cold cylinder. The equivalent problem can then be solved either analytically by the conventional method or directly by experimental stress determination. In either choice, the problem is believed to be greatly simplified. This law of equivalence between hot cylinder and cold cylinder can be called the similarity law.

Stresses and Strains of a Thin-Walled Cylinder

The fact that the thickness of the cylinder is small in comparison to its radius and length allows a great simplification in the strain analysis. To wit, the deformation of every point of the cylinder can be described sufficiently accurately by the displacements of the points on a single surface within the wall of the cylinder. This surface is the so-called median surface. The position of the median surface is so determined that a bending of the median surface will not induce net extensional forces in the plane of the median surface, across the thickness of the wall. When Young's modulus is a constant, as is the case for a cold cylinder, the median surface lies midway between the outer and the inner boundary surfaces of the cylinder. When Young's modulus is not a constant but decreases with increase in temperature, the median surface is displaced toward the cold side, as will be seen presently.

Let x, θ, z be the coordinate system with origin on the cylindrical median surface such that x points in the axial direction of the cylinder, θ is in the circumferential direction, measured on the median surface, and z is normal to the median surface, pointing toward the axis of the cylinder. Let U, V, and W be displacements of a point (x, θ) on the median surface in the directions x, θ, and z, respectively. They are thus functions of x and θ; but not of z. Then the above-mentioned fundamental simplification of thin shells can be stated as follows: If the direct strains in the x and θ directions are e_x and e_θ, and the shear strain $\gamma_{x\theta}$, then

$$\left.\begin{aligned} e_x &= \frac{\partial U}{\partial x} - z\frac{\partial^2 W}{\partial x^2} \\ e_\theta &= \frac{1}{R}\frac{\partial V}{\partial \theta} - \frac{W}{R} - \frac{z}{R^2}\left(\frac{\partial V}{\partial \theta} + \frac{\partial^2 W}{\partial \theta^2}\right) \\ \gamma_{x\theta} &= \frac{\partial V}{\partial x} + \frac{1}{R}\frac{\partial U}{\partial \theta} - 2\frac{z}{R}\left(\frac{\partial^2 W}{\partial x \partial \theta} + \frac{\partial V}{\partial x}\right) \end{aligned}\right\} \quad \ldots [1]$$

Received February 14, 1952.

[1] This paper is based on part of a thesis submitted by the junior author for partial fulfillment of the requirements of Ph.D. in Mechanical Engineering, California Institute of Technology.

[2] Robert H. Goddard Professor of Jet Propulsion.

[3] Graduate Assistant in Mechanical Engineering.

[4] Numbers in parentheses refer to Bibliography on page 162.

where R is the radius of the median cylindrical surface, or the "radius of the cylinder." This result is sometimes described as the Kirchhoff bending assumption: Plane normal to the median surface before bending remains so after bending.

The significant stresses in a thin shell are the direct stresses σ_x and σ_θ in x and θ, and the shear stress $\tau_{x\theta}$. All other stresses are small in comparison to these three. Now let T be the temperature of wall above a reference temperature, say the room temperature. T is assumed to be only a function of thickness ordinate z, but not of x and θ. Thus the heating of the cylinder is assumed to be uniform over the entire surface of the cylinder. This is generally very closely approximated in reality. If α is the coefficient of thermal expansion, the thermal expansion strain is then αT. By Hooke's law one has

$$\left.\begin{aligned} e_x &= \frac{1}{E}(\sigma_x - \nu\sigma_\theta) + \alpha T \\ e_\theta &= \frac{1}{E}(\sigma_\theta - \nu\sigma_x) + \alpha T \\ \gamma_{x\theta} &= \frac{2(1+\nu)}{E}\tau_{x\theta} \end{aligned}\right\} \quad \ldots\ldots\ldots\ldots [2]$$

where E is Young's modulus, and ν is Poisson's ratio. E is, of course, a function of temperature or a function of z. ν, however, will be assumed to be constant for lack of definite information. By solving for the stresses, one obtains from Equation [2],

$$\left.\begin{aligned} \sigma_x &= \frac{E(z)}{1-\nu^2}\{(e_x + \nu e_\theta) - (1+\nu)\alpha T(z)\} \\ \sigma_\theta &= \frac{E(z)}{1-\nu^2}\{(e_\theta + \nu e_x) - (1+\nu)\alpha T(z)\} \\ \tau_{x\theta} &= \frac{E(z)}{2(1+\nu)}\gamma_{x\theta} \end{aligned}\right\} \quad \ldots\ldots [3]$$

For thin-walled cylinders, the equilibrium equations are expressed in terms of "sectional averages" of the stresses given in Equation [3]. That is, one speaks of the normal forces N_x and N_θ, the shearing force $N_{x\theta}$, the bending moments M_x, M_θ, and the twisting moment $M_{x\theta}$. They are related to σ_x, σ_θ, and $\tau_{x\theta}$ by the following equations

$$N_x = \int \sigma_x dz \qquad N_\theta = \int \sigma_\theta dz \qquad N_{x\theta} = \int \tau_{x\theta} dz \quad [4]$$

$$M_x = -\int \sigma_x z dz \qquad M_\theta = -\int \sigma_\theta z dz \qquad M_{x\theta} = -\int \tau_{x\theta} z dz \quad [5]$$

The integrals in the above equations all extend across the thickness of the wall. By substituting Equations [1] and [3] into Equations [4] and [5], one has for example

$$N_x = D_0\left(\frac{\partial U}{\partial x} + \frac{\nu}{R}\frac{\partial V}{\partial \theta} - \nu\frac{W}{R}\right) - D_1\left(\frac{\partial^2 W}{\partial x^2} + \frac{\nu}{R^2}\frac{\partial V}{\partial \theta} + \frac{\nu}{R^2}\frac{\partial^2 W}{\partial \theta^2}\right) - N_T$$

and

$$-M_x = D_1\left(\frac{\partial U}{\partial x} + \frac{\nu}{R}\frac{\partial V}{\partial \theta} - \nu\frac{W}{R}\right) - D_2\left(\frac{\partial^2 W}{\partial x^2} + \frac{\nu}{R^2}\frac{\partial V}{\partial \theta} + \frac{\nu}{R^2}\frac{\partial^2 W}{\partial \theta^2}\right) - M_T$$

where

$$\left.\begin{aligned} D_0 &= \frac{1}{1-\nu^2}\int E(z)dz \\ D_1 &= \frac{1}{1-\nu^2}\int E(z)z dz \end{aligned}\right\} \quad \ldots\ldots [6]$$

$$D_2 = \frac{1}{1-\nu^2}\int E(z)z^2 dz \quad \ldots\ldots [7]$$

and

$$N_T = \frac{\alpha}{1-\nu}\int E(z)T(z)dz \quad \ldots\ldots [8]$$

$$M_T = \frac{\alpha}{1-\nu}\int E(z)T(z)z dz \quad \ldots\ldots [9]$$

The integrals again extend across the thickness of the wall. It is evident from the above expressions for N_x and M_x that considerable simplification can be achieved by choosing the median surface in such a way that

$$D_1 = \frac{1}{1-\nu^2}\int E(z)z dz = 0 \quad \ldots\ldots [10]$$

This is actually the condition to locate the median surface. Since Young's modulus E decreases with increase in temperature, it is seen from Equation [10] that the median surface is nearer to the cold boundary surface than to the hot boundary surface. For a rocket cylinder, hot inside but cold outside, the median surface is near to the outside surface. With this choice of the median surface, the forces and the moments are related to the displacements by the following simpler equations:

$$\left.\begin{aligned} N_x &= D_0\left(\frac{\partial U}{\partial x} + \frac{\nu}{R}\frac{\partial V}{\partial \theta} - \nu\frac{W}{R}\right) - N_T, \\ N_\theta &= D_0\left(\frac{1}{R}\frac{\partial V}{\partial \theta} - \frac{W}{R} + \nu\frac{\partial U}{\partial x}\right) - N_T \\ N_{x\theta} &= \frac{1-\nu}{2}D_0\left(\frac{\partial V}{\partial x} + \frac{1}{R}\frac{\partial U}{\partial \theta}\right) \end{aligned}\right\} \quad \ldots\ldots [11]$$

$$\left.\begin{aligned} M_x &= D_2\left(\frac{\partial^2 W}{\partial x^2} + \frac{\nu}{R^2}\frac{\partial^2 W}{\partial \theta^2} + \frac{\nu}{R^2}\frac{\partial V}{\partial \theta}\right) + M_T, \\ M_\theta &= D_2\left(\frac{1}{R^2}\frac{\partial^2 W}{\partial \theta^2} + \frac{1}{R^2}\frac{\partial V}{\partial \theta} + \nu\frac{\partial^2 W}{\partial x^2}\right) + M_T \\ M_{x\theta} &= (1-\nu)D_2\left(\frac{1}{R^2}\frac{\partial^2 W}{\partial x \partial \theta} + \frac{1}{R^2}\frac{\partial V}{\partial x}\right) \end{aligned}\right\} \quad \ldots [12]$$

It is worthwhile to point out two facts: Firstly, the choice of reference temperature is quite arbitrary. Changing the reference temperature will change the value of N_T, Equation [8]. But a corresponding adjustment in the normal strain will leave the normal forces N_x, N_θ given by Equation [11] unchanged. Therefore the physical problem is quite independent of the choice of reference temperature. M_T is independent of the reference temperature due to Equation [10]. Secondly, the present system of equations reduces to those of the conventional thin shell theory if temperature gradient is absent, or if Young's modulus is independent of the temperature of material. In that case the median surface is midway between the boundary surfaces, and D_2 is simply the usual flexural rigidity of the shell.

Nondimensional Quantities and Equations of Equilibrium

It is useful to introduce nondimensional quantities by taking R as the reference length. Thus

$$\xi = x/R \quad [13]$$

$$u = U/R, \quad v = V/R, \quad w = W/R \quad [14]$$

$$n_\xi = N_x/D_0, \quad n_\theta = N_\theta/D_0, \quad n_{\xi\theta} = N_{x\theta}/D_0, \quad n_T = N_T/D_0 \quad [15]$$

and

$$m_\xi = M_x R/D_2, \quad m_\theta = M_\theta R/D_2, \quad m_{\xi\theta} = M_{x\theta} R/D_2, \quad M_T = M_T R/D_2 \quad [16]$$

Therefore Equations [11] and [12] become now

$$\left.\begin{aligned} n_\xi &= \frac{\partial u}{\partial \xi} + \nu \frac{\partial v}{\partial \theta} - \nu w - n_T, \qquad n_\theta = \frac{\partial v}{\partial \theta} - w + \nu \frac{\partial u}{\partial \xi} - n_T \\ n_{\xi\theta} &= \frac{1-\nu}{2}\left(\frac{\partial v}{\partial \xi} + \frac{\partial u}{\partial \theta}\right) \end{aligned}\right\} \quad [17]$$

and

$$\left.\begin{aligned} m_\xi &= \frac{\partial^2 w}{\partial \xi^2} + \nu \frac{\partial^2 w}{\partial \theta^2} + \nu \frac{\partial v}{\partial \theta} + m_T, \qquad m_\theta = \frac{\partial^2 w}{\partial \theta^2} + \frac{\partial v}{\partial \theta} + \nu \frac{\partial^2 w}{\partial \xi^2} + m_T \\ m_{\xi\theta} &= (1-\nu)\left(\frac{\partial^2 w}{\partial \xi \partial \theta} + \frac{\partial v}{\partial \xi}\right) \end{aligned}\right\} \quad [18]$$

The equations of equilibrium in terms of forces and moments are here exactly the same as the conventional theory (2). The only innovation is to write them in nondimensional form. For this purpose, one has to define the nondimensional quantities q_ξ, q_θ, and p of the dimensional sectional shearing forces Q_x, Q_θ and normal pressure loading P, against z-direction as follows:

$$q_\xi = Q_x/D_0 \quad q_\theta = Q_\theta/D_0 \quad p = PR/D_0 \quad [19]$$

Then the equilibrium equations of forces are

$$\left.\begin{aligned} &\frac{\partial n_\xi}{\partial \xi} + \frac{\partial n_{\xi\theta}}{\partial \theta} - q_\xi \frac{\partial^2 w}{\partial \xi^2} - q_\theta\left(\frac{\partial v}{\partial \xi} + \frac{\partial^2 w}{\partial \xi \partial \theta}\right) - n_{\xi\theta}\frac{\partial^2 v}{\partial \xi^2} - n_\theta\left(\frac{\partial^2 v}{\partial \xi \partial \theta} - \frac{\partial w}{\partial \xi}\right) = 0 \\ &\frac{\partial n_{\xi\theta}}{\partial \xi} + \frac{\partial n_\theta}{\partial \theta} - q_\xi\left(\frac{\partial v}{\partial \xi} + \frac{\partial^2 w}{\partial \xi \partial \theta}\right) - q_\theta\left(1 + \frac{\partial v}{\partial \theta} + \frac{\partial^2 w}{\partial \theta^2}\right) + n_\xi \frac{\partial^2 v}{\partial \xi^2} + n_{\xi\theta}\left(\frac{\partial^2 v}{\partial \xi \partial \theta} - \frac{\partial w}{\partial \xi}\right) = 0 \\ &\frac{\partial q_\xi}{\partial \xi} + \frac{\partial q_\theta}{\partial \theta} + 2n_{\xi\theta}\left(\frac{\partial v}{\partial \xi} + \frac{\partial^2 w}{\partial \xi \partial \theta}\right) + n_\xi \frac{\partial^2 w}{\partial \xi^2} + n_\theta\left(1 + \frac{\partial v}{\partial \theta} + \frac{\partial^2 w}{\partial \theta^2}\right) = p \end{aligned}\right\} \quad [20]$$

The equations for the equilibrium of moments are

$$\left.\begin{aligned} &\frac{\partial m_{\xi\theta}}{\partial \xi} + \frac{\partial m_\theta}{\partial \theta} + m_\xi \frac{\partial^2 v}{\partial \xi^2} + m_{\xi\theta}\left(\frac{\partial^2 v}{\partial \xi \partial \theta} - \frac{\partial w}{\partial \xi}\right) + \beta q_\theta = 0 \\ &-\frac{\partial m_\xi}{\partial \xi} - \frac{\partial m_{\xi\theta}}{\partial \theta} + m_{\xi\theta}\frac{\partial^2 v}{\partial \xi^2} + m_\theta\left(\frac{\partial^2 v}{\partial \xi \partial \theta} - \frac{\partial w}{\partial \xi}\right) - \beta q_\xi = 0 \end{aligned}\right\} \quad [21]$$

where

$$\beta = R^2 D_0/D_2 \quad [22]$$

β is thus a quantity of the order of $(R/b)^2$, b the thickness of the wall. There are eleven individual equations in the system of Equations [17], [18], [20], and [21]. With specified loading p, there are also eleven unknowns, u, v, w, n_ξ, n_θ, $n_{\xi\theta}$, m_ξ, m_θ, $m_{\xi\theta}$, q_ξ and q_θ. The system of equations is thus complete.

Infinite Cylinder Under Uniform Internal Pressure

The simplest special case in the present general problem is the case of very long cylinder under uniform internal pressure. If the rocket cylinder is long in comparison with its diameter, the actual stress system during operation is approximated by this idealized simple case. In this problem of infinitely long uniformly loaded cylinder, the forces n_ξ, n_θ, and moments m_ξ, m_θ are constants independent of ξ and θ. The shearing force $n_{\xi\theta}$ and the twisting moment $m_{\xi\theta}$ vanish. u is proportional to ξ or $\dfrac{\partial u}{\partial \xi}$ is a constant, say k_1. v vanishes. w is a constant, and is negative in the present coordinate system, say $-k_2$. Then Equations [17], [18], and [20] give

$$\left.\begin{aligned} n_\xi^0 &= k_1 + \nu k_2 - n_T \\ n_\theta^0 &= \nu k_1 + k_2 - n_T \\ m_\xi^0 &= m_\theta^0 = m_T \end{aligned}\right\} \quad [23]$$

where the superscript 0 denote the quantities in the present simple stress system. When the temperature distribution and the material properties are specified, Equation [23] gives the strains k_1 and k_2 in terms of the internal pressure p, and the axial load n_ξ. If the axial load is produced by the same internal pressure, then it can easily be shown that

$$n_\xi^0 = p^0/2 \quad [24]$$

It is of interest to note that the bending moment m_ξ and m_θ are equal to m_T and are independent of the conditions of loading.

By solving Equation [23] for k_1 and k_2, one has

$$\left.\begin{aligned} k_1 &= \frac{1}{1-\nu^2}(n_\xi^0 - \nu p^0) + \frac{1}{1+\nu} n_T \\ k_2 &= \frac{1}{1-\nu^2}(p^0 - \nu n_\xi^0) + \frac{1}{1+\nu} n_T \end{aligned}\right\} \quad [25]$$

If the design condition is the maximum strain of the material, then Equation [25] gives the criterion directly from the pressure and temperature loading.

Linearized Theory for General Secondary Loading

As stated in the previous section, the actual stress system in a rocket chamber is approximately that of infinitely long cylinder under uniform internal pressure. This stress system can be called the primary stresses. The deviations from the primary stress system are results of bending due to canted nozzle, to end enclosures, to mounting lugs, etc. These additional stresses or the secondary stresses are, however, only a fraction of the primary stresses. Therefore it is justified to consider the second order terms of additional stresses and deformations as small in comparison to the first order terms, and thus negligible. In other words,

$$
\left.\begin{aligned}
u &= k_1\xi + u' \qquad v = v' \qquad w = -k_2 + w' \\
n_\xi &= n_\xi^0 + n_\xi' \qquad n_\theta = p^0 + n_\theta' \qquad n_{\xi\theta} = n_{\xi\theta}' \\
m_\xi &= m_T + m_\xi' \qquad m_\theta = m_T + m_\theta' \qquad m_{\xi\theta} = m_{\xi\theta}' \\
&\text{and} \\
q_\xi &= q_\xi' \qquad q_\theta = q_\theta' \qquad p = p^0 + p'
\end{aligned}\right\} \quad \ldots [26]
$$

where k_1 and k_2 are given by Equation [25]. The primed quantities are then the secondary deformations and the secondary stresses, they are considered to be small in comparison to the primary deformations and stresses. From Equations [17] and [18], one has the following relations between the deformations and the stresses,

$$
\left.\begin{aligned}
n_\xi' &= \frac{\partial u'}{\partial \xi} - \nu w' + \nu \frac{\partial v'}{\partial \theta}, \qquad n_\theta' = \nu \frac{\partial u'}{\partial \xi} - w' + \frac{\partial v'}{\partial \xi}, \\
n_{\xi\theta}' &= \frac{1-\nu}{2}\left(\frac{\partial v'}{\partial \xi} + \frac{\partial u'}{\partial \theta}\right) \\
&\text{and} \\
m_\xi' &= \frac{\partial^2 w'}{\partial \xi^2} + \nu \frac{\partial^2 w'}{\partial \theta^2} + \nu \frac{\partial v'}{\partial \theta}, \\
m_\theta' &= \nu \frac{\partial^2 w'}{\partial \xi^2} + \frac{\partial^2 w'}{\partial \theta^2} + \frac{\partial v'}{\partial \theta}, \\
m_{\xi\theta}' &= (1-\nu)\left(\frac{\partial^2 w'}{\partial \xi \partial \theta} + \frac{\partial v'}{\partial \xi}\right)
\end{aligned}\right\} \quad \ldots [27]
$$

By substituting Equation [26] into the equilibrium equations, Equations [20], and dropping out the second order terms of the primed quantities, a system of linearized equations is obtained. This system can be further reduced by substituting the q_ξ' and q_θ' obtained from the last two equations of bending moment equilibrium into the third equation. The final result is the following system of three equations: The first is the equilibrium of forces in the axial direction; the second is the equilibrium of forces in the circumferential direction; and the third is the equilibrium of forces in the radial direction:

$$
\left.\begin{aligned}
&\frac{\partial^2 u'}{\partial \xi^2} + \frac{1-\nu}{2}\frac{\partial^2 u'}{\partial \theta^2} + \frac{1+\nu}{2}\frac{\partial^2 v'}{\partial \xi \partial \theta} - \nu \frac{\partial w'}{\partial \xi} = 0 \\
&\frac{\partial^2 v'}{\partial \theta^2} + \frac{1-\nu}{2}\frac{\partial^2 v'}{\partial \xi^2} + \frac{1+\nu}{2}\frac{\partial^2 u'}{\partial \xi \partial \theta} - \frac{\partial w'}{\partial \xi} = 0 \\
&\text{and} \\
&\frac{\partial^4 w'}{\partial \xi^4} + 2\frac{\partial^4 w'}{\partial \xi^2 \partial \theta^2} + \frac{\partial^2 w'}{\partial \theta^4} - \beta\left(\nu \frac{\partial w'}{\partial \xi} - w' + \frac{\partial v'}{\partial \theta}\right) = \\
&\qquad -\beta p' + \beta\left(n_\xi^0 - \frac{m_T}{\beta}\right)\frac{\partial^2 w'}{\partial \xi^2} + \beta p^0 \frac{\partial^2 w'}{\partial \theta^2}
\end{aligned}\right\} \quad \ldots [28]
$$

These equations have been simplified on the basis that β is a large quantity of the order of the square of the radius-thickness ratio.

In the latter equation, p' is the secondary load imposed on the cylinder expressed as a distributed pressure over the surface of the cylinder, directed radially outward. If the load is a concentrated load, then it has to be expanded into a product of Fourier series and Fourier intergral as done by S. W. Yuan (3) in his treatment of concentrated load on a cold cylindrical shell. Other types of loads can be similarly expanded. Then Equation [28] is a system of three equations for three unknowns u', v', and w'. The forces and moments are related to these displacements by Equation [27].

The problem of general secondary loading as expressed by Equations [27] and [28] is very similar to the problem of general loading on a cold cylindrical shell, and can thus be treated by the known methods developed for this conventional problem. In fact, the only difference between the hot cylinder and the cold cylinder is the appearance of the term m_T in Equation [28]. However, even this difference is trivial: The reason is the very large magnitude of β as shown by Equations [6], [7], and [22]. In fact, if, as is generally the case, N_T is of the same order of magnitude as N_x^0, then the above-cited equations show that the ratio of m_T/β and n_ξ^0 is at most of the order of b/R, where b is the thickness of the shell. Since the shell is considered to be thin, or $b/R \ll 1$, the terms involving m_T in Equation [28] can be dropped without impairing the accuracy of the present theory. When this is done, then in the system of equations given by Equations [27] and [28], the effects of thermal stresses and variable Young's modulus are not explicit. As far as the nondimensional equations are concerned, the problem of hot cylinder is identical to the problem of cold cylinder, and the basic equations are now essentially the same as that adopted by L. H. Donnell for his study of the stability of thin cylindrical shells (4). This is the basis of the similarity law discussed in the following section.

Similarity Law for General Loading

If the problem of secondary loading is to be solved analytically, the results of the previous section show that it can be reduced to an equivalent problem of cold cylinder and solved accordingly. However, a more useful application of the equivalence concept lies in the possibility of experimentally determining the stress and the strain on the equivalent cold cylinder and then using the similarity law to determine the stress and the strain in the hot cylinder. There are mainly two advantages of this semi-experimental approach: (*a*) The experiments on a cold cylinder can be done more easily and much more accurately than possible on a hot cylinder. The test period can be as long as desired and not limited to the short burning time of the rocket. (*b*) The stresses induced by mounting lugs, etc., are very difficult to approximate by simple load systems amenable to theoretical calculations. For instance, the loads from a mounting lug are not really a concentrated force and a concentrated moment. To take them as a concentrated force and a concentrated moment would grossly overestimate the actual stress. Such difficulties disappear if the loading is done experimentally.

With such experimental stress determination in mind, it will be convenient to have the hot cylinder and the equivalent cold cylinder of same general sizes. Thus the radius R and the length L will be the same for both cylinders. In order that the nondimensional differential equations, Equation [28], be the same for the hot cylinder as for the cold cylinder, the parameters in these differential equations must be the same. That is, if a quantity of the cold cylinder is denoted by a bar over the quantity

$$\frac{1}{R^2}\beta = \frac{D_0}{D_2} = \frac{\bar{D}_0}{\bar{D}_2} \quad \ldots\ldots\ldots\ldots\ldots\ldots [29]$$

$$n_\xi{}^0 = \frac{N_x{}^0}{D_0} = \frac{\bar{N}_x{}^0}{\bar{D}_0}, \qquad p^0 = \frac{P^0}{D_0} = \frac{\bar{P}^0}{\bar{D}_0} \quad \ldots\ldots\ldots [30]$$

The condition of Equation [29] can be satisfied by making the thickness $\bar{b}$ of the cold cylinder smaller than the thickness b of the hot cylinder. This is of course to be expected, since Young's modulus of the hot material is smaller and hence material is "softer" than the cold material. When the thickness $\bar{b}$ is determined from b by using Equation [29], $\bar{D}_0$ can be computed. Then Equation [30] gives the internal pressure $\bar{P}^0$ and the axial load $\bar{N}_x{}^0$ from the specified P^0 and $N_x{}^0$ for the hot cylinder. These steps then fix the geometry of the cold cylinder and the primary system of loads.

For the additional secondary loads, the fact that Equations [27] and [28] are linear equations can be utilized to introduce an added freedom in specifying the loads. Linear relations are not altered by multiplying the variable by a constant. Therefore for additional loads and additional displacements, the nondimensional quantities for the cold cylinder and the nondimensional quantities for the hot cylinder need not be identical, but differ by a factor ϵ. Thus

$$(\bar{u}', \bar{v}', \bar{w}') = \epsilon(u', v', w')$$

and

$$(\bar{n}_\xi', \bar{n}_\theta', \bar{n}_{\xi\theta}'; \bar{m}_\xi', \bar{m}_\theta', \bar{m}_{\xi\theta}') = \epsilon(n_\xi', n_\theta', n_{\xi\theta}'; m_\xi', m_{\theta\xi}', m_\theta') \ldots [31]$$

Then

$$\bar{p}' = \epsilon p' \quad \ldots\ldots\ldots\ldots\ldots\ldots [32]$$

But the nondimensional pressure loading p is related to the actual pressure loading by Equation [19]. Therefore the secondary pressure loadings $\bar{P}'$ for the cold cylinder and the secondary pressure loading P' for the hot cylinder are related through

$$\bar{P}' = \left(\frac{\bar{D}_0}{D_0}\epsilon\right) P' \quad \ldots\ldots\ldots\ldots\ldots\ldots [33]$$

The ratio of the pressure load is then $\bar{D}_0\epsilon/D_0$. Since the radius R and the length L of both cylinders are the same, other types of loads such as concentrated force, or moment for the cold cylinder and for the hot cylinder must also bear the same ratio. Needless to say, the loads for the cold cylinder must be applied at corresponding points for loads in the hot cylinder.

The additional forces N_x', $N_{x\theta}'$, the additional shear Q_x', and the additional moments N_x', $M_{x\theta}'$ at the ends of the cylinder are controlled by Equations [15], [16], and [19]. It is easily seen that because of Equation [29], the ratio of these quantities for the cold cylinder and the hot cylinder is again $\bar{D}_0\epsilon/D_0$.

Therefore, knowing the load system on the hot cylinder, one can find the corresponding load system for the cold cylinder. The factor ϵ for the secondary loads can be chosen at convenience of the experimenter. For instance, ϵ might be so chosen as to make the ratio $\bar{D}_0\epsilon/D_0$ equal to unity. Then the secondary load system for the cold cylinder is exactly the same as the hot cylinder. When the proper load for the cold cylinder is selected and the corresponding strain on the cold cylinder determined by strain gages, the inverse equivalence problem is then to find the strain in the hot cylinder from the test data on cold cylinder.

Take for instance, the axial strain $e_x(z)$. For the cold cylinder, according to Equations [1] and [25],

$$\bar{e}_x(z) = k_1 - \frac{1}{1+\nu} n_T + \left(\frac{\partial \bar{u}'}{\partial \xi} - \frac{\bar{z}}{R}\frac{\partial^2 \bar{w}'}{\partial \xi^2}\right) \quad \ldots\ldots [34]$$

where $\bar{z}$ is the value of z measured from the median surface of the cold cylinder, midway between the boundary surfaces. Now let $\bar{e}_x$ be the average of the measured axial strains on the outer surface and on the inner surface of the cold cylinder, and let $\Delta\bar{e}_x$ be the difference of the measured axial strains on the outer surface and on the inner surface of the cold cylinder. Then from Equation [34]

$$\bar{e}_x = k_1 - \frac{1}{1+\nu} n_T + \frac{\partial \bar{u}'}{\partial \xi} = k_1 - \frac{1}{1+\nu} n_T + \epsilon \frac{\partial u'}{\partial \xi} \ldots [35]$$

and

$$\Delta\bar{e}_x = \frac{\bar{b}}{R}\frac{\partial^2 \bar{w}'}{\partial \xi^2} = \frac{\bar{b}}{R}\epsilon\frac{\partial^2 w'}{\partial \xi^2}$$

For the hot cylinder, the axial strain is given by

$$e_x(z) = k_1 + \frac{\partial u'}{\partial \xi} - \frac{z}{R}\frac{\partial^2 w'}{\partial \xi^2} \quad \ldots\ldots\ldots\ldots [36]$$

By eliminating $\dfrac{\partial u'}{\partial \xi}$ and $\dfrac{\partial^2 w'}{\partial \xi^2}$ from Equations [35] and [36], one has

$$e_x(z) = \left(1 - \frac{1}{\epsilon}\right) k_1 + \frac{1}{(1+\nu)\epsilon} n_T + \frac{1}{\epsilon}\left(\bar{e}_x - \frac{z}{\bar{b}}\Delta\bar{e}_x\right) \ldots [37]$$

The value of z is measured radially inward from the median surface of the hot cylinder and thus is larger in magnitude for the inside surface than for the outside surface.

Similarly,

$$e_\theta(z) = \left(1 - \frac{1}{\epsilon}\right) k_2 + \frac{1}{(1+\nu)\epsilon} n_T + \frac{1}{\epsilon}\left(\bar{e}_\theta - \frac{z}{\bar{b}}\Delta\bar{e}_\theta\right) \ldots [38]$$

and

$$\gamma_{x\theta}(z) = \frac{1}{\epsilon}\left(\bar{\gamma}_{x\theta} - \frac{z}{\bar{b}}\Delta\bar{\gamma}_{x\theta}\right) \quad \ldots\ldots\ldots\ldots [39]$$

where $\bar{e}_\theta$ is the average of the measured circumferential strain on the outer surface and the inner surface of the cold cylinder, $\Delta\bar{e}_\theta$ is the difference of these strains; $\bar{\gamma}_{x\theta}$ and $\Delta\bar{\gamma}_{x\theta}$ are the corresponding quantities for the shearing strain. In Equations [37] and [38], k_1 and k_2, and n_T are the primary strains computed from Equations [25] and [8]. Therefore these equations allow the calculation of the strains in the hot cylinder from test results from cold cylinder, and thus complete the desired similarity law.

For a stress analyst, the next step is perhaps the calculation of the principle strains at each value of z in the shell, and examine whether the larger of these principal strains exceeds the design limit of the material at the temperature prevailing at that point.

Example of Dimensioning the Equivalent Cold Cylinder

As an example of the procedure outline in the previous section, the data given by Noland (1) will be used to find the equivalent cold cylinder. The temperature distribution in the wall is taken from Fig. 2 of that paper and is reproduced as Fig. 1 here. The material is assumed to be 19-9 DL, and the variation of Young's modulus with temperature is plotted in Fig. 2, again

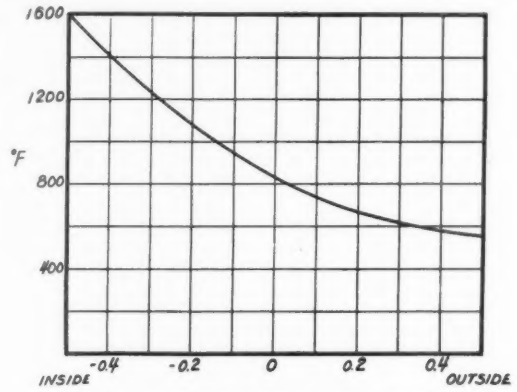

FIG. 1 TEMPERATURE DISTRIBUTION IN THE WALL

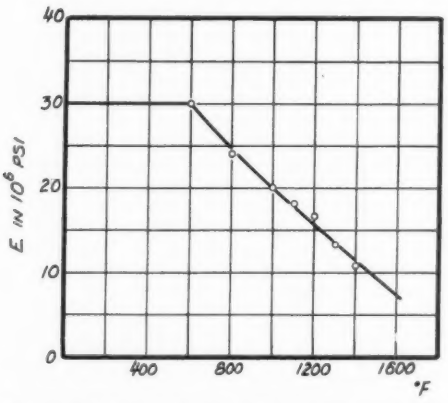

FIG. 2 YOUNG'S MODULUS AS A FUNCTION OF TEMPERATURE

using Noland's data. First, the position of the median surface will be determined, using Equation [10]. This is found to be 0.588 b from the inside surface. Next, by taking the cold cylinder to be at 100° F, the ratio of the thicknesses of the hot cylinder and the equivalent cold cylinder is computed by using Equations [6], [7], and [29]. It is found that

$$\bar{b} = 0.936b$$

Thus the equivalent cold cylinder of the same material is 93.6 per cent as thick as the hot cylinder.

The ratio of the loads on the cold cylinder and the hot cylinder is controlled by $\bar{D}_0/D_0$. This is computed as

$$\bar{D}_0/D_0 = 1.29$$

By taking $\alpha = 10^{-5}/°\text{F}$, and $b = 0.095$ in., the values of thermal stresses are

$$N_T = 22400 \text{ lb/in.}, \qquad n_T = 0.958 \times 10^{-2}$$
$$M_T = 192 \text{ lb.}, \qquad m_T = -0.124$$

If the radius of the cylinder is 2.25 in., and if the internal pressure P^0 is 1500 psi, then

$$p^0 = 1.44 \times 10^{-3}$$

If the axial tension $N_x{}^0$ is due to the same internal pressure, then

$$n_\xi{}^0 = \frac{p^0}{2} = 0.72 \times 10^{-3}$$

Now

$$\beta = 12\left(\frac{R}{\bar{b}}\right)^2$$

Therefore the ratio of m_T/β and $n_\xi{}^0$ is

$$m_T/\beta n_\xi{}^0 = -0.0224$$

This is indeed smaller than the thickness-radius ratio $b/R = 0.0422$. Hence the surmise that m_T/β is negligible against $n_\xi{}^0$ is now justified by numerical calculation.

Junction Stress Between Cylinder and Head

The previous formulation of the similarity law for stresses in the hot cylinder and the cold cylinder is based upon the assumption that the secondary load system is specified. This is not true for the junction stresses induced by fitting, say, a hemispherical head to the cylinder. Such stresses are determined by the equality of deformations of the head and the cylinder at the junction. If the semi-spherical shell has the same thickness as the cylindrical shell, then the temperature distribution in the spherical shell will be the same as in the cylindrical shell. An analysis shows that the "similar" cold test specimen can be made also of uniform thickness $\bar{b}$, determined by Equation [29]. However, the similarity of both the primary loading and secondary loading now requires an additional restriction: ϵ must now be unity. When these conditions are fulfilled, the similarity of junction stresses in the hot cylinder and the cold cylinder will be assured, and the relations previously developed for computing the stresses in the hot cylinder from test data on the cold cylinder remain valid.

Ring Stiffener Around Cylinder

To strengthen the thin cylindrical shell against concentrated loads from the mounting lugs, a ring stiffener is often attached to the outside surface. It remains cold. Young's modulus of the ring material thus is that of cold material. To determine the dimensions of a "similar" ring for the cold cylinder, the conditions to be satisfied are those of Equations [31]. In other words, for a ratio ϵ of deformation of the ring on the cold cylinder to that on the hot cylinder, the force required must bear the ratio $\epsilon\bar{D}_0/D_0$. This means that the ratio of the stiffness of the ring for the cold cylinder to that on the hot cylinder is $\bar{D}_0/D_0$. If the ring is rectangular in section, the correct ratio of the width of the two rings

(*Continued on page 167*)

Heat Flow in Composite Slabs

E. MAYER[1]

The M. W. Kellogg Company, Jersey City, N. J.

This paper presents the solution of the heat flow problem in composite walls under heat transfer conditions which are typical of uncooled rocket engine walls. Analytic expressions in the form of Fourier sums are obtained for the temperature distribution in a composite wall consisting of an inner (refractory) medium and an outer (metallic) medium under Newtonian heat transfer into the first medium with negligible heat transfer from the second medium to the exterior. The expressions obtained are based on a plane parallel composite slab as a representative model for relatively thin cylindrical walls, with thickness-to-radius ratio not exceeding 0.2. The general results for the composite slab are simplified for the limiting cases of a thin refractory shield with a thick shielded medium and a thick refractory shield with a thin shielded medium.

Nomenclature

Most of the symbols listed here are more fully defined in the text as they are introduced.

c	= specific heat
d	= wall thickness
h	= heat transfer coefficient
k	= thermal conductivity
t	= time
x	= space coordinate
$\alpha^2 = k/\rho c$	= thermal diffusivity
λ^2	= characteristic constant of partial differential equation
ρ	= density
A	= Fourier amplitude
$N = \frac{hd}{k}$	= Biot number
T	= temperature above ambient
T_g	= flame temperature above ambient
Λ	= characteristic constant

The subscripts 1 and 2 are used with symbols pertaining to the shield and shielded media, respectively. Additional subscripts m, n, designate running indices in Fourier sums.

1 Introduction

IN MANY rocket engineering applications the problem of transient heat transfer through composite walls has been gaining increasing importance. The typical composite wall consists of an insulating cylindrical shell of refractory material within a cylindrical metal envelope, which, for structural reasons, must not attain excessive temperatures during the firing period. The insulator receives heat by convective heat transfer from the rocket flame. Some of the heat transferred is conducted through the interface between the insulator and envelope, and is accumulated in the envelope. Heat transfer from the envelope to the exterior is generally negligible until the envelope attains excessive temperatures.

Received March 7, 1952.

[1] Research Engineer, Special Projects Department.

The results obtained for heat flow problems in composite cylindrical shells (1, 2)[2] are, as a rule, too complicated to be of practical value in application to the composite rocket wall, especially because of uncertainties in data on material properties and heat transfer coefficients. For typical wall thickness-to-diameter ratios it is sufficient to consider a composite plane parallel slab as a representative model of the cylindrical wall. This paper contains a mathematical description of the temperature transients in a composite slab corresponding to typical heat transfer conditions in rocket motors. While the general results obtained here are still relatively complicated, the solution is reduced to two simple limiting cases of considerable importance; namely, the "thin" insulator and the "thick" insulator.

2 Heat Flow in a Simple Slab

In order to refer the results obtained for the composite shell to a basic problem which has been studied in considerable detail (1, 3) we recall here briefly the temperature distributions obtained in a simple slab receiving heat through one boundary by convective heat transfer and insulated at the other boundary. The slab is contained between the planes $x = 0$ and $x = -d$, as shown on the following sketch. The temperature distribution within the material is governed by the partial differential equation

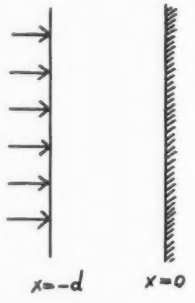

$$k \frac{\partial^2 T}{\partial x^2} = \rho c \frac{\partial T}{\partial t} \quad \text{.....[1]}$$

in which the thermal conductivity k, the specific heat c, and the density ρ are assumed constant. With Newtonian heat transfer at the flame side $x = -d$, the boundary condition at this plane is

$$-k \frac{\partial T(-d, t)}{\partial x} = h\,[T_g - T(-d, t)] \quad \text{.....[2]}$$

where h is the heat transfer coefficient and T_g the flame temperature, both assumed constant. At the other boundary the adiabatic condition is assumed to hold:

$$\frac{\partial T(0, t)}{\partial x} = 0 \quad \text{.....[3]}$$

For convenience, all temperatures T are measured above

[2] Numbers in parentheses refer to the References on page 158.

ambient, and the initial condition satisfied by the solutions of [1] is taken as

$$T(x, 0) = 0 \quad \ldots\ldots [4]$$

The method of separation of variables (4) applied to [1] leads to solutions of the form

$$T(x, t) = e^{-\lambda^2 t} f(x) + C \quad \ldots\ldots [5]$$

in which C is a constant and λ^2 is a separation constant. With the form [5] substituted in [1], the time terms cancel and the spatial dependence of the temperature is contained in

$$\alpha^2 \frac{d^2 f}{dx^2} + \lambda^2 f = 0$$

where $\alpha^2 = k/\rho c$ designates the thermal diffusivity of the material. Thus, the spatial function is sinusoidal

$$f(x) = A \cos \frac{\lambda x}{\alpha} + B \sin \frac{\lambda x}{\alpha} \quad \ldots\ldots [6]$$

The boundary conditions [2] and [3] lead to

$$-\frac{k\lambda}{\alpha}\left[A \sin \frac{\lambda d}{\alpha} + B \cos \frac{\lambda d}{\alpha}\right] e^{-\lambda^2 t} = -h\left[A \cos \frac{\lambda d}{\alpha} - B \sin \frac{\lambda d}{\alpha}\right] e^{-\lambda^2 t} + h[T_g - C] \quad \ldots [2']$$

$$\frac{k\lambda}{\alpha} B e^{-\lambda^2 t} = 0 \quad \ldots\ldots [3']$$

From the time-independent term in [2'] it follows that $C = T_g$. Furthermore, since from (3') B must be zero, Equation [2'] reduces, after cancellation of the of the factor $Ae^{-\lambda^2 t}$, to an eigenvalue equation for λ:

$$\frac{\lambda d}{\alpha} \tan \frac{\lambda d}{\alpha} = \frac{hd}{k} \quad \ldots\ldots [7]$$

Introducing the dimensionless parameters

$$\Lambda = \frac{\lambda d}{\alpha} \qquad N = \frac{hd}{k}$$

we put the eigenvalue equation into the form

$$\Lambda \tan \Lambda = N \quad \ldots\ldots [7']$$

the solutions of which are tabulated in Ref. 1 for the range $0 < N < \infty$. Each value of N determines an infinite set of discrete eigenvalues $\Lambda_n = \lambda_n d/\alpha$, $n = 1, 2 \ldots$. The associated functions f in [6]

$$f_n(x) = A_n \cos \frac{\lambda_n x}{\alpha} = A_n \cos \Lambda_n \frac{x}{d} \qquad n = 1, 2 \ldots$$

form a complete orthogonal set satisfying

$$\int_{-d}^{0} f_n(x) f_m(x)\, dx = 0 \qquad n \neq m$$

which permits the determination of the amplitudes A_n by Fourier analysis of the initial condition [4]

$$T(x, 0) = \sum_n A_n \cos \lambda_n \frac{x}{d} + T_g \equiv 0$$

$$A_n/T_g = -\int_{-d}^{0} \cos \Lambda_n \frac{x}{d}\, dx \Big/ \int_{-d}^{0} \cos^2 \Lambda_n \frac{x}{d}\, dx = -4 \sin \Lambda_n/(2\Lambda_n + \sin 2\Lambda_n)$$

With these results the transient temperature distribution for the simple slab receiving heat by Newtonian heat transfer is represented as a Fourier sum

$$T(x, t) = T_g \left[1 - 4 \sum_n \frac{\sin \Lambda_n}{2\Lambda_n + \sin^2 \Lambda_n} \cdot \cos \Lambda_n \frac{x}{d} e^{-\lambda_n^2 t}\right] \quad \ldots [5']$$

It may be noted here that in practice the above Fourier sum converges rapidly, one or two terms in the sum being sufficient for computation of T/T_g except for very short times when $T/T_g << 1$. Detailed curves of T vs. t for fixed positions x in dimensionless variables appear in the Gurney-Lurie (3) charts, which are based on the Fourier solution corresponding to conditions when only the first term of the sum in Equation [5'] is of importance.

3 Heat Flow in Composite Slabs

The mathematical description of the transient temperatures arising in a composite wall consisting of two plane parallel slabs of different media under Newtonian heat input is obtained with reference to the coordinate system shown on the following sketch.

One of the slabs is contained between the planes $x = -d_1$, and $x = 0$, the other between $x = 0$ and $x = d_2$. The temperature $T(x, t)$ is governed by the heat flow equation

$$\alpha^2 \frac{\partial^2 T}{\partial x^2} = \frac{\partial T}{\partial t} \quad \ldots\ldots [8]$$

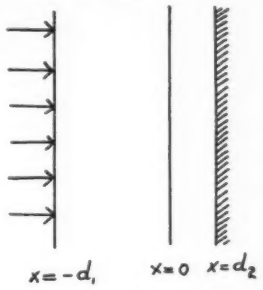

where the thermal diffusivity is constant in each medium having the values

$$\alpha^2 = \begin{cases} \alpha_1^2 = k_1/\rho_1 c_1 \text{ for } -d_1 < x < 0 \\ \alpha_2^2 = k_2/\rho_2 c_2 \text{ for } 0 < x < d_2 \end{cases}$$

With Newtonian heat transfer at the flame side $x = -d_1$, the boundary condition at this plane is

$$h\,[T_g - T(-d_1, t)] = -k_1 \frac{\partial T(-d_1, t)}{\partial x} \quad \ldots\ldots [9]$$

where the heat transfer coefficient h and the flame temperature T_g are assumed constant. At the outer boundary of the composite wall, $x = d_2$ the condition corresponding to vanishing heat transfer is employed:

$$\frac{\partial T(-d_2, t)}{\partial x} = 0 \quad \ldots\ldots [10]$$

While actually there may occur some radiation losses to the exterior as the temperature at the outer boundary rises, the latter heat transfer rates, as estimated from radiation formulas, are negligibly small in practice. Choosing the temperature scale so that the initial uniform temperature of the composite wall is zero, we have as the initial condition

$$T(x, 0) = 0 \quad \ldots\ldots [11]$$

In brief, then the mathematical problem at hand is the solution of the partial differential Equation [8] subject to the boundary conditions [9] and [10] and the initial condition [11].

The solution of Equation [8] is represented by different functional forms in the two regions on the above sketch. Thus:

$$T(x, t) = F_1(x, t) \qquad -d_1 \le x \le 0$$
$$T(x, t) = F_2(x, t) \qquad 0 \le x \le d_2$$

where the F's satisfy the differential equations

$$\alpha_1^2 \frac{\partial^2 F_1}{\partial x^2} = \frac{\partial F_1}{\partial t} \quad \text{[12]}$$

$$\alpha_2^2 \frac{\partial^2 F_2}{\partial x^2} = \frac{\partial F_2}{\partial t} \quad \text{[13]}$$

At the interface $x = 0$, continuity conditions on the temperature T and the heat flux $k\partial T/\partial x$ lead to the following connections between F_1 and F_2:

$$F_1(0, t) = F_2(0, t) \quad \text{[14]}$$

$$k_1 \frac{\partial F_1(0, t)}{\partial x} = k_2 \frac{\partial F_2(0, t)}{\partial x} \quad \text{[15]}$$

Further conditions on the F's are obtained from the boundary and initial conditions on T, Equations [9], [10], and [11]:

$$-k_1 \frac{\partial F_1}{\partial x} = h[T_g - F_1] \qquad \text{at} \qquad x = -d_1 \quad \text{[16]}$$

$$\frac{\partial F_2}{\partial x} = 0 \qquad \text{at} \qquad x = d_2 \quad \text{[17]}$$

$$F_1(x, 0) = F_2(x, 0) = 0 \quad \text{[11']}$$

Seeking solutions by separation of variables we try solutions of the form

$$F_1(x, t) = e^{-\lambda^2 t} f_1(x) + C_1 \qquad F_2(x, t) = e^{-\lambda^2 t} f_2(x) + C_2$$

which lead to

$$\alpha_1^2 \frac{d^2 f_1}{dx^2} + \lambda^2 f_1 = 0 \qquad \alpha_2^2 \frac{d^2 f_2}{dx^2} + \lambda^2 f_2 = 0$$

with the results

$$f_1(x) = A_1 \cos \frac{\lambda x}{\alpha_1} + B_1 \sin \frac{\lambda x}{\alpha_1}$$

$$f_2(x) = A_2 \cos \frac{\lambda x}{\alpha_2} + B_2 \sin \frac{\lambda x}{\alpha_2}$$

From the boundary condition [16] we conclude that $C_1 = T_g$, so that the time dependent terms can be canceled yielding

$$-k_1 \frac{df_1}{dx} = -hf_1 \qquad \text{at} \qquad x = -d_1 \quad \text{[16']}$$

On comparing terms in Equation [14] we find $C_2 = C_1 \equiv T_g$ and

$$f_1 = f_2 \qquad \text{at} \qquad x = 0 \quad \text{[14']}$$

The remaining boundary conditions become, upon cancellation of the time terms,

$$k_1 \frac{df_1}{dx} = k_2 \frac{df_2}{dx} \qquad \text{at} \qquad x = 0 \quad \text{[15']}$$

$$\frac{df_2}{dx} = 0 \qquad \text{at} \qquad x = d_2 \quad \text{[17']}$$

The four boundary conditions lead to a system of homogeneous linear equations for the amplitudes A_1, B_1, A_2, B_2:

$$\begin{aligned} A_1 \qquad &+ 0 \qquad && - A_2 \qquad && + 0 \quad = 0 \quad \text{[14"]} \\ A_1\left[1 - \frac{k_1\lambda}{h\alpha_1} \tan \frac{\lambda d_1}{\alpha_1}\right] &- B_1\left[\tan \frac{\lambda d_1}{\alpha_1} + \frac{k_1\lambda}{h\alpha_1}\right] && && + 0 \quad = 0 \quad \text{[15"]} \\ 0 \qquad &+ B_1 \frac{k_1}{\alpha_1} && && + 0 \quad - B_2 \frac{k_2}{\alpha_2} = 0 \quad \text{[16"]} \\ 0 \qquad &+ 0 \qquad && + A_2 \tan \frac{\lambda d_2}{\alpha_2} && - B_2 \quad = 0 \quad \text{[17"]} \end{aligned}$$

For nontrivial solutions to exist (i.e., solutions other than $A_1 = A_2 = B_1 = B_2 \equiv 0$), the determinant of the coefficients must vanish yielding the eigenvalue equation for λ,

$$\tan \Lambda_2 \frac{\tan \Lambda_1 + \frac{k_1}{hd_1} \Lambda_1}{1 - \frac{k_1}{hd_1} \Lambda_1 \tan \Lambda_1} = \sigma \quad \text{[18]}$$

where:

$$\sigma = \sqrt{\frac{k_1\rho_1 c_1}{k_2\rho_2 c_2}} \qquad \Lambda_1 = \frac{\lambda d_1}{\alpha_1} \qquad \Lambda_2 = \frac{\lambda d_2}{\alpha_2}$$

For given heat transfer coefficient h and the composite wall data (material properties k, ρc and thicknesses d, of each medium) the eigenvalue equation possesses an infinite set of λ's

$$\lambda = \lambda_1, \lambda_2 \ldots \lambda_n \ldots$$

as its solution. With each λ_n there is an associated function f_n and the solution for the temperature distribution is a Fourier sum of the form

$$T(x, t) = \begin{cases} F_1(x, t) = \sum_n f_{1n} e^{-\lambda_n^2 t} + T_g & -d_1 \le x \le 0 \\ F_2(x, t) = \sum_n f_{2n} e^{-\lambda_n^2 t} + T_g & 0 \le x \le d_2 \end{cases} \quad \text{[19]}$$

where the representations of f_n in the two media are

$$f_n(x) = \begin{cases} f_{1n} = A_{1n} \cos \Lambda_{1n} \frac{x}{d_1} + B_{1n} \sin \Lambda_{1n} \frac{x}{d_1} & -d_1 \le x \le 0 \\ f_{2n} = A_{2n} \cos \Lambda_{2n} \frac{x}{d_2} + B_{2n} \sin \Lambda_{2n} \frac{x}{d_2} & 0 \le x \le d_2 \end{cases}$$

In the expressions for f_n only one of the four amplitudes A_{1n}, A_{2n} B_{1n}, B_{2n} is independent, the ratio of any other to this one being determined by the boundary conditions, Equations [14'] to [17']. Thus we may put

$$A_{1n} = A_{2n} \equiv A_n$$

$$\frac{B_{1n}}{A_{2n}} = \frac{B_{1n}}{A_n} = \frac{\tan \Lambda_{2n}}{\sigma} = \mu_{1n}$$

$$\frac{B_{2n}}{A_{2n}} = \frac{B_{2n}}{A_n} = \tan \lambda_{2n} = \mu_{2n}$$

and obtain

$$f_n = \begin{cases} f_{1n} = A_n \left(\cos \Lambda_{1n} \frac{x}{d_1} + \mu_{1n} \sin \Lambda_{1n} \frac{x}{d_1}\right) \\ f_{2n} = A_n \left(\cos \Lambda_{2n} \frac{x}{d_2} + \mu_{2n} \sin \Lambda_{2n} \frac{x}{d_2}\right) \end{cases} \quad \text{[20]}$$

in which the unknown amplitudes A_n are determined by Fourier analysis on the initial condition

$$T(x, t) = \sum_n f_n(x) e^{-\lambda_n^2 t} + T_g \equiv 0 \qquad \text{at} \qquad t = 0 \quad \text{[11"]}$$

It is to be noted at this point that the f_n's are not orthogonal over the range $-d_1 \le x \le d_2$, and hence to perform the indicated Fourier analysis we must first

obtain the orthogonal functions associated with the composite wall system. These functions turn out to be given, as demonstrated below, by

$$\varphi_n(x) = \psi(x) f_n = \begin{cases} \sqrt{\rho_1 c_1}\, f_{1n} & -d_1 \le x \le 0 \\ \sqrt{\rho_2 c_2} f_{2n} & 0 \le x \le d_2 \end{cases}$$

where:

$$\psi(x) = \begin{cases} \sqrt{\rho_1 c_1} & -d_1 \le x \le 0 \\ \sqrt{\rho_2 c_2} & 0 \le x \le d_2 \end{cases}$$

To prove the orthogonality of the ϕ_n's

$$\int_{-d_1}^{d_2} \phi_n(x)\phi_m(x)\, dx = 0 \qquad m \neq n \ldots\ldots\ldots [21]$$

we start with the differential equations satisfied by ϕ_m, ϕ_n

$$\alpha^2 \frac{d^2\phi_m}{dx^2} = -\lambda_m^2 \phi_m$$

$$\alpha^2 \frac{d^2\phi_m}{dx^2} = -\lambda_n^2 \phi_n$$

We multiply the former of these equations by ϕ_n, the latter by ϕ_m, and subtract one from the other, obtaining upon rearrangement and integration over the wall thickness,

$$(\lambda_m^2 - \lambda_n^2) \int_{-d_1}^{d_2} \phi_n(x)\phi_m(x)dx =$$

$$\int_{-d_1}^{0} \alpha_1^2 \left(\phi_m \frac{d^2\phi_n}{dx^2} - \phi_n \frac{d^2\phi_m}{dx^2} \right) dx$$

$$+ \int_{0}^{d_2} \alpha_2^2 \left(\phi_m \frac{d^2\phi_n}{dx^2} - \phi_n \frac{d^2\phi_m}{dx^2} \right) dx$$

Consider now the first integral on the right. After inserting here $\phi_m = \sqrt{\rho_1 c_1}\, f_{1m}$ and $\phi_n = \sqrt{\rho_1 c_1}\, f_{1n}$, we obtain

$$\int_{-d_1}^{0} k_1 \left[f_{1m} \frac{d^2 f_{1n}}{dx^2} - f_{1n} \frac{d^2 f_{1m}}{dx^2} \right] dx$$

which, by partial integrations becomes

$$\Big|_{-d_1}^{0} k_1 \left[f_{1m} \frac{df_{1n}}{dx} - f_{1n} \frac{df_{1m}}{dx} \right]$$

Because of boundary condition [16′] $k_1 \dfrac{df_{1n}}{dx} = h f_{1n}$ at $x = -d_1$, and hence the bracketed terms cancel at the lower limit. Thus, only at $x = 0$ is there a contribution to the first integral considered.

Proceeding similarly with the second integral on the right we obtain cancellations at the upper limit $x = d_2$ by virtue of [17′] and therefore we find

$$(\lambda_m^2 - \lambda_n^2) \int_{-d_1}^{d_2} \phi_n\phi_m\, dx = \Big|_{x=0} k_1 \left[f_{1m} \frac{df_{1n}}{dx} - f_{1n} \frac{df_{1m}}{dx} \right]$$

$$- \Big|_{x=0} k_2 \left[f_{2m} \frac{df_{2n}}{dx} - f_{2n} \frac{df_{2m}}{dx} \right]$$

Employing the continuity conditions at the interface

$$f_{1n} = f_{2n}$$

$$k_1 \frac{df_{1n}}{dx} = k_2 \frac{df_{2n}}{dx} \qquad \text{at} \quad x = 0$$

we obtain a complete cancellation on the right and hence arrive at

$$(\lambda_n^2 - \lambda_m^2) \int_{-d_1}^{d_2} \phi_m(x)\phi_n(x)\, dx = 0$$

Now since $\lambda_n \neq \lambda_m$ for $m \neq n$, we conclude that the integral must vanish and the orthogonality condition [21] is established.

We now determine the amplitude A_n by Fourier analysis on the initial condition [11″] with the aid of the orthogonality properties of the functions ϕ_n. Rewriting Equation [11″] as

$$\sum f_n(x) = -T_0$$

we multiply both sides by the factor $\phi_m(x)\psi(x)$ and integrate over the composite wall:

$$\int_{-d_1}^{d_2} \sum_n \phi_m(x)\phi_n(x)\, dx = -T_0 \int_{-d_1}^{d_2} \phi_m(x)\psi(x)dx \ldots [22]$$

In the summation on the left the product $\psi(x)f_n(x)$ is written as $\phi_n(x)$ in accordance with the definition of the latter. By virtue of the orthogonality condition [21], the summation reduces to a single term $\int \phi_m^2(x)dx$. Reintroducing the explicit forms of ϕ_m,

$$\phi_m(x) = \begin{cases} \sqrt{\rho_1 c_1}\, A_m \left[\cos \Lambda_{1m} \dfrac{x}{d_1} + \mu_{1m} \sin \Lambda_{1m} \dfrac{x}{d_1} \right] & -d_1 \le x \le 0 \\ \sqrt{\rho_2 c_2}\, A_m \left[\cos \Lambda_{2m} \dfrac{x}{d_2} + \mu_{2m} \sin \Lambda_{2m} \dfrac{x}{d_2} \right] & 0 \le x \le d_2 \end{cases}$$

we perform the integrations with the appropriate form of ϕ_m in each of the two regions of the composite wall. With the notation

$$D_{1m} = \int_{-d_1}^{0} \left[\cos \Lambda_{1m} \frac{x}{d_1} + \mu_{1m} \sin \Lambda_{1m} \frac{x}{d_1} \right]^2 dx$$

$$D_{2m} = \int_{0}^{d_2} \left[\cos \Lambda_{2m} \frac{x}{d_2} + \mu_{2m} \sin \Lambda_{2m} \frac{x}{d_2} \right]^2 dx$$

$$N_{1m} = \int_{-d_1}^{0} \left[\cos \Lambda_{1m} \frac{x}{d_1} + \mu_{1m} \sin \Lambda_{1m} \frac{x}{d_1} \right] dx$$

$$N_{2m} = \int_{0}^{d_2} \left[\cos \Lambda_{2m} \frac{x}{d_2} + \mu_{2m} \sin \Lambda_{2m} \frac{x}{d_2} \right] dx$$

we have for Equation [22]

$$A_m^2 [\rho_1 c_1 D_{1m} + \rho_2 c_2 D_{2m}] = -T_0 A_m [\rho_1 c_1 N_{1m} + \rho_2 c_2 N_{2m}]$$

or

$$A_m = -T_0 \frac{\rho_1 c_1 N_{1m} + \rho_2 c_2 N_{2m}}{\rho_1 c_1 D_{1m} + \rho_2 c_2 D_{2m}} \ldots\ldots\ldots [23]$$

Performing the integrations for D and N we obtain

$$D_{1m} = \frac{d_1}{2\Lambda_{1m}} [(1 + \mu_{1m}^2)\Lambda_{1m} + (1 - \mu_{1m}^2) \sin \Lambda_{1m} \cos \Lambda_{1m} - 2\mu_{1m} \sin^2 \Lambda_{1m}]$$

$$D_{2m} = \frac{d_2}{2\Lambda_{2m}} [(1 + \mu_{2m}^2)\Lambda_{2m} + (1 - \mu_{2m}^2) \sin \Lambda_{2m} \cos \Lambda_{2m} + 2\mu_{2m} \sin^2 \Lambda_{2m}]$$

$$N_{1m} = \frac{d_1}{\Lambda_{1m}} [\sin \Lambda_{1m} + \mu_{1m} (\cos \Lambda_{1m} - 1)]$$

$$N_{2m} = \frac{d_2}{\Lambda_{2m}} [\sin \Lambda_{2m} - \mu_{2m} (\cos \Lambda_{2m} - 1)]$$

by which the amplitudes A_m are completely determined.

The procedure, then, of finding temperature transients $T(x, t)$ in the composite wall consists essentially of the following steps. First, with the given material

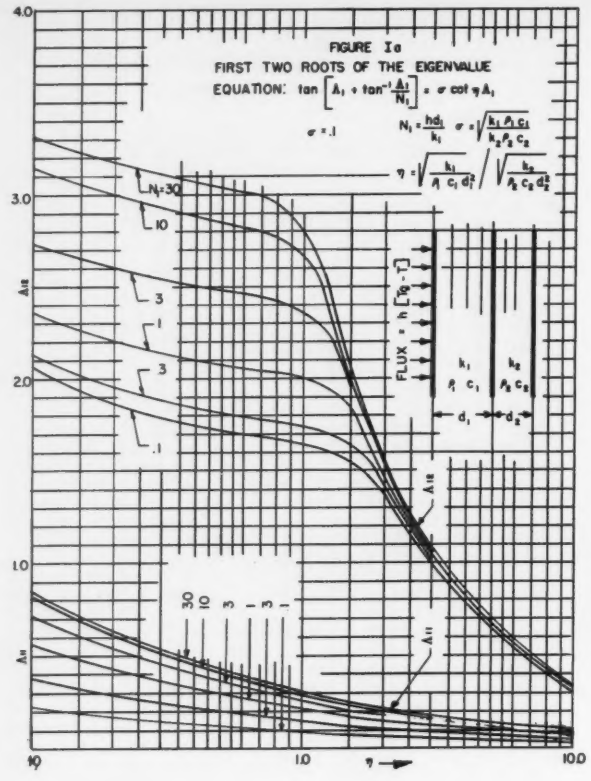
FIGURE Ia
FIRST TWO ROOTS OF THE EIGENVALUE
EQUATION: $\tan\left[\Lambda_1 + \tan^{-1}\frac{\Lambda_1}{N_1}\right] = \sigma \cot \eta \Lambda_1$
$\sigma = .1$
$N_1 = \frac{hd_1}{k_1}$ $\sigma = \sqrt{\frac{k_1 \rho_1 c_1}{k_2 \rho_2 c_2}}$
$\eta = \sqrt{\frac{k_1}{\rho_1 c_1 d_1^2}} \Big/ \sqrt{\frac{k_2}{\rho_2 c_2 d_2^2}}$
$N_1 = 30$
10
3
1
.3
.1
FLUX = h [To - T]
k_1 ρ_1 c_1
k_2 ρ_2 c_2
d_1
d_2
Λ_{12}
Λ_{11}
4.0
3.0
2.0
1.0
Λ_{12}
Λ_{11}
.10
1.0
η →
10.0

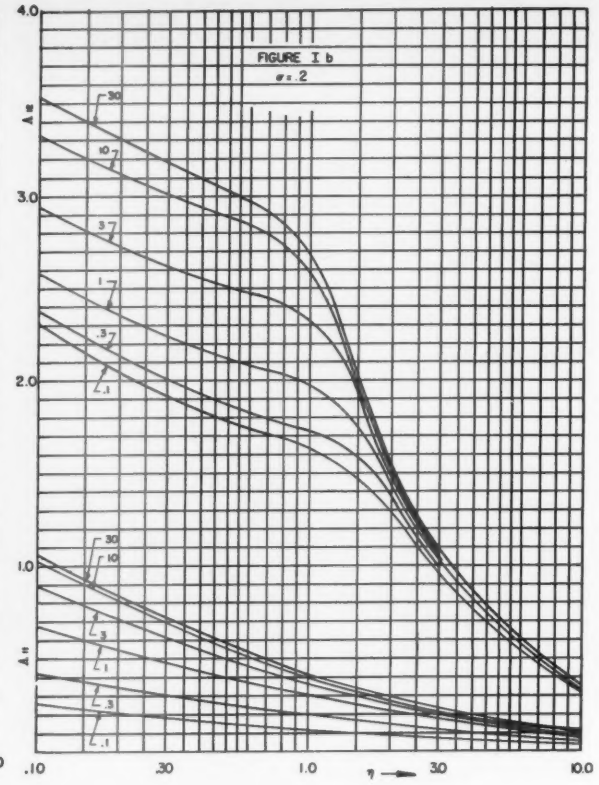
FIGURE I b
$\sigma = .2$
Λ_{12}
Λ_{11}
30
10
3
1
.3
.1
4.0
3.0
2.0
1.0
.10
.30
1.0
3.0
10.0
η →

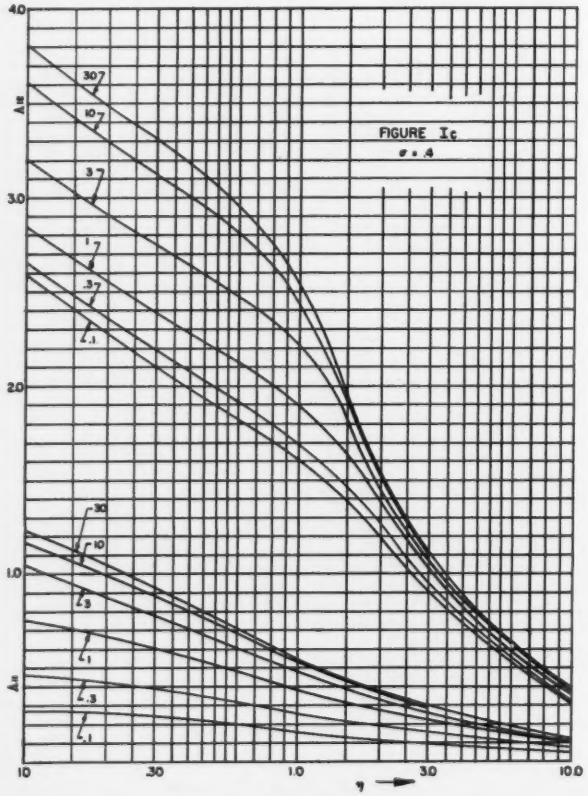
FIGURE Ic
$\sigma = .4$
Λ_{12}
Λ_{11}
30
10
3
1
.3
.1
4.0
3.0
2.0
1.0
10
.30
1.0
3.0
10.0
η →

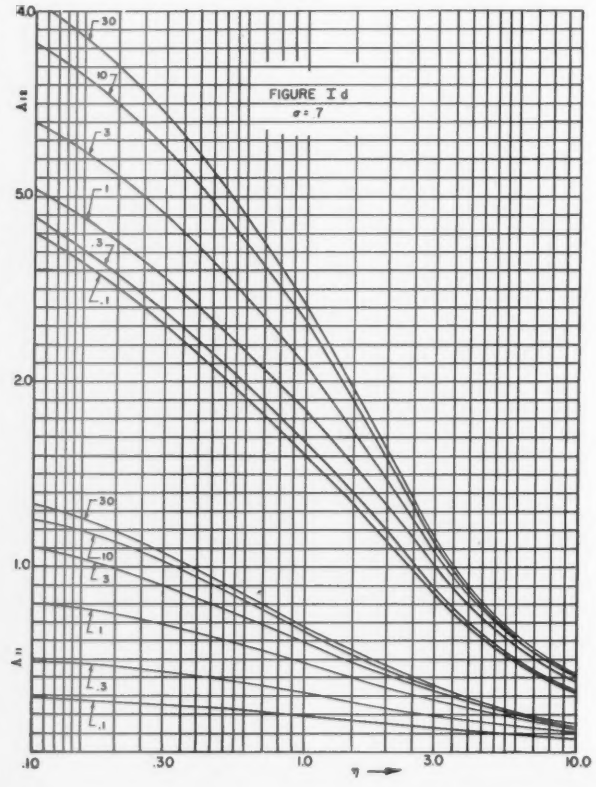
FIGURE I d
$\sigma = .7$
Λ_{12}
Λ_{11}
30
10
3
1
.3
.1
4.0
5.0
2.0
1.0
.10
.30
1.0
3.0
10.0
η →

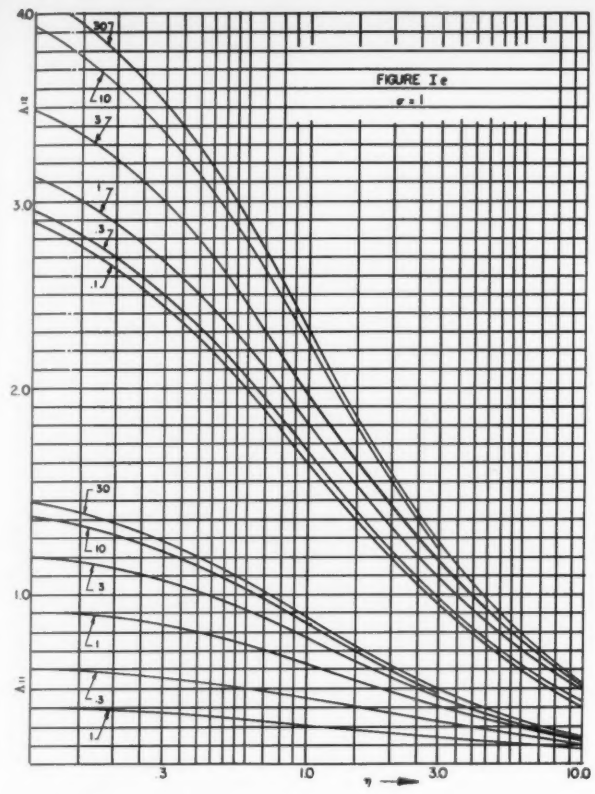

constants, dimensions, and heat transfer coefficient we determine the eigenvalues λ_n or the related eigenvalues $\Lambda_{1n} = \dfrac{\lambda_n d_1}{\alpha_1}$ from the eigenvalue Equation [18]. These immediately yield the time dependence and the amplitude ratios

$$\mu_{1n} = \frac{\tan \Lambda_{2n}}{\sigma} = \frac{\tan \dfrac{\alpha_1 d_2}{\alpha_2 d_1} \Lambda_{1n}}{\sigma}$$

$$\mu_{2n} = \tan \Lambda_{2n} = \tan \frac{\alpha_1 d_2}{\alpha_1 d_1} \Lambda_{1n}$$

Finally, the amplitudes A_n are computed from [23] and the spatial functions f_n are constructed as given by [20]. In this manner all the terms entering into the temperature distribution $T(x, t)$ given by [19] or its alternate

$$T(x,t) = \begin{cases} T_0 + \sum A_n \left(\cos \Lambda_{1n} \dfrac{x}{d_1} + \mu_{1n} \sin \Lambda_{1n} \dfrac{x}{d_1} \right) e^{-\lambda_n^2 t} \\ \qquad\qquad -d_1 \le x \le 0 \\ T_0 + \sum A_n \left(\cos \Lambda_{2n} \dfrac{x}{d_2} + \mu_{2n} \sin \Lambda_{2n} \dfrac{x}{d_2} \right) e^{-\lambda_n^2 t} \\ \qquad\qquad 0 \le x \le d_2 \end{cases} \quad \ldots [19']$$

are uniquely determined in terms of specified material and heat transfer coefficient data.

In the application of Equation [19′], the first two terms in the Fourier sums are usually sufficient for an accurate computation of the temperature in the composite slab. The first two eigenvalues necessary for computations with these Fourier terms, are given in the next section for a wide range of heat transfer and material parameters.

4 The Eigenvalue Equation for Composite Slabs

While the eigenvalues Λ for the simple slab depend only on the parameter $N = hd/k$, as given by Equation [7′], the eigenvalues for the composite slab depend on three parameters, which can be exhibited by rearrangement of the eigenvalue Equation [18] in the form

$$\tan \left[\Lambda_1 + \tan^{-1} \frac{\Lambda_1}{N_1} \right] = \sigma \cot \eta \Lambda_1 \ldots\ldots\ldots [18']$$

where

$$N_1 = \frac{hd_1}{k_1} \qquad \sigma = \sqrt{\frac{k_1 \rho_1 c_1}{k_2 \rho_2 c_2}} \qquad \eta = \frac{\alpha_1}{d_1} \Big/ \frac{\alpha_2}{d_2} \equiv \frac{\Lambda_2}{\Lambda_1}$$

A simple graphical method of determining the eigenvalues of Λ_1 from [18′] involves the following steps. The parameters N_1, σ, and η are computed for the given heat transfer coefficient and material data. Next, each side of Equation [18′] is plotted as a function of Λ_1. The branches of the tangent on the left of [18′] intersect with the branches of the cotangent on the right at an infinite set of points having the eigenvalues as the abscissae of intersections: $\Lambda_1 = \Lambda_{11}$, $\Lambda_{12} \ldots \Lambda_{1n} \ldots$ From these the corresponding Λ_{2n} and λ_n are computed by

$$\Lambda_{2n} = \eta \Lambda_{1n} \qquad \lambda_n = \frac{\alpha_1}{d_1} \Lambda_{1n}$$

By the above graphical procedure the first two eigenvalues Λ_{11}, Λ_{12} were determined for a broad range of the parameters N_1, σ, and η as shown on the curves, Figs. Ia–Ie. The upper limit of unity on σ in these curves was based on the consideration that, in general, the shielding material has a lower thermal conductivity than the envelope material, while the heat capacity per unit volume, ρc, for most materials is of the same order of magnitude. Thus $\rho_1 c_1 \sim \rho_2 c_2$ and $k_1/k_2 < 1$ limit the range of interest of σ in rocket applications to $0 < \sigma \le 1$.

5 The "Thick" Thermal Shield

A considerable simplification in the calculation of temperature transients in composite walls can be effected when, either because of low shield material conductivity, $k_1 << k_2$, or because of large shield thickness $d_1 >> d_2$, the envelope material has no appreciable temperature gradients. Indeed it may be readily visualized that whenever the heat transferred through the interface at $x = 0$ is sufficiently small, the envelope is instantaneously at the interface temperature, $T(0, t)$. Under these conditions the envelope material behaves as though its thermal conductivity were infinite, and the temperature distribution within the shield can be deduced from the general results of Section 3 by a limiting process in which $k_2 \to \infty$.

Consider, for example:

$$\lim_{k_2 \to \infty} \Lambda_{2n} = \lim_{k_2 \to \infty} \frac{\lambda_n d_2}{\sqrt{\dfrac{k_2}{\rho_2 c_2}}} = 0$$

$$\lim_{k_2 \to \infty} \mu_{2n} = \lim_{k_2 \to \infty} \tan \Lambda_{2n} = 0$$

leading to the result that the spatial variation of the temperature within the envelope material vanishes:

$$\lim_{k_2 \to \infty} f_{2n} = \lim_{k_2 \to \infty} A_n \left(\cos \Lambda_{2n} \frac{x}{d_2} + \mu_{2n} \sin \Lambda_{2n} \frac{x}{d_2} \right) = A_n$$

The eigenvalue Equation [18′] can be simplified by noting that for large k_2

$$\eta = \frac{\alpha_1}{d_1} \Big/ \frac{\alpha_2}{d_2} = \sqrt{\frac{k_1}{\rho_1 c_1} \frac{\rho_2 c_2}{k_2}} \frac{d_2}{d_1} \to 0 \quad \cot \eta \Lambda_1 \to \frac{1}{\eta \Lambda_1}$$

so that

$$\lim_{k_2 \to \infty} \sigma \cot \eta \Lambda_1 = \lim_{k_2 \to \infty} \frac{1}{\Lambda_1} \frac{\sigma}{\eta} = \frac{1}{\Lambda_1} \frac{\rho_1 c_1 d_1}{\rho_2 c_2 d_2} \quad \ldots\ldots [24]$$

and, therefore, Equation [18′] reduces to

$$\tan \left[\Lambda_1 + \tan^{-1} \frac{\Lambda_1}{N_1} \right] = \frac{1}{\Lambda_1} \frac{\rho_1 c_1 d_1}{\rho_2 c_2 d_2}$$

The first two eigenvalues computed from the latter are plotted on Fig. 2 for the range

$$0 < \frac{\rho_2 c_2 d_2}{\rho_1 c_1 d_1} < 1$$

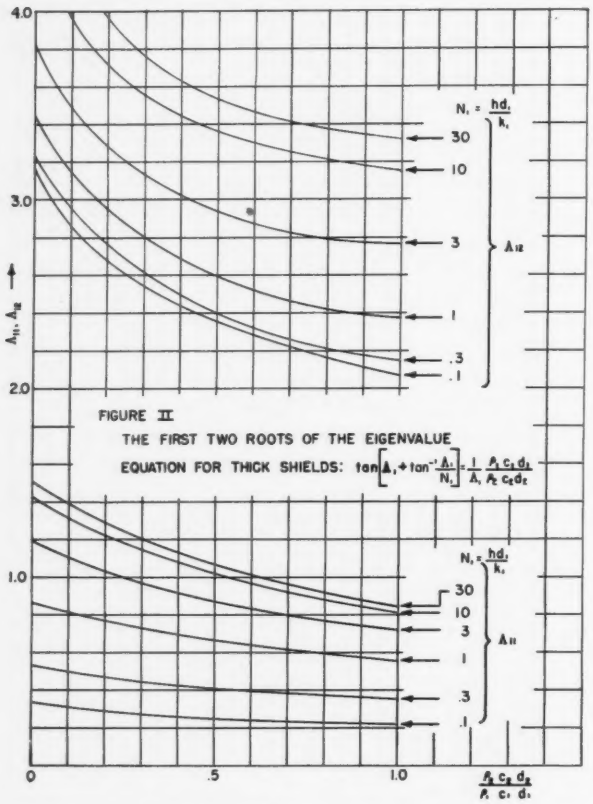

FIGURE II
THE FIRST TWO ROOTS OF THE EIGENVALUE EQUATION FOR THICK SHIELDS: $\tan\left[\Lambda_1 + \tan^{-1}\frac{\Lambda_1}{N_1}\right] = \frac{1}{\Lambda_1}\frac{\rho_1 c_1 d_1}{\rho_2 c_2 d_2}$

For the determination of the expressions D_n, N_n which enter into the amplitude formula [23], the limiting process yields the values

$$\lim_{k_2 \to \infty} D_{2n} = d_2 \qquad \lim_{k_2 \to \infty} N_{2n} = d_2$$

while D_{1n} and N_{1n} remain as derived previously in Section 3, with the additional restriction implicit in [24]

$$\lim_{k_2 \to \infty} \mu_{1n} = \lim_{k_2 \to \infty} \frac{\tan \Lambda_{2n}}{\sigma} = \Lambda_1 \frac{\rho_1 c_2 d_2}{\rho_1 c_1 d_1}$$

Hence, the amplitude formula [23] is reducible to

$$\lim_{k_2 \to \infty} A_n = -2T_v \frac{\sin \Lambda_{1n} + \mu_{1n} \cos \Lambda_{1n}}{(1 + \mu_{1n}^2)\Lambda_{1n} + (1 - \mu_{1n}^2) \sin \Lambda_{1n} \cos \Lambda_{1n} + 2\mu_{1n} \cos^2 \Lambda_{1n}} \quad \ldots [23']$$

With these results Equation [19′] represents the temperature distribution in the composite slab in which the shielded medium behaves essentially as on thermal capacity of magnitude $\rho_2 c_2 d_2$ per unit area, being at any instant at the interface temperature

$$T(0, t) = T_v + \sum A_n e^{-\lambda_n^2 t} \qquad 0 \le x \le d_2$$

It may be noted here that, while the limiting case considered in this section can be formulated directly as a simple slab problem for the shield material receiving heat from the flame as in the boundary condition

$$-k_1 \frac{\partial T(-d_1, t)}{\partial x} = h \left[T_v - T(-d_1, t) \right] \quad \ldots\ldots [2'']$$

and transferring heat to the thermal capacity according to the boundary condition

$$-k_1 \frac{\partial T(0, t)}{\partial x} = \rho_2 c_2 d_2 \frac{\partial T(0, t)}{\partial t} \quad \ldots\ldots [3'']$$

the method of separation of variables does not immediately lead to the solution because of the time derivative present in [3′]. Thus, while the separation of variables yields the eigenvalue Equation [18′], the spatial eigenfunctions obtained are not orthogonal over the range $-d_1 \le x \le 0$ occupied by the slab. [Owing to the presence of the time derivative, this boundary condition is not of the Sturm-Liouville type which assures orthogonality (4)]. In order to perform the Fourier expansion of the initial condition, one must first construct orthogonal functions from the ones yielded by [2′] and [3′]. The limiting procedure employed in this section obviates the need for the construction of orthogonal eigenfunctions from those obtainable with the boundary conditions [2″] and [3″].

6 The "Thin" Thermal Shield

Owing to the role of the expression d^2/α^2 in many heat flow problems, this ratio represents roughly the heat diffusion time, τ, across a thickness d of a material of diffusivity α^2. From this point of view the parameter η is, by definition, related to the diffusion times τ_1 and τ_2 in the two components of the composite slab by

$$\eta = \sqrt{\frac{k_1}{\rho_1 c_1 d_1^2} \frac{\rho_2 c_2 d_2^2}{k_2}} = \sqrt{\frac{\tau_2}{\tau_1}} \equiv \frac{\Lambda_2}{\Lambda_1}$$

For increasing values of η the eigenvalues, Λ_1 diminish, as can be seen from the curves on Fig. 1, and for the first two eigenvalues Equation [18′] may be written in the approximation

$$\tan \left(\Lambda_1 + \frac{\Lambda_1}{N_1} \right) \simeq \Lambda_1 \left(1 + \frac{1}{N_1} \right) = \sigma \cot \eta \Lambda_1 \quad \ldots [18'']$$

This, in turn, may be put into a form for $\Lambda_2 = \eta \Lambda_1$, analogous to the eigenvalue equation for a simple slab

$$\Lambda_2 \tan \Lambda_2 = \frac{\sigma\eta N_1}{1 + N_1} = \frac{hd_2/k_2}{1 + N_1} \quad \ldots\ldots [18''']$$

with an effective (reduced) heat transfer coefficient

$$h_{\text{eff}} = \frac{h}{1 + N_1} \quad \ldots\ldots [25]$$

Furthermore, for $\eta >> 1$, the first two amplitudes A_1 and A_2 in Equation [23] are given approximately by

$$A_n \simeq -T_g \frac{N_{2n}}{D_{2n}} = -T_g \frac{4 \sin \Lambda_{2n} \cos \Lambda_{2n}}{2\Lambda_{2n} + \sin 2\Lambda_{2n}} \quad \ldots\ldots [23'']$$

so that in this case the spatial function reduces to

$$\lim_{\eta >> 1} f_{2n} = \lim_{\eta >> 1} A_n \left(\cos \Lambda_{2n} \frac{x}{d_2} + \mu_{2n} \sin \Lambda_{2n} \frac{x}{d_2} \right) = -T_g \frac{4 \sin \Lambda_{2n} \cos \Lambda_{2n} \left(1 - \frac{x}{d_2}\right)}{2\Lambda_{2n} + \sin 2\Lambda_{2n}}$$

which is analogous to the result for the spatial dependence of the temperature in the simple slab Equation [5']. Here, of course, the "flameside" corresponds to the coordinate $x = 0$, and the insulated boundary is at $x = d_2$.

Thus, for sufficiently large η, the problem of the temperature distribution in a shielded envelope can be reduced to solving for the temperature distribution in a simple slab, with the material data of the envelope and a reduced heat transfer coefficient given by [25] provided that the first two eigenvalues $\Lambda_{1n} = \Lambda_{2n}/\eta$ computed from the solution of [18'''] satisfy the approximation in [18'].

The expression for an effective heat transfer coefficient [25] for thin shielding layers may be inferred from a discussion (Ref. 1, p. 15) of thin surface skins of oxide, grease, scale, and other materials of poor conductivity, in which the thermal capacity may be neglected, and, hence, the temperature gradient may be assumed uniform at any instant. With the notation of Section 3

$$T(x, t) = \begin{cases} F_1(x, t) & -d_1 \leq x \leq 0 \\ F_2(x, t) & 0 \leq x \leq d_2 \end{cases}$$

we obtain for the instantaneously uniform-temperature gradient in the shield material

$$\frac{\partial F_1}{\partial x}(x, t) = -\frac{h}{k_1} [T_g - F_1(-d_1, t)] = \text{const} \ldots [16']$$

which, upon integration, yields

$$F_1(x, t) = -\frac{hx}{k_1} [T_g - F_1(-d_1, t)] + F_1(0, t) \ldots . [16'']$$

Now, the interface boundary condition becomes

$$k_1 \frac{\partial F_1(0, t)}{\partial x} = k_1 \frac{\partial F_1(-d_1, t)}{\partial x} = -h[T_g - F_1(-d_1, t)] = k_2 \frac{\partial F_2(0, t)}{\partial x} \ldots . [15']$$

Substituting the value of $F_1(-d_1, t)$ obtained from [16'']:

$$F_1(-d_1, t) = \frac{N_1 T_g + F_1(0, t)}{1 + N_1}, \qquad N_1 = \frac{hd_1}{k_1}$$

and employing the second interface condition [14] to replace $F_1(0, t)$ by $F_2(0, t)$, we obtain from [15']

$$-\frac{h[T_g - F_2(0, t)]}{1 + N_1} = k_2 \frac{\partial F_2(0, t)}{\partial x} \quad \ldots\ldots [15'']$$

which shows that the temperature distribution F_2 in the shielded material is subject to a boundary condition of Newtonian heat transfer with an effective heat transfer coefficient as given by [25]. With the boundary conditions [15''] and [17], the treatment of envelope as a simple slab leads to the eigenvalue equation [18'''], but the validity of neglecting the thermal capacity of the shield material need be justified by satisfying the approximation in [18''] for the first few eigenvalue which enter into the practical computations of the temperature distribution.

7 Application to Composite Cylindrical Walls

In application to rocket engineering, the temperature transients arising in relatively thin cylindrical walls are, in practice, computed with sufficient accuracy by treatment of the equivalent plane, parallel slab problem. It can be shown by detailed study of the temperature transients in the simple cylindrical shell under Newtonian heat input that, if the thickness-to-radius ratio does not exceed 0.2, the equivalent slab treatment yields results accurate within 0.03 T_g on the conservative side from the design point of view, since the cylinder temperature does not exceed anywhere, at any instant, the corresponding slab temperature. The results of the analysis presented here for composite slabs are also conservative in application to cylindrical walls, but appear sufficiently accurate in practice if the total thickness-to-radius ratio does not exceed 0.2.

As an example of the application of the thin shield formulas we consider the effect of zirconia on a low-carbon steel nozzle in prolonging the duration time before allowed temperatures in the steel are exceeded. We may limit the allowed temperature, T_a, on the flame side to $T_g/2$, where the flame temperature, T_g, is of the order of 4500 F. As a representative value of the heat transfer coefficient in the nozzle we set

$$h = 1500 \frac{\text{Btu/hr}}{\text{ft}^2 \text{ deg F}}$$

and determine the duration times in a $^1/_4$-in. thick, low-carbon steel wall for the following cases: (*a*) no shielding; (*b*) shielding by an 0.02-in. thick layer of zirconia.

The material properties employed are listed in the table below, those for zirconia being taken from Ref. (5).

Property	Material	
	Low carbon steel	Insulating stabilized zirconia
Thermal conductivity k Btu/hr ft² (deg F/ft)	20	0.3
Density ρ lb/ft³	485	175
Specific heat c Btu/lb deg F	.15	.16
Diffusivity $\alpha^2 = \frac{k \text{ ft}^2}{\rho c \text{ hr}}$	.274	.0107

In case (*a*) we have the Biot number

$$N = \frac{hd}{k} = \frac{1500}{20}\left(\frac{.25}{12}\right) = 1.56$$

which yields from Equation [7′] the first two eigenvalues

$$\Lambda_1 = 1.00 \qquad \Lambda_2 = 3.56$$

With these the first two exponents in Equation [5′] become

$$\lambda_1^2 t = \frac{d^2\Lambda_1^2}{d^2}\, t = 630t \qquad \lambda_2^2 t = \frac{d^2\Lambda_2^2}{d^2}\, t = 7950t$$

where t is in units of hours. Inserting the above results in Equation [5′] corresponding to the flameside $x = 0$, we obtain the equation for the duration time t_D in units of seconds:

$$1 - .625e^{-.175t_D} - .095e^{-2.21t_D} = \frac{T_a}{T_g} = .5$$

with the result $t_D = 1.25$ sec.

In case (*b*) the thin shield formulas [18‴] and [25] involve the reduction factor

$$1 + N_1 = 1 + \frac{1500}{.3}\left(\frac{02}{12}\right) = 9.3$$

yielding the effective Biot number and heat transfer coefficient

$$N_{eff} = \frac{N}{1 + N_1} = 1.68 \qquad h_{eff} = \frac{h}{1 + N_1} = 161\ \frac{\text{Btu/hr}}{\text{ft}^2\ \text{deg F}}$$

Use of the simple slab formula [5′] with this N_{eff} shows that only the first term in the Fourier sum is of importance, and that the first eigenvalue is approximately given by

$$\Lambda_1 \tan \Lambda_1 \approx \Lambda_1^2 = N_{eff}$$

whereby [5′] reduces to

$$\frac{T}{T_g} \approx 1 - e^{-h_{eff}t/\rho cd}$$

indicating that the shielded metal now behaves essentially as a thermal capacity with negligible gradients within it. The prolonged duration time t_D' in units of seconds is

$$t_D' = 3600\,\frac{\rho cd}{h_{eff}} \log \frac{T_g}{T_g - T_a} = 24 \text{ sec}$$

The thick shield formulas developed in Section 5 are convenient in the design of insulating refractory liners for rocket chambers with heating times up to the order of a minute, as in some liquid propellant units. Such units are usually regeneratively cooled, but the possibility of using composite chamber walls which are competitive from the weight point of view may be considered. In a composite wall the weight per unit area

$$w = \rho_1 d_1 + \rho_2 d_2 \ldots\ldots\ldots\ldots\ldots\ldots [26]$$

may be minimized subject to the following considerations. The metallic envelope must be sufficiently thick to carry the pressure loads during firing, i.e.,

$$d_2 \geq \frac{pR}{S_2} \ldots\ldots\ldots\ldots\ldots\ldots [27]$$

where p is the chamber pressure, R the chamber radius, and S_2 is the yield stress in the envelope material. The yield stress S_2 is, however, a function of the temperature T_2, generally diminishing as T_2 increases and, therefore, as the duration of the firing t_D increases. Now, for any desired duration time t_D, it is possible to select an infinite set of thicknesses (d_1, d_2) large enough to maintain the inequality in [27]. In the set (d_1, d_2) there is, in general, a particular pair of thicknesses which minimizes the weight per unit area w. As a design criterion we may, therefore, consider the optimum choice of (d_1, d_2) such that, for specified materials and heating parameters, the pair (d_1, d_2) shall make w in Equation [26] a minimum and lead to equality in [27] at the time $t = t_D$.

The comparison of weights for two zirconia-metal composite walls with reference conditions in a chamber given by

$$h = 300\ \frac{\text{Btu/hr}}{\text{ft}^2\ \text{deg F}} \qquad T_g = 4500 \text{ deg F} \qquad pR = 1400\ \frac{\text{lb}}{\text{in.}^2}\ \text{in.}$$

is shown on Fig. 3. The desired duration time has been

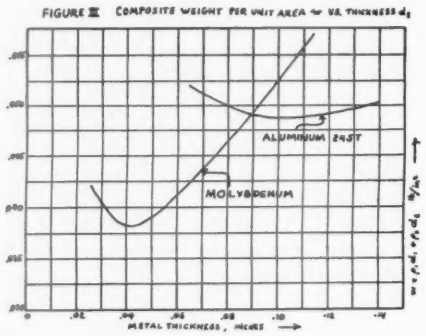

taken as $t_D = 60$ sec. For a regeneratively cooled unit operating under the above chamber conditions, the weight per unit area of the stainless-steel jacket wall and the included coolant is $w = .040$ lb/in.^{2}. From Fig. 3 it is seen that the zirconia-molybdenum combination appears to be weight-wise competitive with the regeneratively cooled unit up to 60 seconds of firing duration.

References

1 "Conduction of Heat in Solids," by H. S. Carslaw and J. C. Jaeger, Oxford University Press, 1947.

2 "Heat Conduction in Composite Circular Cylinders," by J. C. Jaeger, *Philosophical Magazine*, vol. 32, 1941, pp. 324.

3 "Heat Transmission," by W. H. McAdams, New York, McGraw-Hill Book Co., 1942.

4 "Fourier Series and Boundary Value Problems," by R. V. Churchill, New York, McGraw-Hill Book Co., 1941.

5 "Properties and Uses of Pure Oxide Heavy Refractories," by O. J. Whittemore, Jr., Norton Research Laboratories, Worcester, Mass., reprinted from a paper delivered by the author at the 50th Annual Program of the American Ceramic Society, 1948.

A Comparison of Adiabatic and Isothermal Expansion Processes in Rocket Nozzles

H. S. SEIFERT[1] and D. ALTMAN[2]

Jet Propulsion Laboratory, California Institute of Technology, Pasadena, Calif.

An analysis has been made of the expansion of gases through a de Laval nozzle under isothermal conditions. It is shown that for ideal gases, the increase in kinetic energy of the gases is equal to the heat transferred into the gas to maintain constant temperature. The initial energy, or temperature, enters only in the design of the nozzle and determination of the pressure ratio required for the transference of the fixed quantity of heat. Unlike the adiabatic case, the jet velocity is not limited by the initial energy content of the gas but only by the pressure ratio or energy content of the reservoir transferring the heat. Formulas are derived for isothermal exhaust velocity, mass flow, and thrust coefficient which are analogous to those for adiabatic flow.

Nomenclature

a = isothermal sonic velocity = $\sqrt{R_s T}$
a' = adiabatic sonic velocity = $\sqrt{\gamma R_s T}$
c^* = mass flow constant (chamber pressure per unit throat area per unit mass flow rate)
c_p = specific heat at constant pressure
c_v = specific heat at constant volume
C_F = nozzle thrust coefficient
dq = increment of heat energy
e = base of natural logs
E = internal energy
f = nozzle section area
F = thrust exerted due to flow through nozzle
F' = free energy
H = enthalpy
$\dot{m}$ = dm/dt = time rate of mass flow
p = free-stream pressure
R_s = specific gas constant = R/M
S = entropy
T = free-stream temperature
v = mean gas velocity
V = specific volume
γ = c_p/c_v = ratio of specific heats
Γ' = prescribed function of γ
λ = nozzle divergence correction factor
ρ = density of gas

Subscripts

a = adiabatic
c = chamber or initial
e = exit or ambient
i = isothermal
o = atmospheric or standard
t = throat

Received July 9, 1951.
[1] Staff Engineer. Member ARS.
[2] Chief, Chemistry Section. Member ARS.
[3] Numbers in parentheses refer to References on page 162.

THE adiabatic expansion of gases through a de Laval nozzle is well understood and fully documented (1 and 2).[3] It is of some theoretical interest to compare the behavior of such a nozzle with that of the less familiar one in which the expansion process takes place isothermally. A partial treatment of such a nozzle has already been given in this JOURNAL (3). An isothermal expansion would be difficult to realize in practice, since it implies that energy is supplied continuously during expansion to the axial translational degree of freedom of the gas molecules. It might be achieved to a limited extent by the release of chemical energy, by convective heat transfer, or most probably by absorption of radiant energy. An interesting consequence of isothermal expansion is that the velocity of the gas increases without limit as the pressure ratio increases.

Conservation of Energy

Assume that an isothermal process is possible. It will be shown that the thermodynamic function termed free energy F', which has been found useful in chemical calculations (4), will play the same part in isothermal nozzle calculations as the enthalpy H does in adiabatic calculations. The free energy F' is defined as

$$\begin{aligned} F' &= \text{total heat} - \text{unavailable or reversible heat} \\ &= H - TS \\ &= E + pV - TS \end{aligned}$$

F' represents the energy which is available (i.e., free) to do external work. Consider the equations of energy and momentum.

Energy:

$$dq = dE + p\,dV = d(E + pV) - \frac{1}{\rho}\,dp \quad \ldots\ldots [1]$$

Momentum:

$$\rho v\,dv = -dp \quad \ldots\ldots [2]$$

From Equation [2]

$$-\frac{1}{\rho}\,dp = v\,dv = \frac{1}{2}\,d(v^2)$$

Therefore, Equation [1] becomes

$$dq = d(E + pV) + d\left(\frac{1}{2}\,v^2\right)$$

or

$$d\left(E + pV + \frac{1}{2}\,v^2\right) - dq = 0 \quad \ldots\ldots [3]$$

By definition

$$dq \equiv T\,dS$$

For the isothermal case T = const, and

$$T\,dS = d(TS) \quad [4]$$

Using Equation [4] in Equation [3]

$$d\left(E + pV + \frac{1}{2}v^2\right) - d(TS) = 0$$

or

$$(E + pV - TS) + \frac{1}{2}v^2 = \text{const}$$

That is,[4]

$$F' + \frac{1}{2}v^2 = \text{const} \quad [5]$$

This equation may be compared with the usual adiabatic energy relation (5)

$$H + \frac{1}{2}v^2 = \text{const} \quad [6]$$

Exhaust Velocity

The relations [5] and [6] are general and apply to all real fluids. To calculate the exhaust velocity for an isothermal nozzle, it will be necessary to reduce generality by considering a fluid; for example, an ideal gas whose equation of state can be analytically expressed. It is possible to write an equation of state (6) for rocket combustion products, which is a good approximation to real gas behavior because the temperatures are high, pressures are moderate, and corrections due to intermolecular forces are low. This discussion will be limited, however, to the ideal nonreacting gas case.

Assume an equation of state

$$p = R_s T \rho \quad [7]$$

Combining Equations [2] and [7] to eliminate ρ,

$$v\,dv = -R_s T \frac{dp}{p}$$

or

$$\frac{v^2}{2} = -R_s T \ln p + \text{const} \quad [8]$$

Thus it may be seen from Equation [5] that the free energy for isothermal expansion of a perfect gas is

$$F' = R_s T \ln p + \text{const} \quad [9]$$

and that this isothermal process is one in which F' is converted into ordered kinetic energy of the gas. If subscript c indicates chamber conditions, the integration constant in Equation [8] may be evaluated by noting that when $p = p_c$, then $v = v_c$ and $T = F_c$. Thus

$$\frac{1}{2}v^2 - \frac{1}{2}v_c^2 = R_s T_c \ln (p_c/p) = \Delta F' \quad [10]$$

It may be seen from Equation [10] that as $p \to 0$, $v \to \infty$, unlike the adiabatic case in which v approaches a fixed limit v_{max} as $p \to 0$. The conventional adiabatic equation (cf. Equation 24 of Ref. 5) for v^2 is

$$v^2 - v_c^2 = \frac{\gamma}{\gamma - 1} 2R_s T_c \left[1 - \left(\frac{p_e}{p}\right)^{(1-\gamma)/\gamma}\right] \quad [11]$$

If numerical values are inserted in Equations [10] and [11], with v_c^2 neglected, the following ratios for isothermal to adiabatic exit velocity v_i/v_a result (take γ = 1.25 in the adiabatic case, and $R_s T_c$ the same in each case):

p_c/p_e	v_i/v_a
20:1	1.16
100:1	1.24
1000:1	1.36
∞:1	∞

This tabulation indicates a 16 to 36 per cent so-called improvement in exhaust velocity as the pressure ratio goes through the indicated range, and the limiting percentage of improvement is infinite. The limiting infinite value results from the fact that the nozzle absorbs an infinite amount of energy from the heat reservoir in this case.

Equation [10] may be regarded as a special case of Equation [11] in which γ approaches unity. Equation [11] becomes indeterminate of the form 0/0 as $\gamma \to 1.0$. By applying L'Hospital's rule and taking the limit, Equation [11] transforms into Equation [10].

Since $c_p = \gamma R_s/(\gamma - 1)$, the physical meaning of $\gamma = 1$ is infinite specific heat. The more nearly $\gamma \to 1.0$, the smaller the temperature change associated with a unit amount of external mechanical work performed adiabatically by the gas. The more complex the gas molecule, the greater its ability to store energy at a given temperature; that is, the greater the number of ways it can absorb energy in other than translational motion and the nearer γ approaches unity. A gas with $\gamma = 1.0$ has in effect an infinite reservoir of heat within each molecule and can expand both adiabatically and isothermally at the same time. A real gas with $\gamma > 1.0$ may expand isothermally, but only if heat is supplied to it from external sources.

Mass Flow and Throat Area

Equation [10] may be expressed in terms of area f rather than pressure p by using the equation of state (Equation [7]) and of continuity

$$\rho v f = \dot{m} \quad [12]$$

to eliminate p_c/p; thus

$$p_c/p = vf/v_c f_c \quad [13]$$

and Equation [10] becomes

$$f = \frac{v_c f_c}{v} e^{(v^2 - v_c^2)/2R_s T_c}$$

Another combination of the state and continuity equations (Equations [7] and [12]) yields

$$v_c f_c = \frac{\dot{m} R_s T_c}{p_c} \quad [14]$$

Hence

$$f = \frac{\dot{m} R_s T_c}{p_c} \frac{1}{v} e^{(v^2 - v_c^2)/2R_s T_c} \quad [15]$$

[4] The authors are indebted to H. S. Tsien for this derivation of Equation [5].

From the form of Equation [15] it is evident that a throat will exist (minimum of f) since $f \to \infty$ as v approaches either 0 or ∞. To find the throat values of v and f, denoted by a subscript t, differentiate Equation [15] with respect to v and equate to zero. This operation gives

$$\frac{df}{dv} = e^{(v^2 - v_c^2)/2R_sT_c}\left(\frac{\dot{m}R_sT_c}{p_c}\right)\left(\frac{1}{R_sT_c} - \frac{1}{v^2}\right) = 0 \quad \ldots [16]$$

or

$$v_t = \sqrt{R_sT_c} \quad \ldots [17]$$

Equation [17] shows that the gas velocity v_t is also the isothermal sonic velocity at the throat. This equation is to be compared with the adiabatic case (cf. Equation 37 of Ref. 5) for which

$$v_t = \sqrt{\gamma R_sT_t} \quad \ldots [18]$$

The throat area f_t in the isothermal case may now be calculated from Equation [15], neglecting v_c^2 relative to v_t^2,

$$f = \frac{\dot{m}}{p_c}\sqrt{eR_sT_c} \quad \ldots [19]$$

Equation [19] may also be regarded as a means for calculating the mass flow rate $\dot{m}$. If it is desired to define a characteristic velocity $c^* = p_cf_t/\dot{m}$ analogous to the adiabatic case (cf. Equation 52 of Ref. 5), then

$$c^* = \sqrt{eR_sT_c} = \sqrt{e}\,a_c \quad \ldots [20]$$

where a_c is the sonic velocity for a gas with $\gamma = 1$. This c^* may be of value in calculating mass flow and as in the adiabatic case may be considered as a measure of propellant performance. The corresponding adiabatic definition of c^* is

$$c^* = \gamma^{-1}\left(\frac{2}{\gamma+1}\right)^{(\gamma+1)/2(1-\gamma)}\sqrt{\gamma R_sT_c} \quad \ldots [21]$$
$$= \gamma^{-1}\left(\frac{2}{\gamma+1}\right)^{(\gamma+1)/2(1-\gamma)}a'_c$$

where a'_c is the adiabatic sonic velocity in the combustion chamber. As in the case of Equation [10], Equation [20] may be derived from Equation [21] by taking the limit as $\gamma \to 1.0$.

Thrust Coefficient and Expansion Ratio

In order to calculate thrust F and thrust coefficient C_F, customary definitions are used which are unaffected by the nature of the thermodynamic process involved, namely,

$$F = \lambda\dot{m}v_e + (p_e - p_o)f_e \quad \ldots [22]$$

and

$$C_F = F/p_cf_t \quad \ldots [23]$$

Thus, using Equations [10] and [19], with v_c^2 neglected

$$F = \lambda\sqrt{\frac{2}{e}}\,f_tp_c[\ln(p_c/p_e)]^{1/2} + (p_e - p_o)f_e \quad \ldots [24]$$

$$C_F = \lambda\sqrt{\frac{2}{e}}\,[\ln(p_c/p_e)]^{1/2} + \left(\frac{p_e - p_o}{p_c}\right)\frac{f_e}{f_t} \quad \ldots [25]$$

Equations [24] and [25] are to be compared with the adiabatic relations (cf. Equations 49 and 50 of Ref. 5)

$$F = \Gamma'\sqrt{\frac{2}{\gamma-1}}\,f_tp_c\left[1 - \left(\frac{p_e}{p_c}\right)^{(1-\gamma)/\gamma}\right]^{1/2} + (p_e - p_o)f_e \quad \ldots [26]$$

$$C_F = \Gamma'\sqrt{\frac{\gamma}{\gamma-1}}\left[1 - \left(\frac{p_e}{p_c}\right)^{(1-\gamma)/\gamma}\right]^{1/2} + \left(\frac{p_e - p_o}{p_c}\right)\frac{f_e}{f_t} \quad \ldots [27]$$

where

$$\Gamma' = \gamma\left(\frac{2}{\gamma+1}\right)^{(\gamma+1)/2(\gamma-1)}$$

In order to calculate the pressure ratio p_e/p_c used in Equation [25], a relation between area ratio and pressure ratio is needed. If one takes Equation [10] and changes variable from v to f by the successive use of Equations [12] and [7], then neglecting v_c^2

$$\left(\frac{\dot{m}}{\rho f}\right)^2 = \left(\frac{R_sT_c\dot{m}}{pf}\right)^2 = (2R_sT_c)\ln\frac{p_c}{p}$$

Eliminating $\dot{m}$ with Equation [19] gives

$$\frac{f}{f_t} = \frac{p_c/p}{\sqrt{2e}\,[\ln(p_c/p)]^{1/2}} \quad \ldots [28]$$

which may be compared with the corresponding adiabatic equation (cf. Equation 45 of Ref. 5)

$$\frac{f}{f_t} = \Gamma'\left\{\gamma\left(\frac{p}{p_c}\right)^{1/\gamma}\left(\frac{2}{\gamma-1}\right)^{1/2}\left[1 - \left(\frac{p_c}{p}\right)^{(1-\gamma)/\gamma}\right]^{1/2}\right\}^{-1} \quad \ldots [29]$$

To find the critical pressure ratio p_c/p_t, one may differentiate f in Equation [28] with respect to p and equate the result to zero, or simply set $f = f_t$ and solve for p_c/p_t. In either case

$$p_c/p_t = \sqrt{e} = 1.65 \quad \ldots [30]$$

which is independent of γ (as are all of the other isothermal relations). Equation [30] is to be compared with the usual adiabatic relation (cf. Equation 35 of Ref. 5)

$$\frac{p_c}{p_t} = \left(\frac{2}{\gamma+1}\right)^{\gamma/(1-\gamma)} \quad \ldots [31]$$
$$= 1.80 \text{ for } \gamma = 1.25$$

As before, Equation [30] can be obtained from Equation [31] by taking logarithms and applying L'Hospital's rule as $\gamma \to 1.0$.

Conclusions

It may be well to reiterate certain conclusions concerning the isothermal process for ideal gases which might otherwise be obscured among the algebra:

1 Unlike the adiabatic case, none of the performance parameters of an isothermal nozzle depends upon specific heat (or γ).

2 There is no limit to the theoretical exhaust velocity that can be obtained with a finite initial pressure, if sufficient heat is available in the reservoir.

3 The kinetic energy of the exhaust gases is obtained from the heat Δq which is transferred to the expanding gases. This heat is shown to be equal to the change $\Delta F'$ in free energy.

4 The limitations of such a process in practice would probably arise from inadequate heat transfer mechanisms.

References

1 "Rocket Propulsion Elements," by George P. Sutton, John Wiley & Sons, New York, 1949.

2 "Steam and Gas Turbines," by A. Stodola, McGraw-Hill Book Company, Inc., New York, 1927.

3 "Isothermal Expansion in Nozzles," by J. R. Randolph, JOURNAL OF THE AMERICAN ROCKET SOCIETY, No. 74, June 1948, p. 71.

4 "Thermodynamics, "by G. N. Lewis and M. Randall, McGraw-Hill Book Company, Inc., New York, 1923.

5 "Physics of Rockets," by H. S. Seifert, M. M. Mills, and Martin Summerfield, *American Journal of Physics*, vol. 15, 1947, pp. 1–21.

6 "The Computation of the Thermodynamic Properties of Real Gases and Mixtures of Real Gases," by James A. Beattie, *Chemical Reviews*, vol. 44, 1949, pp. 141–192.

The Transfer Functions of Rocket Nozzles

(*Continued from page 143*)

length nozzle, a desirable saving in experimentation. The present investigation also gives the characteristic nondimensional frequency as the angular frequency ω divided by the velocity gradient along the nozzle. The transfer functions for rocket nozzles of different sizes can be correlated through this nondimensional frequency or reduced frequency.

In conclusion then, it is certain that the present paper gives only a general outline of the problem of transfer function of rocket nozzles. The complete detail has yet to be filled in by further studies.

References

1 "Stability of Flow in a Rocket Motor," by D. F. Gunder and D. R. Friant, *Journal of Applied Mechanics*, vol. 17, no. 3, September 1950, p. 327.

2 "A Theory of Unstable Combustion in Liquid Propellant Rocket Systems," by M. Summerfield, JOURNAL OF THE AMERICAN ROCKET SOCIETY, vol. 21, no. 5, September 1951, p. 108.

3 "Aspects of Combustion Stability in Liquid Propellant Rocket Motors, Part I," by L. Crocco, JOURNAL OF THE AMERICAN ROCKET SOCIETY, vol. 21, no. 6, November 1951, p. 163.

4 "Aerodynamic Stability and Automatic Control," by W. Bollay, *Journal of the Aeronautical Sciences*, vol. 18, no. 9, 1951, p. 569, particularly p. 605.

JOURNAL BINDERS AVAILABLE

Handsome binder holds six issues (one year) of the ARS Journal

Approximately 8½" x 11½"

Blue leatherette with stamped letters

Simple metal rack, easy to assemble

- Keeps Journal securely in place
- Stands erect on bookshelf
- Convenient to carry
- Individual copies cannot be misplaced
- Back issues protected against damage

Price $2.00

Please order from

Secretary
American Rocket Society
29 West 39th Street
New York 18, N. Y.

CHANGE OF ADDRESS

Since the Post Office Department does not as a rule forward magazines to forwarding addresses, it is important that the Society be notified of changes in address thirty days in advance of publishing date to insure receipt of every issue of the Journal.

Address such notices as follows:

Secretary
American Rocket Society
29 West 39 Street
New York 18, N. Y.

Letters to the Editor

This section of the Journal is open to letters not exceeding 600 words in length (or one and one-half columns) devoted to brief research reports or technical discussions of papers previously published. Such letters are published without editorial review, usually within two months of the date of receipt. The style and manner of submission of letters are the same as for regular contributions. **(See inside back cover.)**

Jet Propulsion News

C. F. WARNER, Purdue University, *Associate Editor*

with the assistance of W. G. BOHL

Rockets

THE Russians are working on the further development of the following German rocket-propelled missiles: the Wasserfall anti-aircraft rocket; the A9, a winged version of the V-2; the A5, a half-scale V-2; and a rocket of the V-2 type. The work is being done at the reactivated Peenemunde missile center. New facilities, including six new launching ramps for a Matador-type missile, have been installed by the Russians. The airfield at Peenemunde West has been greatly expanded and over 80 MiG-15 interceptors are stationed there for the defense of the area. The base is the most tightly guarded "closed area" in the entire Soviet zone of Germany. A recent giant explosion within the guarded area prompted volunteer firemen of a nearby village to rush to the zone. They were immediately pushed away by Russian police.

✦ ✦ ✦

A PICTURE of the Armstrong-Siddeley "Snarler" liquid propellant rocket motor is presented in Fig. 1. This unit, reported in the January-February issue (p. 39) of the JOURNAL, consists of an externally driven propel-

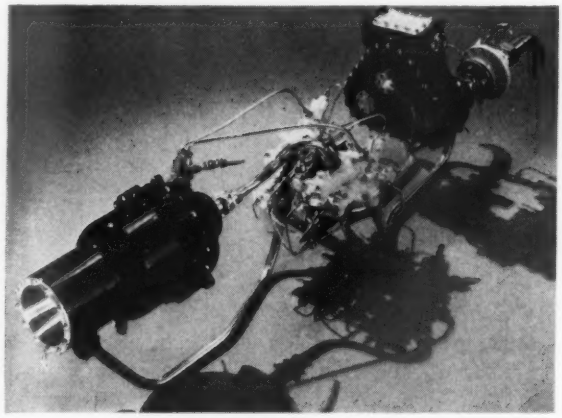

FIG. 1. ARMSTRONG-SIDDELEY ROCKET POWER PLANT FOR AIRCRAFT

lant pumping unit, propellant valve assembly, and thrust chamber. The system operates as follows: When the pilot switches on his master switch, the fuel and liquid oxygen pumps start to rotate. The liquid oxygen pump primes, then the fuel pump primes, and the igniter valves open automatically. The two liquid propellants flow to the igniter chamber, and the spark plug fires. This causes the igniter to light and to provide a pencil of flame in the combustion chamber. The main bipropellant valves now open automatically and the propellants flow into the combustion chamber where they are ignited by the pencil of flame. Finally, the rocket motor fires, the current to the spark plug is cut off, and the flow of propellants to the igniter chamber ceases. The motor may be operated at part-thrust, also.

✦ ✦ ✦

DURING a recent test conducted by U. S. Army Ordnance officers, the guided missile rocket, Nike, intercepted and "destroyed" a remote-controlled crewless B-17. The Nike has been ordered into mass production.

✦ ✦ ✦

RECENT news stories have aroused considerable interest in the guided missiles being developed in this country. Only the names and general field of application of these missiles are available at this time.

NAME	DEVELOPMENT AGENCY	MANUFACTURER	SERVICE
Terrier	Navy Bu Ord.	Convair	Anti-aircraft defense
Sparrow	Navy Bu Aer	Sperry	Air-to-air missile
Nike	Army Ord.	Bell Telephone, Douglas	Anti-aircraft defense
Matador	Air Force	G. L. Martin Co.	Medium-range bombardment
Snark	Air Force	Northrop Aircraft	Long-range bombardment
Hermes	Army Ord.	General Electric	Short-range bombardment
Loki	Army Ord.	Bendix	Anti-aircraft defense
Rascal	Air Force	Bell	Aircraft armament
Lark	Navy Bu Ord.	Fairchild Guided Missile	Anti-aircraft defense

✦ ✦ ✦

ANOTHER assault on the world's altitude record for single-stage rockets will be made next spring by a Navy Martin Viking. The forthcoming Viking will be somewhat different in appearance from its predecessors, however. The redesigned Viking No. 8 is greater in diameter, slightly shorter, and has fins three-quarters the size of the first seven Vikings. This new size will allow considerably more fuel to be carried, thus providing a longer thrust period. The power plant of the present Viking, made by Reaction Motors, Inc., develops approximately 20,000-lb thrust.

✦ ✦ ✦

GEORG M. Lorenian of West Germany has made two patent applications to the Swiss Federal Patent Office at Berne covering the use of liquid propellant rockets to brake the descent of men and equipment dropped from aircraft and to provide a certain amount of steering control. An unmanned model has been built which weighs 120 lb. Nitric acid and a mixture of crude xylidine and triethylamine ("Tonka 250") is forced by compressed air from the supply tanks into the two combustion chambers. Failure of an air valve reduced the

first model to scrap metal during the first drop. A second model is now undergoing bench tests.

✦ ✦ ✦

ARMY Rocket Research fights TB by voluntarily deferring delivery of hydrazine, a chemical compound showing promise as an improved rocket propellant. Hydrazine is also an essential part of a new family of antituberculosis drugs which show encouraging results in treatment of tubercular patients. Only large-scale manufacture of hydrazine has been sponsored by Army Ordnance Corps; release of the compound into commercial channels will assure continuation of clinical tests. Although many TB cases which appeared to be hopeless have shown improvement after treatment, the drugs are not yet considered a cure.

✦ ✦ ✦

THE Navy has taken off the secret list a World War II gadget called the "Gesundheit mine," developed under Project Sneeze. Its details may be of interest to rocket engineers with under-water applications in mind.

Both the Allies and the enemy had proximity mines during the war which would explode without actually being struck by a ship. The trouble was that the proximity mine was no respecter of nationality. It was as effective against friendly ships as against those of the enemy.

Project Sneeze was an attempt to "make the mines choosy." The heart of the modified mine was a small projectile launcher which, aimed by magnetic attraction at a passing ship, would throw aboard a canister loaded with red pepper.

"A sensitive microphone pickup on the mine did the rest," the Navy reported. "If a crew member on the ship said 'Gesundheit' the mine would explode; if he said 'God Bless you' the mine would remain unarmed."

New Use for Rockets

A NEW type of burner, similar in operation to the rocket motor, has been developed by Linde Air Products Division of Union Carbide and Carbon Corp. The Linde Jet Piercing Machine, as it is known, is used to cut holes in rock. The flame produced by burning kerosene in oxygen leaves the burner with a velocity of 6000 fps and literally disintegrates the rock upon which it is directed. One of the machines is now being used in Minnesota in the mining of the iron-producing taconite ore. Because of its extreme hardness, taconite is expensive to mine by conventional drilling methods; however, it is hoped that the Linde machine will greatly reduce the mining cost. Mechanical drilling machines now drill from 1 to 2 ft per hr in taconite, whereas a jet-piercer can do 18 ft per hr, and has done as much as 35 ft per hr.

Pulsejet Engines

THE French have used six Escopette pulsejets to power an Emouchet glider for over 200 test flights. The Escopette, because of its low weight, low speed range, and good fuel consumption, has previously been developed in low power sizes. However, SNECMA is now developing a number of higher speed and higher powered models. Each of the Escopette units develops approximately 22-lb maximum thrust and weighs 11 lb.

The Escopette, a valveless pulsejet, illustrated diagrammatically in Fig. 2, operates upon a pulsating cycle.

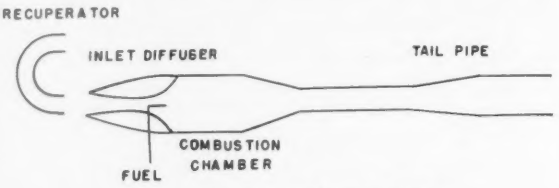

FIG. 2. ESCOPETTE PULSEJET DESIGN

When in operation, air entering the inlet diffuser is mixed with fuel as it enters the combustion chamber. Autoignition occurs and the pressure rises to approximately two atmospheres. A major portion of the hot products of combustion are then discharged through the tail pipe giving the unit a forward thrust. A small fraction of the products is also discharged through the diffuser inlet, thus causing an undesirable thrust tending to retard the forward motion of the unit. Because of this, the Escopette has been fitted with a recuperator which directs these products rearward, resulting in an increased over-all thrust. The elimination of the mechanical valves gives the unit long life and simplifies the injection of fuel. The actual design of the inlet diffuser is the result of many tests by SNECMA and represents the most original feature of the Escopette. The passage is shaped so as to retard the flow of gas outward.

The unit is started by introducing short periodic injections of fuel and compressed air into the mouth of the inlet diffuser. Ignition is obtained by means of an electric spark plug. As soon as ignition takes place the spark is switched off. It has been found that the pulsejet may be restarted with ease in flight at a speed of approximately 47 mph.

Fuel pressures between 0.3 and 1.4 atm are used, and it has been found that the unit will not operate at pressures outside of this range. The thrust can be varied from 6 to 22 lb with fuel consumption from 2 to 5 gram/sec by changing the type of fuel injector. When three units were mounted close together, the thrust of each was decreased by 10 per cent at the same fuel consumption.

Radio to the Moon

SCIENTISTS at Sterling, Va., recently trained a huge radio receiver on the moon and received the message in Morse code: "What hath God wrought." The message originated at the Collins Radio Company's transmitter at Cedar Rapids, Iowa, was reflected from the moon's surface to the Sterling receiver. This message, the first intelligible one to be transmitted by lunar reflection, required only $2^1/_2$ sec to complete the 480,000-

mile round trip. The possibilities opened up by the success of this venture are: Accurate radio control of satellites, and unjammable radio guidance—when the moon is right—of long-range guided missiles.

Aircraft

FIG. 3 is the first photograph released by the Navy of the Chance Vought F7U-3 Cutlass twin-jet fighter. No performance data are available at this time.

✦ ✦ ✦

THE Army Ordnance Department has revealed that its one-man helicopter weighs about 300 lb, can be folded into a 5 × 5 × 14-ft container, and has a top speed of 80 mph. The helicopter carries a 90-min fuel supply of gasoline, kerosene, or diesel oil, and is powered by two 16-lb pulsejet engines mounted at the tips of the rotor blades.

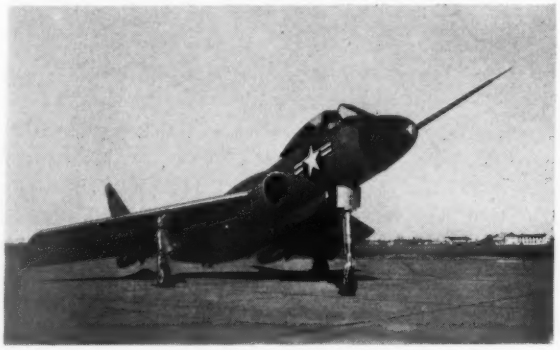

FIG. 3 CHANCE-VOUGHT "CUTLASS" JET FIGHTER

✦ ✦ ✦

A GRUMMAN F9F-6 Cougar has undergone recent flight tests by the Navy. This plane, rated in the "over 600 mph" class, is the swept-wing successor to the Navy's Panther.

✦ ✦ ✦

A FULL-SIZED delta wing section of molded plastic will be displayed in London shortly. The new molding technique was developed at the British government's Royal Aircraft Establishment. Britain plans to build a complete plastic supersonic aircraft within two years.

✦ ✦ ✦

THE revolutionary design of the Hawker-Siddeley Gloster GA5 aircraft is shown in Fig. 4. The delta wing jet is powered by twin Sapphire engines, each of which has a thrust of over 7000 lb, or more than the four engines of a heavy Superfortress bomber.

✦ ✦ ✦

McDONNELL Aircraft Corporation has received an Air Force contract to build its Voodoo XF-88A twin-jet swept wing fighter. This plane, having the longest range of any U. S. jet fighter, will be known as the F-101.

✦ ✦ ✦

NORTH American Aviation Inc. has developed a new 45-deg swept wing fighter, designated the F-100, to be powered by the Pratt & Whitney J-57 jet engine.

✦ ✦ ✦

THE Air Force plans to procure a large number of new Douglas twin-jet-engine bombers, designated the B-66. This plane, a modified version of the Navy's swept wing A3D carrier-based bomber, will weigh over 77,000 lb and will be powered by the 9500-lb thrust General Electric J-73 turbojet with an afterburner.

✦ ✦ ✦

EXPERIMENTAL flight tests are being conducted on the SO6026 by the French Company SNCA du Sud-Ouest. The SO6026, powered by a Hispano "Nene," is equipped with an auxiliary rocket engine in the rear of the fuselage.

✦ ✦ ✦

THE Russians are reported to have a new twin-jet night fighter having a wing span of about 26 ft and a length of about 28 ft. It is believed that axial flow M-012 turbojets having a rating of 6600-lb thrust, power this fighter.

✦ ✦ ✦

UNITED States machine tools combined with French engineering under the Mutual Security Program are making possible the quantity production of a French jet fighter, the Mystére, said to outperform the American Sabre jet. The Mystére MD452, manufactured by the Bordeaux plant of the Marcel Dassault Aircraft Company, was test-flown in a "duel" with the Sabre jets, and the American pilot of the Mystére was greatly impressed by its greater maneuverability. The French plan to be making thirty of these planes per month by the end of the year and to use them in the French Air Force.

✦ ✦ ✦

THE Swedish jet fighter, the Saab J-29, is reported to have attained a flight speed of about 657 mph. The J-29 is supposed to have a rate of climb superior to the Sabre and to have a longer range than the MiG-15.

✦ ✦ ✦

WHEN completed, a fourth prototype of the French Leduc ramjet aircraft will be used as basis for a super-

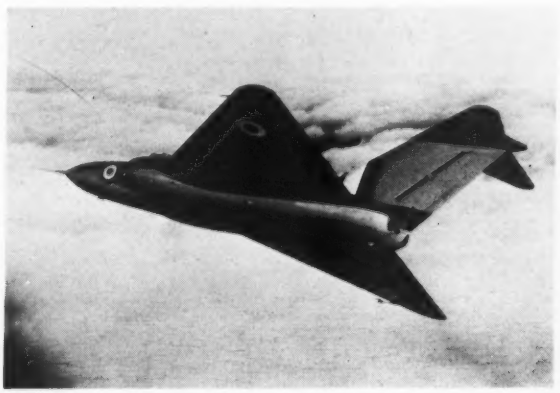

FIG. 4 HAWKER-SIDDELEY LONG-RANGE JET FIGHTER

sonic aircraft development. The third machine is powered by two Turbomeca turbojets mounted on the wing tips.

✦ ✦ ✦

A NEW turbojet unit of 13,230-lb thrust is to be designed and constructed by Turbomeca for new French fighters.

✦ ✦ ✦

BOEING Airplane Company has been awarded an Air Force contract "for an engineering study of the application of nuclear power plants to aircraft," the Department of Defense announced today. A special group of scientists and engineers is engaged in this new project. The contract, under which Boeing is working in close co-operation with Pratt & Whitney Aircraft of East Hartford, Conn., was awarded last year. No details may be revealed as to the scope of the program, or as to specifications of the power plants or airplanes under study.

✦ ✦ ✦

THE first Series-2, long-range de Havilland Comet fitted with four Rolls-Royce Avon engines (6500-lb thrust) has made a successful 2-hour maiden flight. This Comet is capable of carrying 44 passengers, mail, and freight for over 7500 miles nonstop.

Meetings of Interest

THE Applied Mechanics Division of The American Society of Mechanical Engineers will hold a Shock and Vibration Instrument Symposium at Pennsylvania State College, June 19–21, 1952. The program will include papers in the following categories: 1. Survey and historical; 2. One-degree-of-freedom instruments; 3. Sources of error and secondary effects; 4. Peak reading gages; 5. Calibration; 6. Applications. It is expected that the transactions of the symposium will be published in a single volume.

✦ ✦ ✦

A TRAINING course in Statistical Quality Control will be held at the University of Colorado, Boulder, Colorado, June 17–27.

The Fourth Combustion Symposium will be held at the Massachusetts Institute of Technology, September 1 to 5, 1952.

New Instruments

SCIENTISTS at ONR's Naval Research Laboratory have developed a "Vortex" thermometer which allows a correct measurement of ambient air temperature from planes flying 500 mph. In the NRL thermometer, a tube extends axially into the airstream. Within the tube a spiral vane produces a vortex motion. The center of the vortex is a region of lower pressure, which has a cooling effect exactly cancelling the heating effect of the compression caused by the plane's motion. It is said that the new thermometer will record the correct air temperature regardless of plane speed.

✦ ✦ ✦

THERMAL indicators made of paper, capable of determining temperatures from 115 F to 500 F instantly, have been developed by the Army Quartermaster Corps. They consist of white pigment coatings on black paper, each coating designed to melt at a definite temperature. When heated to the designated temperature, the coating melts and disappears into the black porous paper revealing a black background.

✦ ✦ ✦

BELL Aircraft Corp. has constructed a vibration test tower 40 ft high and 15 ft square. Aircraft and missile components weighing up to 3000 lb can be vibrated at from 1 to 15 cps with a maximum amplitude of 5 ft.

✦ ✦ ✦

THE General Electric Co., at its Thomson Laboratory, Lynn, Mass., has developed a new method of fabricating gas-turbine stator and rotor blades. The method is said to require less production equipment, save up to 39 per cent of critical material, and to cut production costs by 55 per cent. Two turbojets equipped with these blades have undergone 500-hr endurance tests and the blades showed no undesirable conditions or signs of failure. Details of the fabrication process are available through the USAF to other manufacturers in the nation.

✦ ✦ ✦

PUNCH-CARD calculators are now being used at the Purdue University Rocket Laboratory to make all performance test calculations. Raw calibration and test data are marked by hand upon the punch cards. The punch-card machines make all of the desired calculations and print the results upon a set of performance result sheets.

✦ ✦ ✦

ENGINEERS of the General Electric Company are using a new "curved light" quartz probing instrument to study flames in jet engines. The heart of the new instrument, known as a flame detector, is a metal-encased pliable quartz filament which transmits light through its length. The visible light from the flame is transmitted through the quartz to a phototube whose output is amplified and recorded. The General Electric engineers use this detector to study the flames in jet engine combustors and tail pipes, and to observe flame leakage into the turbine blades.

New Facilities

ON March 19, Lieut. Gen. Edwin W. Rawlings spoke at the dedication of the new General Electric Company's gas turbine plant at Lockland, Ohio. In his dedication speech, Gen. Rawlings stressed the surprising advance in the design and production of aircraft made by Russia, and the great need for expanded effort on the part of U. S. industry. The Lockland plant, now employing 7500 in the production of the G. E. J-47, will eventually employ 12,000 workers.

✦ ✦ ✦

AIR flow studies at Mach number 10 (ten times the speed of sound) are being made in the hypersonic wind

tunnel at the Naval Ordnance Lab., White Oak, Md. The tunnel has a 5-inch working section and is continuous in operation. Air is supplied at 3000 psi, and heated to 900 F in order to prevent liquidation under operating conditions. Both pressure and optical measurements of air flow are made, in study of air flow characteristics at high speeds and basic aerodynamics for later use in missile and projectile design.

Personalities

EDWARD H. HEINEMANN, Chief Engineer of Douglas Aircraft Company's El Segundo, California Division, has received the Sylvanus Albert Reed Award of the Institute of the Aeronautical Sciences. Mr. Heinemann received this award for his aeronautical investigations accomplished by the *Skyrocket* in 1951.

✦ ✦ ✦

RICHARD W. POWELL has been promoted to the position of Chief Technical Supervisor of the Physical Measurements Division of Aerojet. Mr. Powell has been with Aerojet since 1950 and was formerly associated with G. M. Giannini & Company.

✦ ✦ ✦

MAJOR-GENERAL THOMAS F. FARRELL, assistant general manager of the U. S. Atomic Energy Commission since August 1951, has resigned to become Director of ARO, Inc., which manages and operates the Arnold Engineering Development Center at Tullahoma, Tenn.

✦ ✦ ✦

MAJOR-GENERAL KENNETH D. NICHOLS, Deputy Director of Guided Missiles within the office of the Secretary of Defense, has been named Army service member of the Department of Defense Research and Development Board, in addition to his other duties.

✦ ✦ ✦

JOHN P. LONGWELL, member ARS, a project leader in the Process Division of the Standard Oil Development Company, has been appointed Chairman of the NACA Sub-Committee on Combustion. ALBERT J. BLACKWOOD, assistant director in the Research Division of the Development Company, has been appointed to the NACA Sub-Committee on Aircraft Fuels.

Fluctuations in a Spray Formed by Two Impinging Jets

(*Continued from poge 131*)

sheet velocity and frequency approached a direct proportionality.

References

1 "Stability of Flow in a Rocket Motor," by D. F. Gunder and D. R. Friant, *Journal of Applied Mechanics*, vol. 17, September 1950, pp. 327–333.

2 "A Theory of Unstable Combustion in Liquid Rocket Systems," by Martin Summerfield, JOURNAL OF THE AMERICAN ROCKET SOCIETY, vol. 21, no. 5, September 1951, pp. 108–114.

3 "Aspects of Combustion Stability in Liquid Propellant Rocket Motors. Part I," by L. Crocco, JOURNAL OF THE AMERICAN ROCKET SOCIETY, vol. 21, no. 6, November 1951, pp. 163–178.

4 "Fluctuations in a Spray Formed by Two Impinging Jets," by M. F. Heidmann and J. C. Humphrey, *NACA Technical Note* no. 2349, April, 1951.

A Similarity Law for Stressing Rapidly Heated Thin-Walled Cylinders

(*Continued from page 149*)

for complete similarity is then $\bar{D}_0/D_0$. The ring on the cold cylinder is thus wider than on the hot cylinder. When this condition on the ring dimension is satisfied, the simple similarity relations for the stresses in the shell are again correct.

References

1 "Strengths of Several Steels for Rocket Chambers Subjected to High Rates of Heating," by R. L. Noland, JOURNAL OF AMERICAN ROCKET SOCIETY, vol. 21, no. 6, November 1951, pp. 154–162.

2 See, for instance, "Theory of Plates and Shells," by S. Timoshenko, McGraw-Hill Book Company, New York, 1940, p. 389.

3 "Thin Cylindrical Shells Subjected to Concentrated Loads," by S. W. Yuan, *Quarterly of Applied Mathematics*, vol. 4, 1946, pp. 13–26.

4 "Stability of Thin-Walled Tubes Under Torsion," by L. H. Donnell, *NACA Technical Report* 473, 1933.

MPB

"Suppliers to the World's Foremost Instrument Manufacturers"

For vital requirements, aviation instrument makers and diversified manufacturers of precision equipment choose MPB miniature ball bearings as standard.

Available to critical tolerances in over 70 different types and sizes from .100" to 5/16" O.D.

A Few Examples of Typical Stock Sizes:

Complete and competent engineering assistance for your applications is promptly available. Comprehensive catalog on request.

MINIATURE *Precision* BEARINGS INCORPORATED
KEENE, NEW HAMPSHIRE

MEMBER, ANTI-FRICTION BEARING MANUFACTURERS ASSOCIATION

American Rocket Society News

H. K. WILGUS, *Associate Editor*

ARS Becomes Voting Member of IAF

During the Second International Astronautical Congress held in London, September 3–8, 1951 (see the November 1951 issue of the JOURNAL) the groundwork was laid for the formation of an International Astronautical Federation. A constitution has now been drafted and the National Board, after reviewing it carefully, has agreed unanimously that the American Rocket Society should become the American voting member of this organization. The other voting members are the British Interplanetary Society and the German Gesellschaft für Weltraumforschung.

Some of the General Aims, Objects, and Activities of the IAF are: (1) To promote and stimulate the achievement of space flight, and to attempt to insure that space flight shall be achieved as a peaceful, not a military project; (2) to do all in its power to secure the widespread dissemination of technical and other information on space flight through the medium of exchange of publications, collaboration on research, etc., as between its members; (3) to stimulate work on astronautical subjects by international and national research establishments, universities, commercial firms, individual specialists, etc.; (4) to hold, at one-year intervals if possible, or less frequently if so desired by its Council, international meetings to be attended by delegates from among its members; (5) to found and administer an international astronautical research institute, charged with the task of achieving space flight for nonmilitary purposes.

The present IAF officers elected at the London Congress are—*President*, Eugen Sanger; *Vice-Presidents*, G. Loeser (European affairs), and Andrew G. Haley (American affairs); *Secretary*, J. Stemmer.

The permanent secretariat of the IAF is to be located in Switzerland. It is believed that this decision to affiliate the American Rocket Society with the IAF is a progressive and constructive action, the outcome of which must await the test of time. The terms of the IAF constitution under which the American Rocket Society has agreed to become a member permit withdrawal at any time.

Third International Astronautical Congress

The German Gesellschaft für Weltraumforschung (Stuttgart-Zuffenhausen) has announced that the Third International Astronautical Congress will be held from September 1–6, 1952, at Stuttgart, Germany. The G. f. W. will be host to the member societies this year. Last year the British Interplanetary Society was host at the London Congress.

ARS delegates to the Congress will be selected and announced at a later date. Members of the ARS who may be able to attend the Congress are requested to forward their names to Mr. Andrew G. Haley, Vice-President (American affairs) IAF, 1101 Connecticut Avenue, N. W., Washington, D. C. The program for the Congress will be published in the next issue of the JOURNAL.

Papers Invited

The ARS is now considering papers on astronautics, space travel, and related subjects for presentation before the assembled national societies at the Third International Astronautical Congress.

The subjects of these papers may be technical or philosophical in nature, but should represent original thought or concept. In the absence of the author, papers will be read by an ARS delegate.

To be considered for presentation, papers must be received in the New York office by August 1, 1952. Address: Secretary, American Rocket Society, 29 West 39th Street, New York 18, N. Y.

2000 Hear von Braun Lecture at Washington-Baltimore Section Meeting

The Washington-Baltimore Section meeting on March 19, 1952, held in the Administration Building Auditorium, Naval Ordnance Laboratory, White Oak, Md., was a lecture open to the general public. The speaker was Wernher von Braun, rocket expert, and technical director for guided missile development, Redstone Arsenal, Huntsville, Ala. If the response to his subject, "Let's Tackle the Space Ship," is any indication, Washingtonians are impatient to get to Venus or Mars or waypoints in between.

More than 2000 persons heard the lecture, according to H. J. Archer, president of the Washington-Baltimore Section. The auditorium was filled, loudspeakers had been installed in the corridors, and a large number of cars were turned away by the time Dr. von Braun had commenced his talk at 8 o'clock.

Dr. von Braun described the possibility, within the next 10 or 15 years, of a man-made satellite—a 250-ft wide, wheel-shaped space station—that could be either a force for peace or a weapon of war, depending on who makes or controls it. This artificial moon, which will be carried into space, piece by piece, by rocket ships, will have specially designed powerful telescopes

Photograph Courtesy of Naval Ordnance Laboratory

ROCKET SHIP AND SPACE STATION MODELS ARE VIEWED BY THE LECTURER, WERNHER VON BRAUN, AND GUESTS AT THE WASHINGTON-BALTIMORE SECTION LECTURE

(*Left to right*): LCmdr. F. C. Durant, III, ARS vice-president; Dr. Wernher von Braun, rocket expert; Willy Ley, author; Harry J. Archer, Jr., president of ARS Washington-Baltimore Section; and Andrew G. Haley, ARS general counsel

attached to optical screens, radarscopes, and cameras. It will travel along a celestial route 1075 miles above the earth, completing a trip around the globe every two hours, at a speed of 15,840 mph. Nature will provide the motive power, a balance between its speed and the earth's gravitational pull.

Dr. von Braun also envisioned the huge rocket ship capable of carrying a crew and some 30 or 40 tons of cargo into the "two-hour" orbit. He described this as a three-stage rocket, 24 stories tall, weighing 7000 tons, and its three power plants driven by a combination of hydrazine and nitric acid. The first stage will be powered by 51 rocket motors having a combined thrust of 14,000 tons, and consuming a total of 5250 tons of propellants in 84 seconds. The second stage (middle section) will have 34 rocket motors with a 1750-ton total thrust, and burning 770 tons of propellants. The third stage (nose section), carrying the crew, equipment, and pay load, will have 5 rocket motors with a 220-ton combined thrust. This "body" or cabin stage carries 90 tons of propellants, including ample reserves for the return trip to earth.

Following the lecture, a panel of experts discussed various aspects of interplanetary travel. The moderator was Milton W. Rosen, section head, rocket section, Rocket Sonde Research Branch, Naval Research Laboratory. The speaker's panel consisted of Dr. Martin A. Mason, formerly with the Beach Erosion Board and now Dean of the School of Engineering, George Washington University, Washington, D. C.; Dr. Paul B. Pearson, chief, biology branch, Atomic Energy Commission; Rear-Admiral Kenneth H. Noble (retired), now of Aerojet Engineering Corporation; and Esterly C. Page, formerly vice-president in charge of engineering, Mutual Broadcasting System, and now head of the E. C. Page Consulting Radio Engineers, Washington, D. C.

X-1 Experimental Rocket Plane Described at Indiana Section Meeting

On February 12, 1952, in joint session with the Purdue University chapter of the Institute of the Aeronautical Sciences, the ARS Indiana Section held a meeting attended by approximately 300 persons from the central Indiana area, including ARS members from Indianapolis and Kokomo.

R. Bruce Foster, head of the rocket research division, Bell Aircraft Corporation, discussed the problems in designing, constructing, and testing the six X-1 aircraft built to date. He began his talk with a film depicting the X-1 in operation to familiarize the audience with the airplane. The X-1, Mr. Foster pointed out, was conventional in its design, being a straight-winged aircraft built as nearly as possible symmetrical about its longitudinal axis.

Photograph Courtesy of Naval Ordnance Laboratory

SPEAKERS' PANEL AT LECTURE SPONSORED BY WASHINGTON-BALTIMORE SECTION ON MARCH 19, 1952

(*Left to right*): Dr. Paul B. Pearson, Atomic Energy Commission; Dr. Martin A. Mason, dean, school of engineering, George Washington University, Washington, D. C.; Esterly C. Page, ARS member; and Rear-Adm. (ret.) Kenneth H. Noble, of Aerojet Engineering Corp.

He emphasized the extreme strength of the aircraft and the fact that the design loading of the structure was 18 times the force of gravity. For a comparison, he pointed out that the thin wings of the X-1 could support the entire weight of a B-36 without structural failure. He concluded his talk with another movie of the X-1 in action, climaxed by its taking-off and climbing to altitude under its own power in contrast to the usual procedure of air-launching it from a B-29 airplane.

Mr. Robertson Youngquist, chief development engineer for Reaction Motors, Inc., then spoke on the general progress and development taking place in the rocket power plant field in the United States. Of the several related rocket engine design and installation problems, the most difficult, he stated, were the corrosive action of propellants, the pumping pressures involved, the space limitations, low-temperature valving, and the high combustion temperatures and pressures. A film showing the growth of the Reaction Motors, Inc., from meager beginnings to its present facilities at Dover, N. J., was narrated by Mr. Youngquist. The film included pictures of test-firings and comparisons of rocket engine performance up to and including the V-2 power plant of 57,000-lb thrust.

Aerojet Rocket Engineer Speaks at Purdue

Mr. B. L. Dorman, president of the ARS Southern California Section, and chief of the rocket test division, Aerojet Engineering Corporation, was the guest speaker at the Indiana Section meeting on March 7, 1952. Mr. Dorman's talk, illustrated with slides, centered on present-day problems in the rocket propulsion industry and some of the goals which are a constant guide to improvement.

The two major problems at present confronting the industry, Mr. Dorman said, are the need for better propellant combinations or entirely new propellants, and better materials from which to construct nozzles, high-speed pumps, and other components. An important phase of the search for new materials embraces experimental work in the field of ceramics for use as nozzles and combustion chamber liners. Some ceramic components, he pointed out, are now in limited production.

The four goals which will require considerable developmental work rather than any radical technology changes, Mr. Dorman said, are increased reliability, improved performance, light weight, and the ability to mass-produce needed units.

Mr. Dorman concluded his talk with some comments on the employment prospects in the rocket industry. Although the industry is still small, it is advancing rapidly, he said, and can offer rewarding and secure employment to all those interested in this field of engineering.

Indiana Section Tours Purdue Rocket Laboratory

On the afternoon of March 15, 1952, about 35 members and guests of the Indiana Section were conducted on a specially arranged tour of the Purdue Rocket Laboratory. Clair M. Beighley, research associate, Purdue University, in charge of the tour, explained various pieces of equipment in the laboratory and described briefly the work being done at Purdue University for the Navy's SQUID Project.

Moving pictures of test firings were shown to the group following the tour. One film, in color, depicted the different phases of construction of the laboratory buildings and also the initial test firings. The climax of the film consisted of shots, taken from two different angles, of a spectacular explosion of one of the rocket engines in its test cell.

Dr. Gamow Addresses Washington-Baltimore Section Meeting

On April 25, 1952, the ARS Washington-Baltimore Section held a meeting in the Department of Commerce auditorium, Washington, D. C. Approximately 500 members and guests were present to hear Dr. George Gamow, professor of physics at George Washington University, Washington, D. C., give a lecture on "Rockets in Relativity Theory."

The meeting was opened by Harry J. Archer, Jr., president of the Section. Andrew G. Haley, ARS General Counsel and chairman of the Section's program committee, introduced Dr. Gamow who is known throughout the scientific world for his theory of radioactive decay and for his more recent work on the application of nuclear physics to the problems of stellar evolution.

The main part of Dr. Gamow's talk was a discussion of a fanciful relativistic rocket—one traveling near the speed of light. He showed that with this type of rocket it would be possible to visit the Andromeda nebula (680,000 light years distant) within three or four hours, due to the slowing of time with velocity.

Following the lecture there was a panel discussion under the direction of C. J. Libby, project engineer on the Matador missile for the Glenn L. Martin Company. Members of the panel included George P. Adair, formerly chief engineer of the Federal Communications Commission and now a consulting engineer in the fields of radio, communications, and electronics; Dr. Ralph J. Havens, head of the Atmospheric Physics Section in the Rocket Sonde Research Branch, Naval Research Laboratory; Dr. G. Loeser, project scientist, Air Force Cambridge Research Center, and vice-president, International Astronautical Federation; and Lt. Gen. Kenneth B. Wolfe, USAF (ret'd), president of the Oerlikon Tool and Arms Corporation.

The Washington-Baltimore Section is planning a dinner meeting on May 27 at the National Press Club, Washington, D.C.

Northeastern New York Section

The newly organized Northeastern New York section of the ARS reports a recent election at which the following officers were chosen: *President*, F. M. Cooper; *Vice-President*, Kurt Berman; *Secretary*, S. W. Crawford; *Treasurer*, A. J. Orsino; *Directors*, L. R. Bollinger, H. Lopez, and H. M. Weber.

On April 8, 1952, Kurt R. Stehling, of the Bell Aircraft Corporation, gave a lecture on "Satellite and Space Flight," accompanied by sound and color films of the Bell Aircraft's X-1 rocket.

The formation of the technical lecture series on jet propulsion elements has proved a successful undertaking and has attracted many new members to the ARS group. Several General Electric Company engineers and scientists have presented talks on various jet propulsion topics. The series will be concluded with lectures by Edwin H. Hull, ARS Fellow member, Thomas M. Pettey, Jr., ARS member, and Dr. R. W. Porter, ARS Board of Directors.

Alabama Section Meets

The second meeting of the recently organized ARS section at Redstone Arsenal, Huntsville, Ala., took place on Feb. 20, 1952. Dr. Harold W. Ritchey acted as president pro tem, and the following officers were elected to serve until the regular annual election in November: *President*, Dr. Martin B. Schilling; *Vice-President*, Hans Hueter; *Treasurer*, Arthur Andrews; *Secretary*, James L. Stamy.

After the business meeting an address was given by Krafft A. Ehricke, chief of the gas dynamics section of the Propulsion and Fuels Branch, Guided Missile Development Group, Redstone Arsenal. The subject of his talk was "The Development of Guided Missiles and the Foundation of Interplanetary Flight." Mr. Ehricke explained the application of rockets to space travel, pointing out the problems to be encountered and their possible solutions, and how present developments might be applied to space travel.

On March 26, 1952, the Alabama section (formerly Redstone), with its newly chosen officers presiding, held a meeting to elect a Board of Directors. The members of the Board are: Dr. Kurt Debus, Krafft A. Ehricke, James J. Fagan, Gerhard Heller, George Henderson, Dr. W. M. Mebane, Dr. George Messerly, Dr. Harold W. Ritchey, and Dr. Wernher von Braun.

At this meeting a set of By-Laws was adopted, and with its acceptance by the ARS National Board, the group has now become an officially recognized Section of the ARS, known as the "Alabama Section of the American Rocket Society, Inc."

The program for the evening was an illustrated lecture, "Civilian Help Needed for Space Rockets," given by Pfc. Geo. S. James, assistant technical editor of the Guided Missile Development Group, and a director of the Rocket Research Institute, Redstone Arsenal.

Mr. James traced the history of the rocket engine from the early efforts of Dr. Robert H. Goddard, through World War II, to the present, where a sufficient rocket engine technology exists, he said, to construct a space station.

Mr. James pointed out that the need for supplementing present military and technological rocket and guided missile development with civilian education could be accomplished through the medium of rocket societies. As an example of how such societies could participate, color films showing the activities of the Rocket Research Institute were presented.

ARS New York Section Visits IBM

On Friday evening, March 21, 1952, some 100 New York Section members, through the courtesy of the International Business Machines Corporation, met at the IBM offices, 590 Madison Avenue, New York, N. Y., for an inspection of the IBM Selective Sequence Electronic Calculator, one of the earliest large calculators, and smaller electronic computers and other machines. After a general explanation of the various calculators and a résumé of their potentialities, small groups were guided around to observe how these mechanical calculators advance scientific knowledge by relieving mathematicians of the necessity for doing masses of computations.

According to brochures distributed to the group, the Selective Sequence Control Calculator reads numbers involved in the problem and reads the instructions for its solutions. By means of a "central nervous system," the program devised by the scientist for the problem in hand directs automatically the sequence of operation, selects the proper number from the various

RECENTLY ELECTED OFFICERS OF NEW ALABAMA SECTION

(*Left to right*): Arthur Andrews, treasurer; Dr. Martin B. Schilling, president; Hans Hueter, vice-president; and James L. Stamy, secretary

memory units or from reference tables, directs them to the calculating unit, guides the calculating processes, and routes the results back to the proper places in the memory unit. This busy "brain" will tell the machine to record the results of its work when they are obtained.

At the conclusion of the evening the ARS members were shown a computer working on actual rocket problems. As the last members were departing, the machine was busy computing the answer to: "If we shoot off Rocket X at White Sands, will it land outside the reservation?"

Copies of BIS Journal Still Available to ARS Members

The American Rocket Society currently receives from the British Interplanetary Society, on an exchange basis, a limited number of copies of its Journal. Since insufficient copies are received to permit distribution to all ARS members, the Board of Directors has decided to distribute these Journals upon request, within the limit of copies available. A handling fee of $1.00 is charged for a subscription to all six 1952 issues. Address your request, together with check or money order, to Secretary, American Rocket Society, 29 West 39th Street, New York 18, N. Y.

ARS National Board Sets Up Space Flight Committee

The extent to which the American Rocket Society should devote its energies and techniques to the problems of space travel has long been a question facing the national organization. Several proposals in connection with space flight recently have been placed before the National Board of Directors, and to meet this growing interest, C. W. Chillson, ARS president, has appointed an Ad Hoc Space Flight Committee. This committee, of which Andrew G. Haley, ARS General Counsel, is chairman, consists of R. W. Porter, ARS Board of Directors, F. C. Durant, III, ARS vice-president, Kurt R. Stehling, Bell Aircraft Corporation, Milton Rosen, Naval Research Laboratory, John R. Youngquist, Glenn L. Martin Company, and W. E. Zisch, Aerojet Engineering Corporation.

The Committee is "to investigate and recommend to the Board the ways in which the American Rocket Society can best serve its members and fulfill its aims outlined in the By-Laws, by activity in the field of space flight, satellite stations, astronautics, etc., and to define the extent to which the American Rocket Society should become active in these fields."

New ARS Publicity Committee Organized

At the April 7th, 1952, meeting of the ARS National Board of Directors, Mr. David A. Anderton, engineering editor of *Aviation Week*, was appointed Chairman of a newly formed Publicity Committee. The duties of this Committee (as broadly framed in a study by G. Edward Pendray, ARS National Board) are to implement the work of the Society in increasing the prestige of rocket and jet propulsion engineering as a profession; to extend the general knowledge of jet propulsion; and to stimulate active interest by present members and encourage new members to contribute to the work of the American Rocket Society.

Mr. Anderton is considered ideally qualified for this work on the basis both of interest and training. An aeronautical engineering graduate of Rensselaer Polytechnic Institute in 1941, he spent 5 years in aircraft design, for the most part at Grumman on jet aircraft. He subsequently spent 4 years with General Electric's Project HERMES, on which he was a project engineer. Since May of 1950 he has been with *Aviation Week*. Readers of this magazine will recall his many contributions to this publication in the fields in which the Society is active.

G. M. GIANNINI & CO., INC., Pasadena 1, California

Hycon Mfg. Company

2961 East Colorado Street

Pasadena, California

Designers and Manufacturers of photographic and electronic equipment and ordnance devices including metal parts for aircraft rockets and JATO'S.

Technical Literature Digest

H. S. SEIFERT, California Institute of Technology, *Associate Editor*

CONTRIBUTORS: D. Altman, D. I. Baker, R. B. Canright, F. C. Gunther, H. S. Seifert, F. H. Wright

Book Review

HELICOPTER ANALYSIS, by Alexander A. Nikolsky, John Wiley & Sons, Inc., New York, 1951, 340 pp. $7.50.

Reviewed by MAX L. WILLIAMS, JR.
California Institute of Technology

This book is presumably an outgrowth and expanded version of Professor Nikolsky's original "Notes on Helicopter Design Theory" (Princeton University Press, 1944), and as such contains much of the original work. The main difference is that nearly half of this later version is devoted to dynamic stability and control analysis, and it is in this respect that the book will appeal to the practicing engineer. Longitudinal stability in forward flight is considered in detail, and the method for analyzing the lateral case is indicated. Automatic stabilization is also considered. For the most part the book is directed to students, and the author has made it very useful for this purpose by employing clear notation, adequate detail, illustrative examples, and class problems.

The bibliography, while not extensive, is representative, the latest reference extending into 1950.

Detailed performance methods are not discussed in detail nor is the effect of various rotor configurations on the analysis dwelt upon at any great length. The author has also chosen to exclude any discussion of the alternate various types of power supply, such as the pressure jet or pulsejet.

While a chapter on modern power-plant possibilities and their effects upon helicopter analysis might have been included, the book is thought to fulfill a definite need in this rapidly expanding field by introducing students to helicopters and in providing engineers with a ready reference for stability and control work

Books

Thermodynamics of Irreversible Processes, by S. R. DeGroot, Interscience Publishers, Inc., N. Y.; North Holland Publishing Co., Amsterdam, 1951, xvi + 242 pp. $5.

Bibliography of Books and Published Reports on Gas Turbines, Jet Propulsion and Rocket Power Plants, by E. F. Fiock and C. Halpern, U. S. Nat. Bur. Standards Circ. 509, 1951. 25 cents.

Automatic Feedback Control, by W. R. Ahrendt and J. F. Taplin, McGraw-Hill Book Co., Inc., N. Y., 1951, 14 + 412 pp.

The Magnetic Amplifier, by J. H. Reyner, Stuart & Richarts, London, 1950, 119 pp. + 18 plates. 15 shillings.

The Preparation of Programs for an Electronic Digital Computer, by M. V. Wilkes, D. J. Wheeler, and S. Gill, Addison-Wesley Press, Inc., 1951, 167 pp. $15.

Jet Propulsion Engines

Measurement of the Efficiency of Turbo-Reactor Combustion Chambers by Determination of the Carbon Dioxide in the Exhaust Gases, by J. Rappeneau, *Recherche Aéronaut. (Paris)*, vol. 21, 1951, pp. 19–23.

Flame Speeds of Methane-Air, Propane-Air, and Ethylene-Air Mixtures at Low Initial Temperatures, by G. L. Dugger and S. Heimel, NACA Tech. Note 2624, Feb. 1952.

Tests on a Working Model Ram Jet in a Supersonic Wind Tunnel, by J. R. Singham, R & M Report 2508, 1951, 16 pp.

S.N.E.C.M.A. "Escopette" Pulse-Jet Unit, unsigned, *Aircraft Eng.*, vol. 24, Jan. 1952, p. 17.

Escopette Pulsejet, unsigned, *Flight*, vol. 61, Jan. 25, 1952, pp. 101–102.

Rocket Propulsion Engines

Rockets for Aircraft Propulsion, by S. Allen, *The Aeroplane*, vol. 81, Dec. 7, 1951, pp. 726–727.

Rockets of the Navy, by W. H. Keighley, *Ordnance*, vol. 36, Jan.–Feb. 1952, pp. 577–578.

The Viking Rocket, by W. G. Purdy, *Aeronaut. Eng. Rev.*, vol. 11, Jan. 1952, pp. 16–20.

Red Rockets, by D. A. Anderton, *Aviation Week*, vol. 56, Jan. 14, 1952, pp. 37–38.

Rockets for Bazookas, by J. Geschelin, *Automotive Ind.*, vol. 106, Jan. 1, 1952, pp. 34–36.

Heat Transfer and Fluid Flow

Steam Heat Transfer to Small Drops of Water, by S. Weinberg, *Brit. J. Appl Phys.*, vol. 2, Dec. 1951, pp. 363–366.

Engineering Aspects of Liquid Metals for Heat Transfer, by Y. Trocki, *Nucleonics*, vol. 10, Jan. 1952, pp. 28–32.

The Free Vibration of a Gas Contained Within a Spherical Vessel, by H. G. Ferris, *J. Acoust. Soc. Am.*, vol. 24, Jan. 1952, pp. 57–60.

The Passage of Turbulence Through Wire Gauzes, by A. A. Townsend, *Q. J. Mech. and Appl. Math.*, vol. 4, Sept. 1951, pp. 308–320.

Experimental Study of Isothermal Wake Flow Characteristics of Various Flame Holder Shapes, by G. G. Younger, *NACA Research Memo.* E61K07, Jan. 28, 1952, 45 pp. + 6 plates.

Design of Two-Dimensional Channels With Prescribed Velocity Distributions Along the Channel Walls. II—Solution by Green's Function, by J. D. Stanitz, *NACA Tech. Note* 2595, Jan. 1952.

The Propagation in a Compressible Fluid of Finite Oblique Disturbances with Energy Exchange and Change of State, by F. W. Ross, *J. Appl. Phys.*, vol. 22, Dec. 1951, pp. 1414–1421.

On Shock-Wave Phenomena; Refraction of Shock Waves at a Gaseous Interface, by H. Polachek and R. J. Seeger, *Phys. Rev.*, vol. 84, Dec. 1, 1951, pp. 922–929.

A Note on Prandtl's Formula for the Wave-Length of a Supersonic Gas Jet, by D. C. Pack, *Q. J. Mech. and Appl. Math.*, vol. III, 1950, pp. 173–181.

On Supersonic Flow of a Two-Dimensional Jet in Uniform Stream, by S. I. Pai, *J. Aeronaut. Sci.*, vol. 19, Jan. 1952, pp. 61–65.

The Rapid Discharge of Gases from Vessels, by J. Kestin and J. S. Glass, *Aircraft Eng.*, vol. 23, Oct. 1951, pp. 300–304.

On the Interaction Between Multiple Jets and an Adjacent Surface, by J. Jonas, *Aeronaut. Eng. Rev.*, vol. II, Jan. 1952, pp. 21–25.

The Boundary Layer in the Converging Nozzle of a Swirl Atomizer, by G. I. Taylor, *Q. J. Mech. and Appl. Math.*, vol. III, 1950, pp. 129–139.

The Application of Boundary-Layer Theory to a Swirling Liquid Flow Through a Nozzle, by A. M. Binnie and D. P. Harris, *Q. J. Mech. and Appl. Math.*, vol. III, 1950, pp. 89–106.

Recent Investigation of Temperature Recovery and Heat Transmission on Cones and Cylinders in Axial Flow in the N.O.L. Aeroballistics Wind Tunnel, by G. R.

EDITOR'S NOTE: This collection of references is not intended to be comprehensive, but is rather a selection of the most significant and stimulating papers which have come to the attention of the contributors. The readers will understand that a considerable body of literature is unavailable because of security restrictions. We invite contributions to this department of references which have not come to our attention, as well as comment on how the department may better serve its function of providing leads to the jet propulsion applications of many diverse fields of knowledge.

Eber, *J. Aeronaut. Sci.*, vol. 19, Jan. 1952, pp. 1–6.

Combustion

Vapor Phase Oxidation of Hydrocarbons, by F. H. Garner, *Trans. Faraday Soc.*, vol. 47, Aug. 1951, pp. 877–899.

Determination of Aldehydes in Combustion Products, by H. C. Bailey and J. H. Knox, *J. Chem. Soc.*, vol. 75, Oct. 1951, pp. 2741–2742.

Material Transfer in a Turbulent Flame, by V. J. Berry, D. M. Mason, and B. H. Sage, Jet Propulsion Lab. Progress Report 20–148, Aug. 24, 1951, 36 pp.

Application of the Phase Behavior of Binary Systems to the Improvement of Combustion, by H. B. Palmer, J. O. Hirschfelder, and C. A. Boyd, U. Wisc. Naval Research Lab., Dept. of Chemistry CM-702, Jan. 2, 1952.

The Structure of the Boundary Layer in the Burning of Solid Fuel, by N. P. Voznesenkiy and A. B. Chernyshev, *Chem. Abstracts*, vol. 46, Jan. 25, 1952, p. 703f.

Summary of Combustion Studies for Generation of Inert Gas, by J. F. Hill, SAE Nat. Aeronaut. Meeting, Los Angeles, Oct. 3–6, 1951, Preprint 660, 6 pp.

The Design of a Combustion Tunnel, by R. McCarthy and H. Emmons, Harvard Div. Appl. Sci., Combustion Tunnel Lab., Jan. 1952.

Blowoff of Flames from Short Burner Ports, by C. W. Wilson and N. J. Hawkins, *Ind. Eng. Chem.*, vol. 43, 1951, pp. 2129–2135.

Calculated Data for the Combustion with Liquid Oxygen Diluted Alcohols and Paraffin in Rocket Motors, by I. C. Hutcheon, *R & M* 2572, 1951, 13 pp.

Heats of Combustion of Some Nitro Alcohols, by R. M. Currie, C. O. Bennett, and D. E. Holcomb, *Ind. Eng. Chem.*, vol. 44, Feb. 1952, pp. 329–331.

Combustion Characteristics of Diesel Fuels as Measured in a Constant-Volume Bomb, by R. W. Hurn and K. J. Hughes, *Q. Trans. Soc. Automotive Engrs.*, Jan. 1952, pp. 24–35.

Investigation of Hydrocarbon Ignition, by C. E. Frank and A. U. Blackham, *NACA Tech. Note* 2549, Jan. 1952, 33 pp.

New Technique Simplifies Evaluation of Precombustion Reactions, by E. B. Rifkin, *J. Soc. Automotive Engrs.*, vol. 60, Feb. 1952, pp. 50–55.

Hydrocarbons (a Symposium), Discussions Faraday Soc., The Aberdeen University Press, Ltd., no. 10, 1951, 339 + vii pp. 35 shillings.

This collection of articles, published as part of an irregular series by the same organization which produces the *Transactions of the Faraday Society*, is the result of a symposium on Hydrocarbons held at Oxford in April, 1951. It is of wider interest than the title would indicate, since many of the articles include general discussions of possible combustion mechanisms. Two general topics are covered: I. Hydrocarbon Structure and Bond Properties (pp. 1–128), twelve articles; and II. Hydrocarbon Reactions, subdivided into *A*. Thermal Reactions (pp. 129–235), eight articles; and *B*. Oxidation Reactions (pp. 236–338), ten articles.

Density Measurements in Gaseous Detonation Waves, by G. B. Kistiakowsky, *J. Chem. Phys.*, vol. 19, Dec., 1951, pp. 1611–1612.

Considérations théorique sur la propagation des flammes: I. Vitesses. II. Domaines de propagabilité, by P. Blanquet and M. F. Hoare, *J. Chimie phys.*, vol. 48, Sept.–Oct. 1951, pp. 399–406.

Effect of Preheat on Burning Velocity, by G. Dixon-Lewis, *Fuel*, vol. 30, 1951, pp. 287–288.

Propagation d'une déflagration dans un tube recouvert d'une pellicule d'huile, by R. Loison, *Compt. rend.*, vol. 234, Jan. 28, 1952, pp. 512–513.

Théorie simplifiée de la hauteur des flammes laminaires de diffusion, by F. Guyomard, *Compt. rend.*, vol. 234, Jan. 2, 1952, pp. 67–69.

Flammenfortpflanzung in Rohrstrecken. II, by H. Behrens, *Z. Elektrochem.*, vol. 55, Dec. 1951, pp. 695–696.

Basic Research on Combustion, Detonation and Shock Waves at the Laboratoire de Recherches Techniques de Saint Louis of the Direction des Études et Fabrication d'Armement, Office of Naval Research, London, Tech. Report ONRL-130-51, American Embassy, London, England, 1952.

Inflammation of Methyl and Ethyl Nitrate Vapors: Characteristics of the Explosion Process and Intermediate Reactions Involving Nitrogen Dioxide, by P. Gray and A. D. Yoffe, *J. Chem. Soc.*, 1950, pp. 3180–3185.

Experimental Study of the Radiation of Diffusion Flames (in French), by F. Guyomard, *Compt. rend.*, vol. 233, July 16, 1951, pp. 237–239.

A Spectroscopic Investigation into the Structure of Diffusion Flames, by H. G. Wolfhard and W. G. Parker, *Proc. Phys. Soc. (London)*, vol. 65, pt. 1, Jan. 1, 1952, pp. 2–19.

Spectroscopic Studies of the Hydrogen-Oxygen Explosion Initiated by Flash Photolysis of Nitrogen Dioxide, by R. G. W. Norrish and G. Porter, *Proc. Roy. Soc., Series A*, vol. 210, Jan. 22, 1952, pp. 439–460.

Spectroscopic Study of Combustion, by G. H. Rothgery and J. T. Grey, USN. USAF Proj. Squid Tech. Memo. CAL-34, Sept. 28, 1951.

Flame Radiation Research Joint Committee: Reports of 1949 Trials at Ijmuiden (Holland), by J. J. Broeze, G. Ribaud, and O. A. Saunders, *J. Inst. Fuel*, vol. 24, no. 140, Suppl., 1951.

Fuels, Propellants, and Materials

Quantitative Evaluation of Rocket Propellants, by S. S. Penner, *Am. J. Phys.*, vol. 20, Jan. 1952, pp. 26–31.

High Reaction Energy Substances for Jet and Rocket Propulsion, a Review of Existing Literature, by L. E. Swearingen and A. Veis, USAF-AMC/TR-6633, May 1951.

Rocket Propellants, by J. D. Clark, *Ordnance*, vol. XXXVI, Jan.-Feb. 1952, pp. 661–663.

Jet Fuel Quality Requirements, by D. P. Barnard, *Petroleum Processing*, vol. 6, 1951, pp. 1229–1232.

The Heats of Combustion of Magnesium and Aluminum, by C. E. Holley, Jr., and E. J. Huber, Jr., *J. Am. Chem. Soc.*, vol. 73, Dec. 1951, pp. 5577–5579.

Ni-Al-Titanium Carbide Cermets, by C. C. McBride, USAF-AMC TR-6458, Jan. 1951.

Compacts of Pure Tungsten Carbide, by A. E. Williams, *Metal Treatment*, vol. 18, Oct., 1951, p. 45.

New Ordnance Materials, by B. S. Mesick, *Ordnance*, vol. 36, Jan.–Feb. 1952, pp. 573–576.

Elastic and Flow Properties of Dense, Pure Oxide Refractories, by J. F. Wygant, *J. Am. Ceram. Soc.*, vol. 34, Dec. 1951, pp. 374–380.

Apparatus for Low-Temperature Tension Tests of Metals, by R. J. Nosborg, ASTM Bull., Oct. 1951, pp. 41–45.

The Behavior of Graphite Under Alternating Stress, by L. Green, *J. Appl. Mech.*, vol. 18, Dec. 1951, pp. 345–349.

Ceramics in Jet Propulsion, by F. Zwicky, *Aviation Age*, vol. 17, Jan. 1952, pp. 31–32.

Cermets May Answer Jet Designers' Prayers, Pt. I, by W. J. Koshuba and J. A. Stavrolakis, *Iron Age*, vol. 168, Nov. 1951, pp. 77–80; Pt. II, *Iron Age*, vol. 168, Dec. 6, 1951, pp. 154–158.

A Preliminary Study of the Oxidation and Physical Properties of Ti C-Base Cermets, by C. C. McBride, H. M. Greenhouse, and T. S. Shevlin, *J. Am. Ceram. Soc.*, vol. 35, Jan.1952, pp. 28–32.

New Chromium Carbides Have High Temperature and High Corrosion Resistance, unsigned, *Materials and Methods*, vol. 34, Dec. 1951, pp. 69–70.

Silicon Carbide Refractories Used as Alternates for Special Service Alloys, by J. L. Everhart, *Materials and Methods*, vol. 33, Nov., 1951, pp. 71–75.

Refractory Bodies Composed of Boron and Titanium Carbides Bonded with Metals, by J. A. Nelson, *J. Electrochem. Soc.*, vol. 98, Dec. 1951, pp. 465–473.

Boron Carbide as a Base Material for a Cermet, by H. J. Hamjian and W. G. Lidman, *J. Am. Ceram. Soc.*, vol. 35, Feb. 1952, pp. 44–48.

Elevated Temperature Properties of Titanium Carbide Base Ceramals Containing Nickel or Iron, by A. L. Cooper and L. E. Colteryahn, *NACA Research Memo.* E51I10, Dec. 1951, 47 pp.

Solar's Ceramic Coatings, by G. C. Close, *Aviation Age*, vol. 16, Sept. 1951, pp. 21–22.

Trends in Powder Metallurgy, by H. W. Greenwood, *Metallurgia*, vol. 44, Dec. 1951, pp. 291–294.

Speedier Powder Quality Control Made Possible, unsigned, *Metallurgia*, vol. 45, Jan. 1952, pp. 49–51.

Arc-Cast and Powdered Molybdenum Tested, by J. H. Bechtold, *Iron Age*, vol. 167, Nov. 22, 1951, pp. 92–95.

Mechanical Properties of Arc-Cast and Powder Metallurgy Molybdenum, by J. H. Bechtold, *J. Electrochem. Soc.*, vol. 98, Dec. 1951, pp. 495–504.

Cast Molybdenum of High Purity, by G. W. P. Rengstorff, *J. Metals*, vol. 192, Feb. 1952, pp. 157 et seq.

Effect of Strain Hardening and Tempering on 18-8 Stainless Steels, by P. Bastien, *Metal Treatment*, vol. 51, Oct. 1951.

Impact Properties of Stainless Steel and

9 Per Cent Nickel Steel After Exposure Under Stress to Liquid Nitrogen, by T. N. Armstrong, *ASTM Bull.*, Oct. 1951, pp. 35–36.

Corrosion Aspects of Fusion Welded Aircraft High-Strength Aluminum Alloys, by L. W. Smith, *Corrosion*, vol. 7, Dec. 1951, pp. 423–437.

Sprayed Aluminum-Base Coatings for Aluminum Alloys, by F. A. Champion, *Metal Indus.*, vo.. 79, Oct. 26, 1951, pp. 355–358.

Physical-Chemical Topics

Autoignition by Rapid Compression, by J. C. Livengood and W. A. Leary, *Ind. Eng. Chem.*, vol. 43, Dec. 1951, pp. 2797–2805.

Heat Capacity Lag in Gases, by R. Walker, *NACA Tech. Note* 2537, Nov. 1951, 40 pp.

The Critical Constants of Polar Gases, by J. S. Rowlinson, *J. Chem. Phys.*, vol. 19, 1951, pp. 831–833.

Theoretical Foundations of the Kinetics of Gas Reactions in Flow Systems (in Russian), by M. F. Nagiev, *Doklady Akad. Nauk USSR*, vol. 80, 1951, pp. 397–400.

Spherical Interface. I. Thermodynamics, by F. P. Buff, *J. Chem. Phys.*, vol. 19, Dec. 1951, pp. 1591–1594.

Temperature of Evaporation of Droplets (in Russian), by N. P. Tverskaya, *Izvest. Akad. Nauk USSR, Ser. Geog. Geophys.*, vol. 15, 1951, pp. 74–81.

Experimental Values of the Surface Tension of Supercooled Water, by P. T. Hacher, *NACA Tech. Note* 2510, Oct. 1951, 20 pp.

Evaporation Rate of Liquid Helium, by A. Wexler, *J. Appl. Phys.*, vol. 22, Dec. 1951, pp. 1463–1470.

Transport Phenomena in Polyatomic Gases, by C. S. Wan Chang and G. E. Uhlenbeck, Mich. U. Eng. Research Inst., Report no. CM-681, July 10, 1951, 46 pp.

Thermodynamic and Transport Properties of Liquids. Problem I. Thermal Conductivities of Liquids, by E. Johnson, Jr., and W. Sheffy, USN and AF Project Squid, TM PR-17, Oct. 1951.

Absorption of Sound in Fluids, by J. J. Markham, R. T. Byer, and R. B. Lindsay, *Revs. Modern Phys.*, vol. 23, Oct. 1951, pp. 353–411.

Behavior of Gas Discharge Plasma in High-Frequency Electromagnetic Fields, by L. Goldstein, *Elec. Commun.*, vol. 28, Dec. 1951, pp. 305–321.

Thermodynamics of Carbon Disulfide Synthesis, Equilibrium in Some Reactions Involving Hydrogen Sulfide, Sulfur Dioxide, Carbon Dioxide, and Carbon, by A. J. Owen, K. W. Sykes, and D. J. D. Thomas, *Trans. Faraday Soc.*, vol. 47, 1951, pp. 419–428.

Autoxidation of Hydrazine; Effect of Dissolved Metals and Deactivators, by L. F. Audrieth and P. H. Mohr, *Ind. Eng. Chem.*, vol. 43, 1951, pp. 1774–1779.

Some Semiempirical Methods for Estimating the Entropies of Oxides, Silicates, and Titanates, and the Prediction of Reaction Equilibria and Yields, by W. J. Knapp and W. D. Van Vorst, *J. Am. Ceram. Soc.*, vol. 34, Dec. 1951, pp. 384–387.

Absolute Density of Nitromethane Vapor Above Its Boiling Point, by R. M. Corelli, *Ann. chim. applicata*, vol. 39, 1949, pp. 591–596.

The Critical Temperature and Critical Pressure of Nitrogen by D. White, A. S. Friedman, and H. L. Johnston, *J. Am. Chem. Soc.*, vol. 73, Dec. 1951, pp. 5713–5715.

Solubility of Fluorine Gas in Various Fluorocarbons and Concentrated Acids, by W. B. Burford, III, C. E. Weber, H. C. Anderson, M. B. Rogers, et al., Nat. Nuclear Energy Ser., Div. VII, 1, Prepn., Properties, and Technol. of Fluorine and Org. Fluorine Compds., 1951, 188 + 97 pp.

Thermal Data, Vapor Pressure, and Entropy of Chlorine Trifluoride, by J. W. Grisard, H. A. Bernhardt, and G. D. Oliver, *J. Am. Chem. Soc.*, vol. 73, Dec. 1951, pp. 5725–5727.

Preparation and Heats of Combustion of Some Amine Nitrates, by T. L. Cottrell and J. E. Gill, *J. Chem. Soc.*, 1951, pp. 1798–1800.

Empirical Equations for the Calculation of the Dissociation Energies of C–H and C–C Bonds in the Molecules of Saturated Hydrocarbons and Free Aliphatic Radicals, by V. V. Voevodskii, *Doklady Akad. Nauk USSR*, vol. 79, 1951, pp. 455–458.

Vibrational Intensities. III. Carbon Dioxide and Nitrous Oxide, by D. F. Eggers, Jr., and B. L. Crawford, Jr., *J. Chem. Phys.*, vol. 19, Dec. 1951, pp. 1554–1561.

Heats of Solution and Reaction in Liquid Ammonia. VIII, by H. D. Mulder with F. C. Schmidt, *J. Am. Chem. Soc.*, vol. 73, Dec. 1951, pp. 5575–5577.

Crystal Structure of Nitric Acid, by V. Luzzati, *Mém. services chim. état (Paris)*, vol. 35, 1950, pp. 7–59.

Instrumentation and Experimental Techniques

Ambient Temperature Independent Thermopiles for Radiation Pyrometry, by W. G. Fastie, *J. Opt. Soc. Am.*, vol. 41, Nov. 1951, pp. 823–829.

Line Reversal Techniques in the Determination of Temperature of Gun Flash and Other Rapid Transient Phenomena, by J. T. Agnew, Am. Soc. Mech. Eng., Paper No. 51—F-6, June 5, 1951.

Problems of Fluid Measurement, by M. Schatzmann, *Engineers' Digest*, vol. 13, Jan. 1952, pp. 15–16.

Fundamentals of Orifice Measurement, by F. M. Partridge, *Instruments*, vol. 25, Feb. 1952, pp. 207–209.

An Induction Flowmeter Design Suitable for Radioactive Liquids, by W. G. James, *Rev. Sci. Instruments*, vol. 22, Dec. 1951, pp. 989–1002.

On the Generation of Magnetism by Fluid Motion, by H. Bondi and T. Gold, *Monthly Notices Roy. Astron. Soc.*, vol. 110, 1950, pp. 607–611.

How to Transfer Volatile Liquids Under Pressure, by R. J. Sweeney, *Chem. Eng.*, vol. 58, Nov. 1951, pp. 158–161.

Field Inspection of Boiler Tubes with Ultrasonic Reflectoscope, by J. A. Tash, *Trans. Am. Soc. Mech. Engrs.*, vol. 74, Feb. 1952, pp. 201–206.

Methods and Instruments for Measuring Smallest Gas Pressures (in German), by H. Schwarz, *Arch. Tech. Messen*, vol. 188, Sept. 1951, pp. T96-T97.

Measurement of Instantaneous Vector Air Velocity by Hot-Wire Methods, by C. E. Pearson, *J. Aeronaut. Sci.*, vol. 19, Feb. 1952, pp. 73–82.

Bibliography on the Measurement of Gas Temperature, by P. D. Freeze, Nat. Bur. Standards Circular 513, Aug. 20, 1951 (Supt. of Documents, U.S. Gov. Printing Office, Wash., D. C. 15 cents).

High-Temperature Arcs, by D. W. Rudorff, *Engineers' Digest*, vol. 13, Jan. 1952, pp. 6–8.

The Panradiometer: an Absolute Measuring Instrument for Environmental Radiation, by C. H. Richards, A. M. Stoll, and J. D. Hardy, *Rev. Sci. Instruments*, vol. 22, Dec. 1951, pp. 925–933.

Radiation Measuring Instruments for the Infra-Red to Ultra-Violet Waveband, by A. C. Menzies, *Proc. Inst. Elect. Engrs., Pt. II*, vol. 98, Dec. 1951, pp. 771–780.

Multiple Shielded High Temperature Probes; Comparison of Experimental and Calculated Errors, by E. M. Moffett, SAE Report T13, Jan. 1952, 20 pp. + 3 plates.

A New Method for Determining the Static Temperature of High-Velocity Gas Streams, by J. A. Clark, *Trans. Am. Soc. Mech. Engrs.*, vol. 74, Feb. 1952, pp. 219–228.

A Solar Furnace of 120 Inches Diameter for Studying Highly Refractory Substances, by W. M. Conn, *Rev. Sci. Instruments*, vol. 23, Dec. 1951, pp. 945–951.

Calorimeter for the Determination of the True Heat Capacity and of Latent Heats at High Temperatures, by V. A. Sokolov, *Zhur. Tekh. Fiz.*, vol. 18, 1948, pp. 813–822.

New Precision Calorimeter for Determining Heats of Combustion, by A. Magnus and F. Becker. *Z. physik. Chem.*, vol. 196, 1951, pp. 378–396.

Semiconductors Capable of Withstanding High Temperatures (Refractory Thermistors), by N'Guyen Thien Chi and J. Suchet, *Ann. Radio-électricité*, vol. 6, April 1951, pp. 99–105.

Accurate Time for Scientific Observations, by F. E. Fowler, *Electronics*, vol. 25, Jan. 1952, pp. 98–101.

The Performance Equations of the Eddy Current Gyroscope, by R. Clay and R. Harrison, USN-BuOrd/NAVORD-R-1397, Oct. 26, 1951.

The Impact of Servomechanism Techniques on Instrumentation, by A. Porter, ASME Paper No. 51—SA-22, March 20, 1951, 22 pp.

Flight, Ballistics, and Vehicle Development

Life on Mars in View of Physiological Principles, by H. Strughold, *CADO Tech. Data Digest*, vol. 16, Nov. 1951.

Dirigibility of Rockets, by H. Bartenbach, *J. Space Flight*, vol. 3, Dec. 1951, pp. 1–2.

The Artificial Satellite, by E. Burgess, *The Engineer*, vol. 192, Oct. 12, 1951, pp. 456–458.

Advance Man to the Moon, unsigned, *Aero Digest*, vol. 63, Oct. 1951, pp. 25–32.

Power Sources for Orbital Rockets, by L. J. Grant, *J. Space Flight*, vol. 3, Nov. 1951, pp. 1–3.

Preview of Space Flight, by L. S. Black,

Aero Digest, vol. 63, Oct. 1951, pp. 17–24.

The Brainwork Is Done, by R. McLarren, *Aero Digest*, vol. 63, Oct. 1951, pp. 34, 36, 38, 42, 44, 46, 50, 52, 54, 56, 58, 60, 63, 64.

Shapes of Craters Formed in Plaster of Paris by Ultra-Speed Pellets, by J. S. Rhinehart and W. C. White, *Am. J. Phys.*, vol. 20, Jan. 1952, pp. 14–18.

Thermal Stresses in a Rotating Elastic Solid of Revolution, by C. E. Iliffe, *Engineer*, vol. 173, Dec. 28, 1951, pp. 835–836.

Slingshots or Precision Weapons, unsigned, *Interavia*, vol. VI, Oct. 1951, pp. 541–547.

Rocket Away!, unsigned, *Interavia*, vol. VI, Oct. 1951, pp. 556–557.

Guided Anti-Aircraft Missiles, unsigned *Interavia*, vol. VI, Oct. 1951, pp. 554–555.

The Pilotless Aircraft Type Missile, by S. E. Weaver, SAE Report 731, Jan. 1952, 9 pp. + 1 plate.

USAF's Guided Missile Test Center, Pt. II, by R. E. Stockwell and R. Hawthorne, *Aviation Age*, Dec. 1951, pp. 40–43.

What We Have Learned from V-2 Firings, unsigned, *Aviation Week*, Nov. 26, 1951, vol. 55, pp. 23–30.

Some General Aspects of Missile Testing, by J. H. Zabriskie, SAE Report 733, Jan. 1952, 6 pp.

Bumblebee Program, by J. E. Arnold, *Aviation Age*, vol. 17, Jan. 1952, pp. 31–35.

Peenemunde, 1951, unsigned, *Aviation Age*, vol. 117, Feb. 1952, p. 33.

Supersonic Flight from the Pilot's View, by W. B. Bridgeman, *Aeronaut. Eng. Rev.*, vol. 11, Feb. 1952, pp. 24–28.

Atomic-Powered Aircraft, unsigned, *Flight*, vol. 60, Dec. 21, 1951, p. 780.

P-W to Build Atomic Aircraft Engine, unsigned, *Aviation Week*, vol. 55, Dec. 24, 1951, p. 18.

Other Classifications

(Meteorology, Astrophysics, Etc.)

The Scintillation of Starlight, by A. H. Mikeseli, *J. Opt. Soc. Am.*, vol. 41, Oct. 1951, pp. 689–695.

Trends in U. S. Air Force Research and Development, by D. L. Putt, *Tech. Data Digest*, vol. 17, Jan. 1952, pp. 7–12.

Post-War Developments in Operational Research, by A. W. Swan, *Engineer*, vol. 173, Dec. 21, 1951, pp. 812–814.

High Altitude Research at the Applied Physics Laboratory, by L. W. Fraser, Bumblebee Report No. 153, APL, Johns Hopkins U., May 1951.

Guided Missiles, a New Field for the Radio Engineer, by S. Ramo, *Proc. Inst. Radio Engrs.*, vol. 40, Jan. 1952, p. 3.

Methods Developed at the Naval Ordnance Test Station for Rapid Calculation of Air Density, by N. R. Williams and K. L. Coulson, USN-BuOrd/-NAVORD-R-1910, Aug. 28, 1951.

The Temperature of the Upper Atmosphere, by D. R. Bates, *Proc. Phys. Soc.*, (*London*), vol. B, Sept. 1951, pp. 895–821.

Interpretation of the Polarization of Light Reflected by the Different Regions of the Surface of the Planet Mars (in French), by A. Dollfus, *Compt. rend.*, vol. 233, Aug. 6, 1951, pp. 467–469.

Meeting of the Space Medicine Association, unsigned, *J. Aviation Med.*, vol. 23, Dec. 1951, pp. 544-547.

A new achievement in *automatic data analysis* . . .

the Teleplotter

plots graphs 10 times faster than by hand

operates from IBM or keyboard digital input

A new problem has developed in modern science and engineering—the problem of manual plotting.

The slowness, fatigue, human errors of manual plotting frequently cause serious time lags, increase expenses and overhead.

The Teleplotter solves that problem. Plotting 40 points per minute, it is faster, cheaper, more accurate than manual plotting.

Vital data:

Plotting speed—40 points per minute, approximately 10 times faster than manual plotting
Plotting area—26 x 55 inches or less
Plotting accuracy—±.25 mm(paper stretch does not affect accuracy)
Scale factors—five factors, with independent selection for each axis
Plots X-Y data on linear or logarithmic paper
Time required to set up Teleplotter for operation—negligible

How it operates:

Data is introduced into the Teleplotter by IBM equipment or by the Teleplotter keyboard.

The Teleplotter Reading-Head, housing photo-electric "eyes," travels over the graph paper, counts grid lines and spaces, prints a symbol when its counts coincide with the IBM or keyboard data.

Applications:

Experimental uses

Plots wind tunnel data; static and structural test data; fractionating tower design data, etc.

Plots results of manual calculations and results of automatic electronic calculating machines to detect random errors.

Theoretical uses

Plots theoretical curves and results of theoretical calculations.

General uses

Plots insurance tables; stock market, statistical and financial records; production control data; results of engineering studies and analyses; management control data.

Plots results of continuous process operations for supervision and control purposes.

Write for brochure, "Automatic Data Analysis," giving full details on the Teleplotter and other Telecomputing Instruments. Coupon on the right is for your convenience.

Mr. John H. Weaver, Engineering, Dept.—RT-5
Dear Sir: Please send me "Automatic Data Analysis."

Name

Company

Street address

City and State

TELECOMPUTING
CORPORATION, BURBANK, CALIFORNIA
"Turn hours into minutes with Automatic Data Analysis"

Here is a better lining material for uncooled rocket motors

Shown here is a group of liner and throat shapes made by The Carborundum Company.

Exceptional resistance to the high temperature and severe erosive conditions developed in uncooled rocket motors is offered by special silicon carbide liners and throats. In comparative tests they have outlasted metals by several times.

Information is available upon request to Dept. RS-52, Refractories Div., The Carborundum Co., Perth Amboy, N. J.

Silicon Carbide linings by

CARBORUNDUM
Trade Mark

"Carborundum" is a registered trademark indicating manufacture by The Carborundum Company.

GROVE
SELF-ACTUATED
CONTROLS AND REGULATORS

for

High pressure liquids and gases

•

Pressure Reducing
Back Pressure
Relief and By-Pass
Manual Valves

•

Special light weight units
for air-borne service.

•

Special materials for corrosive
or low-temperature applications.

•

GROVE CONTROLS, INC.
6529 Hollis Street

Emeryville — GROVE SIMPLICITY ACCURACY SAFETY — California

Get the Facts about your Future with Martin!

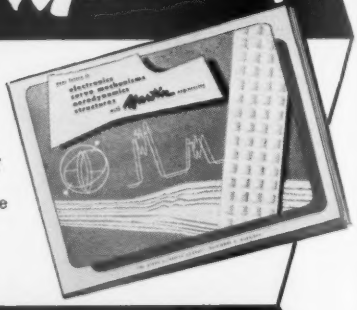

Discover the greater opportunities offered engineers by the greatest diversity of projects of any aircraft company in the East! Write today for fact-packed brochure.

SEND FOR ENGINEERING BROCHURE

THE GLENN L. MARTIN COMPANY
Personnel Dept. • Section A • Baltimore 3, Md.
Please send me your brochure describing engineering opportunities at Martin.
Name .....
Address .....
City and state .....
Engineering field .....

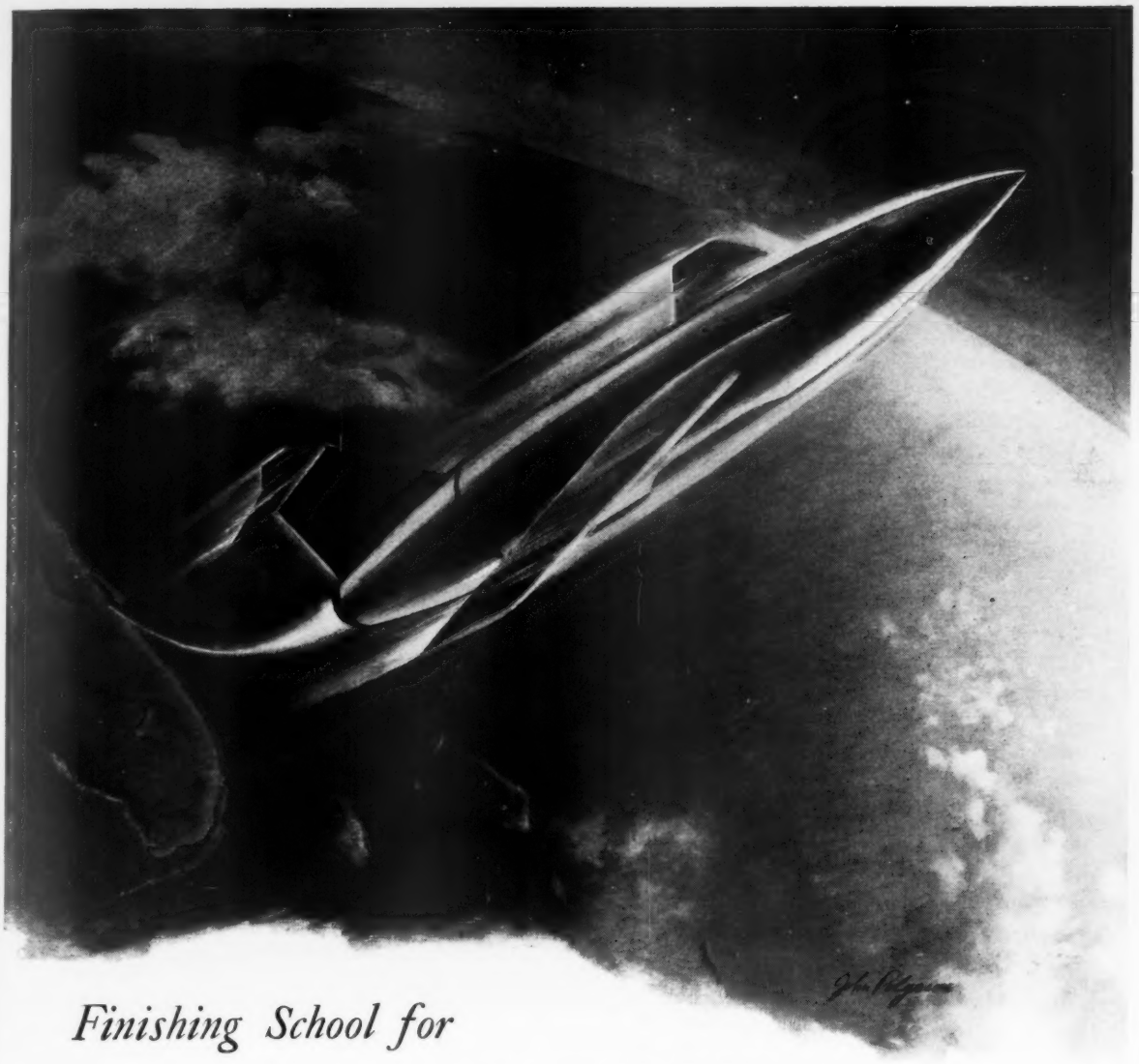

Finishing School for
GUIDED MISSILES

The Air Force Missile Test Center, used by all our military services as a long-range proving ground, stretches thousands of miles from Florida, out over the Bahamas, into the South Atlantic.

A pilotless bomber roars away from its launching stand, picks up speed, zooms into the blue. Setting its course for a far-off target in the ocean, it rockets over a chain of tiny islands where men and machines check its flight, its behavior, the operation of its guidance and control systems. It's a vital part of our air power of the future—aeronautical research and development laying the foundation for continued U. S. air supremacy!

Operated by the USAF's Air Research and Development Command, the Missile Test Center is geared up to test the wide variety of missiles, rockets and pilotless aircraft vital to modern air power. It reached its full stature with the recent completion of down-range observation stations. And the dramatic B-61 pilotless bomber, the Matador, designed and produced by Martin as part of its diversified missiles program, was the first to use the completed range. THE GLENN L. MARTIN COMPANY, Baltimore 3, Maryland.

Martin AIRCRAFT

Builders of Dependable Aircraft Since 1909

DEVELOPERS AND MANUFACTURERS OF: Navy P5M-1 Marlin seaplanes • Air Force B-57A Canberra night intruder bombers • Air Force B-61 Matador pilotless bombers • Navy P4M-1 Mercator patrol planes • Navy KDM-1 Plover target drones • Navy Viking high-altitude research rockets • Air Force XB-51 developmental tactical bomber • Martin airliners • Guided missiles • Electronic fire control & radar systems • **LEADERS IN** Building Air Power to Guard the Peace, Air Transport to Serve It.

Illustration is artist's conception of Air Force B-61 Matador pilotless bomber.

PHYSICISTS AND SENIOR RESEARCH ENGINEERS

• • • •

POSITIONS NOW OPEN

• • • •

Senior Engineers and Physicists having outstanding academic background and experience in the field of:

- Microwave Techniques
- Moving Target Indication
- Servomechanisms
- Applied Physics
- Gyroscopic Equipment
- Optical Equipment
- Computers
- Pulse Techniques
- Radar
- Fire Control
- Circuit Analysis
- Autopilot Design
- Applied Mathematics
- Electronic Subminiaturization
- Instrument Design
- Automatic Production Equipment
- Test Equipment
- Electronic Design
- Flight Test Instrumentation

are offered excellent working conditions and opportunities for advancement in our Aerophysics Laboratory. Salaries are commensurate with ability, experience and background. Send information as to age, education, experience and work preference to:

NORTH AMERICAN AVIATION, INC.

Aerophysics Laboratories
Box No. S-4
12214 South Lakewood Blvd.
Downey, California

INDUSTRIAL SOUND CONTROL • INDUSTRIAL SOUND CONTROL • INDUSTRIAL SOUND CONTROL • INDUSTRIAL SOUND CONTROL • INDUSTRIAL SOUND CONTROL

rocket ROAR silenced by ISC mufflers

● In the laboratory, in the test cell, on the airfield, hundreds of INDUSTRIAL SOUND CONTROL installations are subduing the noise, heat and gas velocities generated during testing of the big jets.
Whatever *your* noise problem, ISC's skilled engineering, design, and installation "know how" — gained through years of practical experience — can help you, and is at your instant service.
We welcome the challenge of the unusual problem. For full information

WRITE ISC TODAY

Foreign Licensees:
Cementation (Muffelite) Limited, London
Les Travaux Souterrains, Paris

Industrial Sound Control, Inc.

45 Granby Street, Hartford, Conn.
2119 So. Sepulveda Blvd., Los Angeles, Calif.

CURRAN ENGINEERING CO.

Manufacturer of

MECHANICAL COMPONENTS
from
METALS, CERAMICS, AND PHENOLICS

Consultants and Specialists of
ROCKET IGNITER ASSEMBLIES
and
LONGITUDINAL SHAPED CHARGE CUTTERS

"CENCO" Process for
HIGH TEMPERATURE-HIGH DIELECTRIC INSULATING OF METALLIC ASSEMBLIES

7614 Santa Monica Blvd.
Los Angeles 46 California.

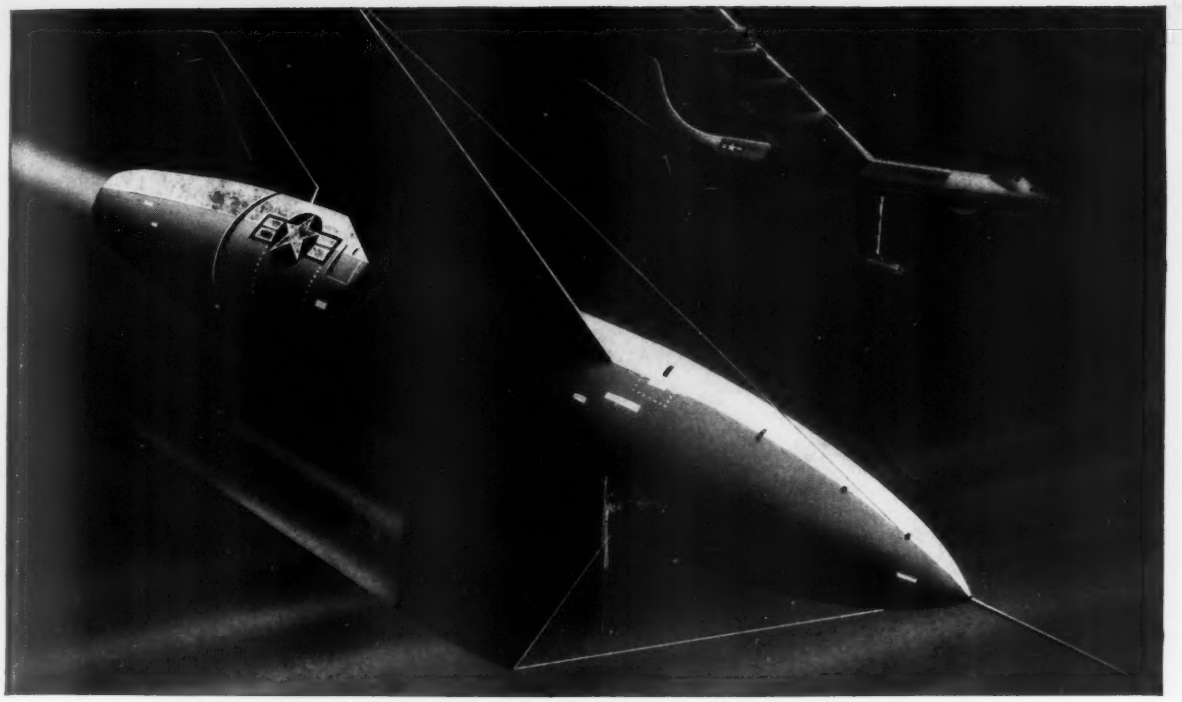

It's got a target by the tail!

THIS GUIDED MISSILE may go through some mighty tight turns to stay on target . . . and that means G loads go up, *fast*. But the Greer Accumulator in the circuit will take it.

New Guided Missiles Count On Greer Accumulators to Supply Power Actuate Controls and Mechanisms

There's a Greer guided missile accumulator for almost every requirement, or Greer will build to your exact specifications.

For Greer Accumulators are designed to operate under the high G loads caused by tight maneuvers and high accelerations. Their volumetric efficiency is extremely high. They are practically impervious to temperature; function under operating pressures as high as 6000 psi; can vary in capacity from 2 cubic inches to 25 gallons.

Uses for Greer Accumulators in a guided missile are many, varied, and important. They actuate Servo controls and mechanisms, function as a source of instantaneous energy, power supply for primary and secondary circuits, a pressurized reservoir, pressure-transfer barrier, and eliminate pressure pulsations. These compact, lightweight power sources can be designed to fit almost any given space. They are unusually flexible in shape, capacity and pressure, and can be planned as an integral part of the missile itself.

Developing accumulators for guided missiles is just one interest of the *Greer Special Products Division*. If you are confronted with a problem relating to the field of aviation, call Greer engineers for a consultation. There is no cost, no obligation.

GREER
GUIDED MISSILE ACCUMULATORS

SPECIAL PRODUCTS DIVISION • GREER HYDRAULICS INC.
454 Eighteenth Street, Brooklyn 15, New York

Field Office: 298 Commercial Bldg., Dayton, O. • Thomson Engineering Service, 708 Hemphill St., Fort Worth 4, Tex. • Harold E. Webb, 918 N. Kenilworth Ave., Glendale 2, Calif

The California Institute of Technology

Jet Propulsion Laboratory

Pasadena, California

. . . has several openings in the following engineering fields:

Preliminary Design
Engineering Analysis
- **Aerodynamics**
- **Aerodynamic Heating**
- **Heat Transfer**
- **Thermodynamics**
- **Dynamics**
- **Structural Studies**
- **Statistical Studies**

Structural Design
Propulsion System Development
Test Engineers—Wind Tunnel
- **Experience in supersonic wind-tunnel tests desirable**

Excellent opportunity exists to learn all phases related to missiles, rockets and wind tunnel test operations. Apply giving details pertaining to academic background and work experience to

JET PROPULSION LABORATORY
4800 Oak Grove Drive
Pasadena 2, California

ANGULAR accelerometers are made by Statham Laboratories for measurement in ranges as low as ±1.5 radians per second per second.

The design permits close balance against linear acceleration effects with a high degree of mechanical shock resistance and leads to a damping characteristic relatively insensitive to temperature.

The transducer element, an unbonded strain gage bridge, provides an electrical output proportional to applied angular acceleration for recording or telemetering in conventional a.c. or d.c. circuits.

Please request Bulletin No. 4.5.

Statham
LABORATORIES
Los Angeles 64, Calif.

SCINTILLA MAGNETO DIVISION

BENDIX AVIATION CORPORATION

SIDNEY, NEW YORK

Manufacturers of Ignition Systems for Jet, Turbine and Piston Power Plants, Fuel Injection Equipment for Railway, Marine and Industrial Diesel Engines, Electrical Connectors, Ignition Analyzers, Moldings and Special Components.

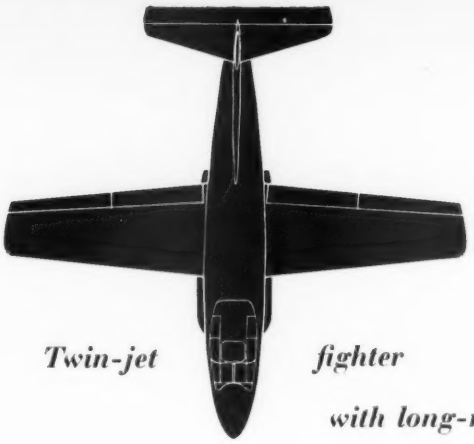

Twin-jet fighter with long-range radar eyes

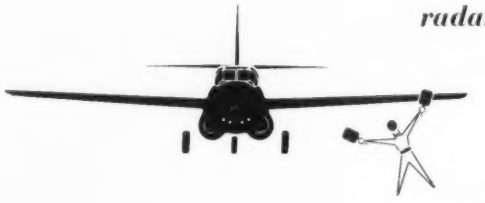

—the Douglas Skyknight

Designed and built for Navy carriers, the Douglas F3D Skyknight provides our fleets with round-the-clock protection. Attack, patrol, reconnaissance, or escort, Skyknight can handle them all.

Aided by its radar eyes, the Skyknight can search out distant targets 24 hours a day. The pilot of this unique two-man, twin-jet, long-range fighter—guided by his radar operator—comes in on targets with split-hair accuracy . . . to hit with both rockets and bullets. And although Skyknight approaches sonic speeds, its hydraulic flaps can slow it down for combat maneuvers or carrier landings.

The carrier-based F3D Skyknight, now in volume production, is typical of Douglas leadership in aviation. Planes that can be mass-produced to *fly further and faster with a bigger payload* is the basic rule of Douglas design.

Depend on *DOUGLAS* 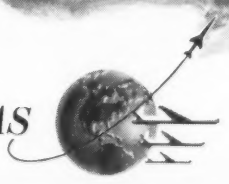 **First in Aviation**

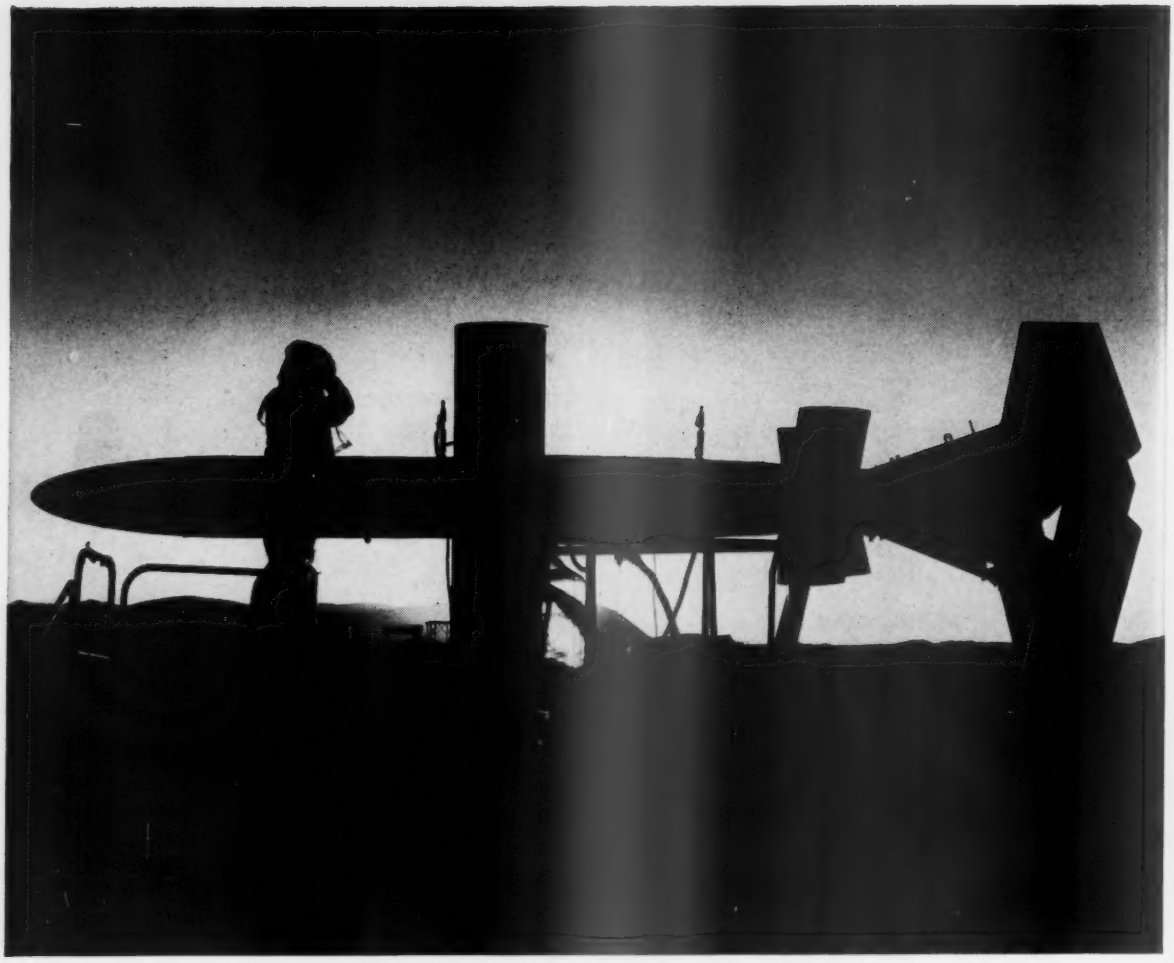

ADVANCED TRAINER...

FOR THE FIRST GUIDED MISSILES GROUP, U.S. ARMY

The United States Army Field Forces today is training its first Guided Missiles Group with Fairchild Missiles. In firing these advanced type anti-aircraft missiles, the Army Field Forces is preparing now for the day when missile batteries will defend cities and vital military installations.

Firing on the desert missile range at Ft. Bliss, Texas, officers and enlisted cadres are learning the skills and techniques necessary for the tactical application of these new weapons under conditions similar to those in actual combat.

Fairchild's Guided Missiles Division also is providing similar anti-aircraft missiles for the United States Navy and the United States Air Force. Its advanced engineering and technical facilities are being devoted to the design and development of new missiles and improved versions of current missiles to provide our Armed Forces with the latest and best possible weapons.

The Fairchild Plant at Wyandanch, L. I.—The World's First Privately Built Missile Plant

ENGINE AND AIRPLANE CORPORATION
FAIRCHILD *Guided Missiles Division*
WYANDANCH, L.I., N.Y.

Fairchild Aircraft Division, Hagerstown, Maryland • Fairchild Engine and Stratos Divisions, Farmingdale, Long Island, New York

MINUTE IN SIZE... GIANTS IN PERFORMANCE!

MYCALEX 410

8-PIN SUB-MINIATURE TUBE SOCKETS

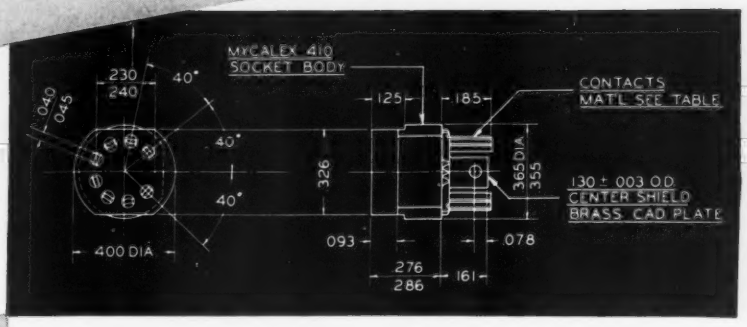

TOP VIEW

BOTTOM VIEW

- **LOW LOSS FACTOR OF .015 at 1 MC.**
- **INSULATION RESISTANCE (min.) 50,000 Megohms**
- **ARC RESISTANCE, ASTM SECS. 250+**
- **OPERATING TEMPERATURE 135°C (limitation due to contact metal)**
- **Q-value at 40°C—50% RH—not less than 1000**
- **Q-value at 40°C—90% RH min.—not less than 333**

WRITE FOR DATA SHEETS

Mycalex 8-Pin Sub-Miniature Tube Sockets are fully described in the new Data Sheets. Other catalogs are available on Mycalex Insulation for every electronic or electrical application.

New MYCALEX 410 Sub-Miniature Tube Sockets are designed for use in electronic and electrical equipment where space is at a premium. Because they are extremely compact, these sockets offer a ready solution to numerous design problems involving spatial limitations. Installation is simple, mounting being accomplished without screws or rivets in shaped chassis holes.

Improved electrical performance and greater mechanical protection for the tube than are available with ordinary insulating materials are afforded by this socket through the use of MYCALEX 410 glass-bonded mica. MYCALEX 410 is rated Grade L-4B insulation under N.M.E.S. JAN-I-10. It offers superior electrical and mechanical properties in combination with practical cost per unit.

MYCALEX TUBE SOCKET CORPORATION
Under Exclusive License of
MYCALEX CORPORATION OF AMERICA
30 ROCKEFELLER PLAZA, NEW YORK 20, N. Y.

SINCE 1919 MYCALEX THE INSULATOR

MYCALEX CORPORATION OF AMERICA
Owners of 'MYCALEX' Patents and Trade-Marks
Executive Offices: 30 ROCKEFELLER PLAZA, NEW YORK 20 — Plant & General Offices: CLIFTON, N.J.

NITRO SOLVAY MEMO

TO: ROCKET DEVELOPERS

SUBJECT: SHIPMENT OF NITROGEN TETROXIDE

Nitrogen Tetroxide is no longer a laboratory curiosity. If you are designing rocket motors to use liquid propellants, you should consider this oxidizer. Solvay is prepared to ship it in I.C.C. approved cylinders or ton containers. Free technical literature is available.

If you would like to test Nitrogen Tetroxide, we will gladly furnish cost and shipping information.

Send your inquiry to:

Product Development Department
THE SOLVAY PROCESS DIVISION
Allied Chemical & Dye Corporation
40 RECTOR STREET • NEW YORK 6, N. Y.

Representative Solvay Nitrogen Products: ANHYDROUS AMMONIA • AMMONIUM NITRATE • SODIUM NITRATE • NITROGEN SOLUTIONS • NITROSYL CHLORIDE • METHANOL